To Prof. T. J. Dolan with regards
Geoff. Liu

CRACK PROPAGATION IN THIN METAL SHEET UNDER REPEATED LOADING

by

HAO WEN LIU

ACKNOWLEDGMENT

This investigation was conducted under the supervision of Professor H. T. Corten in the Fatigue of Metals Laboratory of the Department of Theoretical and Applied Mechanics as a part of the work of the Engineering Experiment Station, University of Illinois, in cooperation with the Wright Air Development Center under Contract Code No. 46-22-60-305. Special acknowledgment is due to Professor T. J. Dolan, Head of the Department, and Professor G. M. Sinclair for their criticism and helpful suggestions. Acknowledgment is due to J. P. Bruen, Mrs. N. E. Dahl, Mrs. A. R. Feltner, G. E. Mercer, Miss V. A. Moberg, R. E. Price, and E. M. Wu, who assisted in various phases of this project.

TABLE OF CONTENTS

CRACK PROPAGATION IN THIN METAL SHEET UNDER REPEATED LOADING

Hao Wen Liu, Ph.D.

Department of Theoretical and Applied Mechanics

University of Illinois, 1959

Fatigue fracture involves two processes: crack initiation and crack propagation. The effect of range, mean, and state of stress appears to be different for crack initiation and crack propagation. Therefore, to understand basic damage phenomena it is advantageous to separate the studies of crack initiation and crack propagation.

An experimental and analytical investigation were undertaken to study the fundamental law of crack propagation in a thin metal sheet under repeated axial loading.

Sheet specimens of 2024-T3 aluminum alloy four inches wide and containing a central hole were used in the experimental investigation. Various combinations of stress range and mean stress were covered by this investigation. Time lapse photography was used to record the crack length and the number of cycles of loading at regular intervals. The crack length was then measured from the recording film.

The experimental results indicated that the propagation life consisted of three periods. In the initial period, the cracks propagated sporadically and slowly. In the middle period, the relationship between the crack length and the number of cycles of loading was well represented by an exponential function. In the final period, crack propagation was greatly accelerated, leading rapidly to fracture.

Based on the concept of geometrical similarity of crack configuration, an expression for crack length was derived in terms of a stress dependent propagation factor and an exponential function of the number of cycles of loading, for a semi-infinite sheet subjected to repeated loads consisting of a constant stress range and mean stress. This expression was in good agreement with the experimental results for the middle periods of the propagation lives. The propagation factor was related experimentally to the stress range and the mean stress.

Modification of the expression was made for the effect of increasing stress range and mean stress as the crack propagated in a finite specimen. Accurate prediction of the propagation life, was possible using the modified equation.

Photomicrographic observations indicated that the size of the plastic zone increased as the crack propagated and that the crack often branched along the path. This branching phenomenon is a possible cause of hesitation periods.

The equation by Head and the hypothesis by Paris were used to analyze the experimental data. However, the results indicated that, without further development, the analyses by Head and Paris et. al. were not as promising as the analysis developed in this investigation.

I. INTRODUCTION

As early as 1858, Wohler found that fatigue or progressive fracture was caused by initiation and propagation of one or more cracks.(1)* In 1903, this observation was substantiated by Ewing and Humphrey by microscopic examination.(2) However only recently, in the last 25 years, have the advantages of separating the phenomena of crack initiation and propagation been recognized.(3,4,5)

Studies of both initiation and propagation of fatigue cracks have proved to be of practical as well as academic interest. The fatigue strength of a member is determined primarily by the stress necessary to <u>initiate</u> a fatigue crack, while safety and prolongation of fatigue life are two major applications of information from propagation studies.(6,7,8) Optimization of the strength to weight ratio and the severe operating conditions encountered in all types of vehicles, high speed machinery and some pressure vessels, produce peak stresses that are high enough to initiate and propagate fatigue cracks, thus limiting the useful life of the member. Further, attainment of a critical crack length frequently quite small, produces catastrophic unstable fracture of the structural member. Therefore, the safety as well as the economy of modern structural members depends greatly upon a rational method of accurate predicting fatigue crack propagation.

Recent studies indicate that fatigue cracks may be detected at a very early stage in the life of the specimen. Thompson(9) reported that cracks can be observed with a microscope after about 5 per cent of the life has expired. Love(10) reported

---

* Numbers in parentheses refer to the references listed in the bibliography.

observing a crack with an electron microscope after about 0.1 per cent of the fatigue life had expired. It is obvious that a large part of the life of the specimen is spent in crack propagation, a fact which emphasizes the importance of studying the influence of the important variables on crack propagation.

This investigation was undertaken to study experimentally and analytically the macroscopic behavior of the fatigue crack propagation.

Thin sheet specimens loaded in repeated tension were used because of the simplicity of analysis and experimental observations. Various combinations of stress range and mean stress were employed to study their effect on crack propagation. Crack lengths were recorded by time lapse photography at regular cycle intervals, and measured from the film. Metallographic observations of the crack tip and slip band region were made to study the size of the plastic zone.

Crack propagation in the semi-infinite sheet under constant stress range and mean stress was analyzed using dimensional analysis. An expression for crack length in terms of number of cycles of load and a stress dependent propagation factor was obtained. In the derivation of this expression, no mechanism of fatigue fracture was assumed, therefore the equation is general in this respect. The propagation factor was related to the stress range and mean stress empirically. Modification of the equation was made for specimens of finite width.

The experimental results were compared with Head's relation[11] and also analyzed in terms of Irwin's stress intensity factor under the premises of Paris and others.[12]

II. REVIEW OF LITERATURE

This review considers two aspects of crack propagation phenomena: first, observations of the relationship between the crack initiation stage, the crack propagation stage, and the total fatigue life are summerized, and second, a detailed review is made of recent crack propagation studies.

The boundary between the crack initiation and the crack propagation periods is controversial and arbitrary, yet this concept provides a useful basis for analysis and evaluation of the many significant variables. Because the presence of a crack changes the geometrical configuration of a member, the effects of range, mean, and state of stress, notches, surface finish, specimen size, and environment appear to be different during crack initiation as compared with crack propagation.

One obvious criterion for judging the effect of any one of these variables is concerned with the size of the region that is affected. If the effect is localized to the region where a crack is initiated, only the initiation period will be affected. On the other hand, if the effect encompasses the entire path of the crack, the initiation as well as the propagation periods may be changed. For example, surface cold work has been used to prolong the crack initiation period or even to prevent crack initiation; however, once a crack is present, it has but a small effect or no effect at all on the propagation period.[4] Conversely, an increase of the amount of various alloying elements has been observed to prolong the initiation as well as the propagation periods.[13]

For notched specimens subjected to the same nominal stress, it has been observed that the crack initiation period became shorter as the notch was made more severe, and the proportion of the total life consumed in crack propagation increased with increasing notch severity.[14] Conversely, if the notch root stress was maintained constant, the fatigue life was lengthened with increasing notch severity because of slower crack propagation in the material away from the notch.[14] For the same total life, the proportion of the life devoted to crack propagation increased with increasing notch severity.[14,15,16] These observations are all consistent with the fact that in a severely notched specimen the highly stressed zone is localized to the region near the surface where a crack is initiated, where as in a mildly notched specimen the highly stressed zone penetrates more deeply into the specimen and influences both crack initiation and propagation.

Most of the early investigations in which crack propagation was measured were made using round rotating beam specimens. More recently, plate or sheet specimens have been used[15,17,18,19,20,21,22]; the simpler geometry facilitates the measurement of crack size and simplifies the analysis. Only those investigations which employed axially loaded plate or sheet specimens will be considered in the remainder of this review.

Wilson and Burke[17] studies 11-1/2 in. wide steel plate specimens containing a 2-7/8 in. long saw cut to initiate cracks. For a given stress, the rate of crack propagation was found to be approximately constant over the range of the crack lengths from 2-7/8 in. to 3-5/8 in. In view of most recent results, this constant rate of crack propagation is unusual but probably was due to the relatively small range of large crack lengths (by comparison to specimen width) used in that investigation.

Martin and Sinclair[18] measured crack length as a function of number of cycles and stress amplitude in 2024-T3 aluminum alloy sheet specimens. Crack length was described by a power function of number of cycles and the crack propagation rate was analyzed in terms of nominal stress, theoretical stress at the tip of the crack,* Irwin's crack driving force,[23,24] and Bowie's rate of strain energy release.[25] These analyses as well as comparison with Head's propagation equation[11] indicated that more accurate and refined theory was needed.

Lipsitt et.al.[19] conducted low-cycle, high-stress fatigue tests on 1.25-in. wide specimens of 1100-H18 aluminum alloy sheet with a single semi-circular notch of 0.0625-in. radius on one side as a crack starter. The data indicated that the growth of a fatigue crack increased very rapidly as the length of the crack increased for this unsymmetrical configuration; however, from motion pictures it was established that, in general, a fatigue crack propagates in short bursts or jumps followed by periods of no measurable growth.

McEvilly and Illg[20] assumed Orowan's mechanism of fatigue fracture and divided each increment of the crack propagation process into two stages. During the first stage, the material near the tip of a crack was cyclically work hardened to the fracture strength of the material. During the second stage, the work hardened material fractured and the crack propagated through this region but stopped when it reached material which had not yet been

---

* The theoretical stress was calculated by assuming a constant root radius of 10^{-3} cm at the tip of an elliptical crack.

completely work hardened. This fracture process was then repeated to provide for crack propagation.

During the work hardening stage the rate of increase of stress at the critical site (rate of work hardening) was assumed to be inversely proportional to the number of cycles since the last increment of crack growth, as well as a function of the endurance limit and the theoretical maximum stress at the tip of the crack. This peak stress at the crack tip was expressed as $K_N\sigma_n$, where K_N is a stress concentration factor, and σ_n is the nominal stress across the net cross-sectional area. It was further assumed that the increment of crack growth during the second stage also depended upon the theoretical maximum stress at the tip of the crack. Based on the above assumptions, the rate of crack propagation was written as

$$\log_{10} \frac{d\ell}{dN} = \log_{10} f_2 (K_N\sigma_n) - \frac{k_1}{2.3} f_1 (K_N\sigma_n, \sigma_e) \qquad (\underline{1a})$$

where ℓ = crack length

N = number of cycles of load

σ_e = endurance limit

k_1 = constant

The constant k_1 and the functions f_1 and f_2 were determined empirically, and upon substitution into Eq. (1a) gave

$$\log_{10} \frac{d\ell}{dN} = 0.00509\, K_N\sigma_n - 5.472 - \frac{34}{K_N\sigma_n - 34} \qquad (\underline{1b})$$

This equation provided a good description of the experimental results for both 2-in. and 12-in. wide specimens of both 2024-T3 and 7075-T6 aluminum alloys. The direct relationship between ℓ and N was obtained by numerical integration.

Weibull[15,21] assumed that the rate of crack propagation was a function of the stress at the tip of the crack, σ_t only. Thus, assuming a parabolic relation,

$$\frac{d\ell}{dN} = k_1 \sigma_t^{a_1} \tag{2}$$

where ℓ is the crack length, N is the number of cycles of load, and k_1 and a_1 are constants. Another parabolic relationship was assumed between σ_t and the nominal stress across the net cross-sectional area, σ_n; that is,

$$\sigma_t = k_2 \sigma_n^{a_2} \tag{3}$$

where k_2 and a_2 are also constants. For a constant amplitude of load, σ_n can be expressed in terms of the <u>initial</u> nominal stress σ_o by

$$\sigma_n = \frac{\sigma_o}{z} \tag{4}$$

where

$$z = \frac{L-\ell}{L-\ell_o} \tag{5}$$

and L is the width of the specimen, ℓ is the crack length at N cycles and ℓ_o is the initial crack length. Equation (2) can be rewritten as

$$\frac{d\ell}{dN} = k\sigma_n^{a} \tag{6}$$

or

$$\frac{dz}{dN} = -\frac{k}{L-\ell_o} \frac{\sigma_o^{a}}{z^a} \tag{7}$$

where k and a are constants, that is $k = k_1 k_2^{a_2}$ and $a = a_1 a_2$.

By integration, Eq. (7) becomes

$$z^{a+1} = -\frac{k(a+1)}{L - \ell_o} \sigma_o{}^a N + k' \qquad (8)$$

According to Eq. (6), the rate of crack propagation should be constant if the net nominal stress, σ_n, is maintained constant. Equation (8) indicates that a diagram of z^{a+1} versus N should be a straight line. Both predictions were substantiated by Weibull's experimental results. Eqs. (6) and (8) have not provided a good description of the data obtained by other investigators. The good agreement obtained by Weibull was apparently due to a combination of fortuitous circumstances including several over simplifications which compensate for one another and the fact that the data were for cracks that were long compared with the specimen width. Equation (3) states that the stress at the tip of the crack remains the same as the crack length increases if σ_n is maintained constant. This is valid only when the crack is very small in comparison to the width of the plate. For long cracks, the stress at the tip of the crack decreases as the crack length increases, if σ_n is kept constant.* Therefore, as the crack length increased, the constant crack propagation rate for constant σ_n is due to the

---

* For an infinite plate containing a circular hole the elastic solution indicates that the maximum stress is $3\sigma_n$. However, for a plate of finite width with a hole diameter of one-half of the width of the plate, the maximum stress is only 2.15 σ_n. Therefore if σ_n is kept constant, the maximum stress is reduced as the diameter of the hole increases relative to the width of the plate. A similar phenomenon of larger magnitude exists for the stress at the tip of a crack.

following two opposing effects at the tip of the crack: a gradual reduction of the peak stress and an increasing zone of inelastic deformation. These two opposing effects apparently cancelled one another for the specimen configuration employed by Weibull.

The derivation of Eqs. (6) and (8) was based on the assumption that the minimum stress is zero. Therefore, the maximum stress alone was sufficient to specify the stress condition of the specimen. In the present investigation, the minimum as well as the maximum stress was a variable. Consequently, Eqs. (6) and (8) are not suitable for analysis of the results of this investigation.

Frost and Dugdale[22] made an extensive study of crack propagation using sheet specimens of mild steel, aluminum alloy, and commercially pure copper. The specimens were 9 or 10-in. wide and used a central slit as a crack starter. On a diagram of logarithm of crack length, ℓ, versus the number of cycles of load, N, the data plotted as a straight line for cracks shorter than 1/8 of the width of the specimen. Therefore, the rate of crack propagation under repeated loading was described by

$$\frac{d\ell}{dN} = C\ell \tag{9a}$$

or

$$\ln \frac{\ell}{\ell_o} = C(N-N_o) \tag{9b}$$

where C is a function of the applied stresses and the subscript "o" indicates the initial condition. Frost and Dugdale suggested Eq. (9) based on the premise of geometrical similarity of the crack configuration at each stage of propagation assuming elastic conditions at all points throughout the specimen.

From measurement of the plastic zone at the tip of the crack in steel specimens, it was found that the length of the plastic zone was proportional to the current crack length. This phenomenon is consistent with Eq. (9) because, as will be shown later, the rate of crack propagation is proportional to the length of the plastic zone if the stress distribution within the elastic and plastic zones remains geometrically similar as the crack length increases.

Bennett[26] and Shanley[27] suggested similar equations on emperical grounds for crack propagation. Equation (9) will be derived by dimensional analysis in the next section.

Head[11] derived a fatigue crack propagation formula based on a physical model of fatigue crack propagation. Paris[12] and others analyzed the fatigue crack propagation in terms of Irwin's[23,24] stress intensity factor. The relation developed by Head and the hypothesis of Paris will be considered in detail in Section V, and thus will not be discussed further at this time.

III. ANALYSIS OF CRACK PROPAGATION IN THIN SHEET UNDER REPEATED LOADING

A thin sheet of material of thickness t and width L, and containing a crack of length ℓ as shown in Fig. 1, is loaded by a combination of a constant amplitude repeated stress and a constant main stress. The origin of the coordinates is at the center of the crack, and the x-axis coincides with the longitudinal direction of the crack.

It is the purpose of this analysis to determine the rate of cycle propagation, $d\ell/dN$, of the crack in terms of the geometry of the crack. The method of dimensional analysis will be employed. It is assumed that the mechanism at crack propagation is the same in every region of the material and that the conditions for crack propagation are adequately specified by the stress-strain relations, the state of stress and the stress- or strain-cycle history at each point in the material.

Neglecting the microscopic variables, the stress $\sigma_\Theta(x,y)$ at point P(x,y) in the direction of Θ can be written as

$$\sigma_\Theta(x,y) = f(\sigma_o,\ x,\ y,\ \Theta,\ t,\ L,\ \text{configuration of the crack, complete stress-strain relation of the material}) \qquad (10)$$

where σ_o is the nominal stress in the specimen, and x and y are the coordinates of the point.

If plane stress is assumed and the width L is large relative to the crack length ℓ, the variables t and L can be excluded. If the shape of the crack for a given value of σ_o remains geometrically similar independent of the crack length,* the configuration of

---

* This assumption will be discussed in detail later in this section.

the crack can be specified by crack length alone. Therefore, Eq. (10) can be written as

$$\sigma_\theta(x,y) = f(\sigma_o,\ x,\ y,\ \theta,\ \ell,\ \text{complete stress-strain relation of the material}) \qquad (11)$$

The stress-strain relations depend on the intrinsic properties of the material as well as on the stress or strain history. Upon repeated loading different points in the specimen experience different stress or strain histories. Therefore, the stress-strain relations will be different for the material at different points in the sheet. Without the exact solution to this stress analysis problem, as well as an exact description of the behavior of the material, it is impossible to specify the stress-strain relations of the material of the whole specimen with one set of parameters.

For the purpose of analysis, divide the specimen into rows and columns of small square elements of side b. The squares can be made as small as necessary to insure that the stress-strain relations are the same for all of the material in each element. The complete stress-strain relations for the entire specimen are the aggregate of the stress-strain relations for each of the small squares which constitute the specimen.

The general stress-strain relations for an element are

$$d\epsilon'_{ij} = \frac{3\sigma'_{ij}\, d\,\bar{\sigma}}{2\bar{\sigma}\, H'} + \frac{d\,\sigma'_{ij}}{2G}$$
$$d\epsilon_{ii} = \frac{(1 - 2\mu)}{E}\, d\,\sigma_{ii} \qquad (12)$$

where

ϵ'_{ij} = deviatoric strain tensor

σ'_{ij} = deviatoric stress tensor

$\bar{\sigma}$ = equivalent stress or effective stress

H' = the slope of an equivalent stress vs. plastic strain diagram

G = Lame constant

ϵ_{ii} = $\epsilon_{11} + \epsilon_{22} + \epsilon_{33}$

σ_{ii} = $\sigma_{11} + \sigma_{22} + \sigma_{33}$

E = Young's modulus

μ = Poisson's ratio

Therefore, the stress-strain relations of any square can be specified by a set of six quantities: $d\sigma_{\alpha\beta}$, $\sigma_{\alpha\beta}$, $H'_{\alpha\beta}$, $G_{\alpha\beta}$, $E_{\alpha\beta}$, and $\mu_{\alpha\beta}$. The subscripts α and β specify the position of the square element in terms of α'th column and β'th row. All of these quantities have the dimensions of σ_o except μ, which is dimensionless. The complete stress-strain relations of the material of the whole specimen can be specified by M sets of such quantities where M is the total number of squares.

Written in the form of dimensionless quantities, Eq. (11) becomes

$$\sigma_\theta(x,y) = \sigma_o \, F_1\Big(\frac{x}{\ell}, \frac{y}{\ell}, \frac{b}{\ell}, \theta, ------, \frac{d\bar{\sigma}_{\alpha\beta}}{\sigma_o}, ------ ----, \frac{\bar{\sigma}_{\alpha\beta}}{\sigma_o}, ------, \frac{H'_{\alpha\beta}}{\sigma_o}, ------, \frac{G_{\alpha\beta}}{\sigma_o}, ------, \frac{E_{\alpha\beta}}{\sigma_o}, ------, \mu_{\alpha\beta}, ------\Big) \tag{13}$$

To apply the methods of dimensional analysis, consider a "model" and a "prototype" of the sheet of material containing a crack. For complete similarity, the model laws require that the stress-strain relations of homologous squares* be identical, if σ_o is the same for both model and prototype. In addition, the following conditions also must be satisfied:

$$\frac{\sigma_\theta(x,y)_1}{\sigma_\theta(x,y)_2} = \frac{\sigma_{o1}}{\sigma_{o2}} = 1 \qquad (\underline{14a})$$

$$\frac{x_1}{x_2} = \frac{\ell_1}{\ell_2} \qquad (\underline{14b})$$

$$\frac{y_1}{y_2} = \frac{\ell_1}{\ell_2} \qquad (\underline{14c})$$

$$\theta_1 = \theta_2 \qquad (\underline{14d})$$

$$\frac{b_1}{b_2} = \frac{\ell_1}{\ell_2} \qquad (\underline{14e})$$

where subscripts 1 and 2 denote model and prototype respectively.

Eq. (14) states that if the stress σ_o is the same for both model and prototype, and if the stress-strain relations of all homologous squares are the same, then the state of stress at any homologous points is the same. The condition of identical stress-

---

* In general, there is a point-to-point correspondence between a model and its prototype. Two points that correspond to each other are homologous.

strain relations for material of homologous squares presupposes that the homologous squares experience the same stress or strain history. If $\Delta \ell_1$ and $\Delta \ell_2$ are homologous lengths, i.e., if they satisfy the condition

$$\frac{\Delta \ell_1}{\ell_1} = \frac{\Delta \ell_2}{\ell_2} = C_1 \qquad (\underline{15})$$

then the number of cycles of load to propagate a crack through $\Delta \ell_1$ and $\Delta \ell_2$ must be the same. Therefore, Eq. (15) can be written as

$$\frac{\Delta \ell_1}{\ell_1 \Delta N} = \frac{\Delta \ell_2}{\ell_2 \Delta N} = C \qquad (\underline{16})$$

Now consider the subscripts 1 and 2 as two stages in the course of crack propagation through one specimen rather than crack propagation in two similar specimens.* Eq. (16) describes the basic law of crack propagation in a thin infinite sheet.

Since the subscripts do not specify any particular stages in the course of crack propagation, but only earlier and later stages, they can be provisionally dropped. Written in differential and integrated forms, Eq. (16) becomes

$$\frac{d\ell}{dN} = C\ell \qquad (\underline{17a})$$

$$\ln \ell - \ln \ell_o = C(N - N_o) \qquad (\underline{17b})$$

In the course of the derivation of Eq. (17), two assumptions were made which now must be investigated. The shape of the crack for

---

* Consideration of two stages in the course of crack propagation in one specimen necessarily introduces different stress histories for the two stages. The significance of this limitation will be discussed later.

each value of σ_o was assumed geometrically similar independent of the crack length, and the stress-strain relations of homologous squares were assumed to be identical. These two assumptions have to be examined by comparison with the final solution, Eq. (17). The solution and the assumptions are valid only if they are compatible with one another.

The assumption that the shape of the crack remains geometrically similar independent of the crack length for each value of σ_o will now be verified. Under any stress, σ_o, the displacement, $u_\theta(x,y)$, of a point $P(x,y)$ in the direction θ can be written as

$$u_\theta(x,y) = \ell F_2\Big(\frac{x}{\ell}, \frac{y}{\ell}, \frac{b}{\ell}, \theta, \text{------}, \frac{d\bar{\sigma}_{\alpha\beta}}{\sigma_o}, \text{------}, \frac{\bar{\sigma}_{\alpha\beta}}{\sigma_o}, \text{------}, \frac{H'_{\alpha\beta}}{\sigma_o}, \text{------}, \frac{G_{\alpha\beta}}{\sigma_o}, \text{------}, \frac{E_{\alpha\beta}}{\sigma_o}, \text{------}, \mu_{\alpha\beta}, \text{------}\Big) \qquad (18)$$

Based on Eq. (18) and following the same general procedure employed in the derivation of Eq. (17), it can be concluded that the displacements $u_\theta(x,y)$, of homologous points under the same stress, σ_o, are proportional to their crack lengths, provided the stress-strain relations of homologous squares are the same. Thus, if the initial shapes of the crack, i.e., the shapes of the crack when the stress σ_o was zero, were geometrically similar at any two stages of crack propagation, the shapes of the crack must remain geometrically similar under any identical stress, σ_o. Therefore, this assumption of geometrical similarity of the shapes of crack is contingent on the condition of identical stress-strain relations for homologous squares.

It is now necessary to examine the assumption that the homologous squares have identical stress-strain relations as the crack propagates. Examine the stress histories of two homologous points $P_1(x_1,y_1)$ and $P_2(x_2,y_2)$ at two stages of crack propagation. The crack length at stage 1, after N_1 cycles, is ℓ_1, and at stage 2, after N_2 cycles, is ℓ_2. Initially assume identical stress-strain relations at these two stages. Eq. (14) indicates immediately that these two homologous points experience the same additional stress history if no crack propagation occurs. Now consider an increment of crack propagation and let ℓ_1' be the crack length after ℓ_1 increases by $\Delta\ell_1$, and let ℓ_2' be similarly defined. According to Eq. (16) ℓ_1' and ℓ_2' are

$$\left.\begin{aligned} \ell_1' &= \ell_1 + \Delta\ell_1 \\ &= \ell_1 + C\ell_1\Delta N \\ &= \ell_1 (1 + C\Delta N) \\ \ell_2' &= \ell_2 + \Delta\ell_2 \\ &= \ell_2 + C\ell_2\Delta N \\ &= \ell_2 (1 + C\Delta N) \end{aligned}\right\} \qquad (19)$$

Eq. (19) indicates that

$$\left.\begin{aligned} \frac{x_1}{x_2} &= \frac{\ell_1'}{\ell_2'} \\ \frac{y_1}{y_2} &= \frac{\ell_1'}{\ell_2'} \end{aligned}\right\} \qquad (20)$$

Eq. (20) states that P_1 and P_2 remain homologous points as the crack propagates to ℓ_1' and ℓ_2' respectively. Therefore, by Eq. (14) these two points have experienced the same increment of stress history, and have identical stress-strain relations at the end of the interval if the stress-strain relations were identical at the beginning of stages 1 and 2.

The one remaining consideration which determines the compatibility of the initial assumptions and the final solution is the influence of previous stress history.

Consider the stress history of two points, $P_1(x_1,y_1)$ and $P_2(x_2,y_2)$ during the interval from the first load cycle until a crack is initiated at N_o cycles. During each cycle, each point experiences the same stress history,* since the original specimen configuration remains unchanged. Thus, all points* exhibit identical stress-strain relations at N_o cycles.

With the initiation of a crack at N_o cycles, points $P_1(x_1,y_1)$ and $P_2(x_2,y_2)$ experience different stress histories, since these two points are homologous points but at two different stages of crack propagation. For the purpose of determining the condition for compatibility of the assumptions and the solution, assume that the stress-strain relations for points $P_1(x_1,y_1)$ and $P_2(x_2,y_2)$ are identical at stage 1 and stage 2 respectively. According to Eqs. (19) and (20), each increment of stress history preceding stage 1 was identical to a corresponding increment of stress history preceding stage 2.

---

* This is not applicable to points that are within the influence of a geometrical discontinuity employed as a crack starter.

Upon tracing the stress history for both points, $P_1(x_1,y_1)$ and $P_2(x_2,y_2)$, backwards, increment by increment, for a total of $(N_1 - N_o)$ cycles, it is clear that point $P_1(x_1,y_1)$ experiences a cycle of stress at N_o cycles that is, by definition, not influenced by the crack. At this same stage of stress history, that is, at $[N_2 - (N_1 - N_o)]$ cycles, point $P_2(x_2,y_2)$ experiences a cycle of stress that is influenced by the presence of the crack.* Thus point $P_2(x_2,y_2)$ experiences an increment of stress history from N_o cycles to $[N_2 - (N_1 - N_o)]$ cycles that is different from point $P_1(x_1,y_1)$. The condition of compatibility of the assumption and the solution requires for the material at point $P_2(x_2,y_2)$, that the stress-strain relations remain unchanged during this cycle interval. Since the two points are any homologous points, this cycle interval may be short or long depending upon the relative location of these two points.

The significance of this condition will be fully discussed later; however, to satisfy this condition, it is evident that all of the material must exhibit a stable response to cycles of stress, σ_o (and slightly higher) following the $N_o{}^{th}$ cycle. For sufficiently low values of σ_o it may be anticipated that the condition will be satisfied. For some high value of σ_o, as compared with the properties of the material, the stress-strain relations for any point $P_2(x_2,y_2)$ will continue to undergo change even after N_o cycles. Thus it appears that the realm of validity of Eq. (17) may be specified in terms of a dimensionless ratio involving the applied stress

---

* If the concept of "model" and "prototype" had been retained, N_o cycles would correspond to crack initiation in both members.

σ_o and some material property representing the response of the material after N_o cycles.

It is concluded that within the limitation imposed by the influence of stress history as outlined above the assumptions made in the above derivation are compatible with the final solution, and Eq. (17) is the law of crack propagation in a thin sheet of infinite width under repeated loading of a given amplitude and mean stress. In the derivation, no assumptions were made concerning the mechanism of crack propagation, the stress or strain distribution, or the material properties. Therefore, the solution is general in these three respects.

For the over-all problem of crack propagation, the geometry, the mechanism of crack propagation, the stress or strain distribution, and the material properties all must be taken into consideration. The geometry will determine the general form of the equation as given by Eq. (17); the mechanism of crack propagation, the stress or strain distribution, and the material properties will relate the parameter or parameters, such as C in Eq. (17), to the applied stress. Therefore, Eq. (17) is the partial solution to the over-all problem of crack propagation in thin sheet. The constant C in Eq. (17) will be correlated empirically to the stress amplitude and mean stress in this investigation.

The solution, Eq. (17), is for a thin sheet of infinite width. For this configuration, the stress distribution remains similar at different stages of crack propagation. For a specimen of finite width under constant amplitude repeated load, the stress amplitude as well as the mean stress increases as the net section of the specimen is reduced by the propagation of the crack. Thus, appropriate modifications should be made. For a specimen of finite width, the stress distribution changes as the crack length increases, and the change becomes considerable as the crack approaches a critical size. Thus, an exact solution for a sheet of finite width appears to be very difficult because for various stages of crack propagation the exact stress distribution is unknown, and the concept of similarity is not applicable.

IV. EXPERIMENTAL INVESTIGATION

1. Material and Specimens

Specimens were cut from 2024-T3 aluminum alloy sheets 0.02 in. thick. According to specifications the aluminum was solution heat treated, tempered, and cold rolled to final thickness by the manufacturer. The mechanical properties were measured as follows:

Yield Strength (0.03% offset)	51,500 psi.
Yield Strength (0.2% offset)	53,500 psi.
Ultimate Strength	69,500 psi.

A typical stress-strain curve is shown in Fig. 2.

The critical dimensions of the specimens are shown in Fig. 3. A circular hole, 0.033-in. in diameter and located at the center of the 4-in. wide specimen, was used as a stress raiser to initiate the fatigue cracks.

The specimens were buffed and hand polished by a standardized process* to produce a uniform, smooth, and reflective surface across the entire width of the central region.

2. Apparatus and Experimental Procedures

The specimens were loaded axially using various combinations of minimum and maximum tensile loads to obtain a planned sequence of values of range of stress and mean stress. For each combination, except one, at least two specimens were tested under

---

* The specimens were buffed for two minutes with 4-in. diameter cotton buffs and type XXX buffing compound of white coloring composition. The buffs were held against the specimen with a force of 2.5 lb. The specimens were then hand polished with a fine cloth and lapping compound, which contained medium hard alumina of grit size 900.

identical conditions to provide an indication of the reproducibility and scatter of the data.

A schematic diagram and a photograph of the experimental apparatus are shown in Fig. 4a, and Fig. 4b, respectively. The stress amplitude was controlled by an adjustable eccentric crank which loaded the specimen at 600 rpm. The eccentric crank was connected to a loading beam by a turnbuckle, which controlled the mean stress. Both stress amplitude and mean stress could be adjusted easily and accurately.

The load to the specimen was measured by four SR-4 electric resistance strain gages mounted two on the inside and two on the outside of a circular ring load cell. The gages were wired to form the four arms of an external bridge and connected to an SR-4 strain indicator. The over-all experimental error in the measurement of stress was estimated to be $\pm$ 200 psi.

The crack length and the number of cycles of load were recorded by time lapse photography at regular cycle intervals. The camera* was operated electrically, and could take 420 successive frames without reloading. It was controlled by an electromechanical system which performed two functions: (1) taking pictures at regular cycle intervals and (2) taking each picture when the stress was within 90 per cent of the maximum stress in order to obtain maximum definition of the cracks on the film. This

---

* A Praktina FX 35mm camera was used.

electro-mechanical system is shown schematically in Fig. 4a*.

Fifty to three hundred successive frames were obtained for each specimen. The crack length was measured by viewing the film through a microscope mounted on a calibrated travelling mechanical stage. The measurements were reproducible to within 0.0005 in., and considering all sources of error, were estimated to be accurate to 0.001-in.** In Fig. 5, pictures of a crack at three different stages of propagation are reproduced from the recording film. The cycle counter contained a 10 to 1 reduction; thus the number of cycles of load that was recorded was accurate to within ten cycles. The grid lines at the top of the pictures were 0.100-in. apart, and served as reference calibration for the measurements.

Since the crack propagation rate depends on the total crack length, the crack lengths were measured from the tip of one crack to the tip of the other. The stress distribution at the tip

---

* The cyclic interval was controlled by a gear reducer which was driven by the machine motor. The reduction ratio of the gear reducer determined the size of cyclic interval between pictures. The pip on cam A, which was attached to the shaft of a gear reducer, activated solenoid A through micro-switch A. When activated, solenoid A raised micro-switch B to the depressed portion of cam B.

The phasing of the picture and the applied load were coordinated by cam B which was positioned on the shaft connecting the machine motor to the eccentric load crank. When the raised portion of cam B contacted micro-switch B, solenoid B was activated, and the release switch of the camera was closed.

** During the early stages of the program certain difficulties were encountered, such as small scratches close to the crack and poor focus of the camera, which introduced somewhat greater error, including apparent "crack shortening" in a few cases.

of the crack depends on the configuration of the crack. If the longitudinal dimension of the crack is large compared to the lateral dimension, the region near middle of the crack, away from the tips, experiences a stress field of very low intensity. Therefore, the presence of a circular hole at the middle of the crack will not disturb the stress distribution at the crack tips, provided the crack is considerably longer than the diameter of the hole. It was found that the effect of the hole on crack propagation diminished and could no longer be detected as the crack length approached 0.07-in., which was approximately twice the diameter of the hole.

All experimental procedures were performed in a consistent manner throughout the entire investigation. Special care was taken to maintain the maximum and the minimum loads constant during each experiment. The first few cycles of load were turned by hand, and the loads were checked and adjusted to the specified values. Four or five small adjustments of load were made during the first third of the lives of the specimens. Throughout the remainder of the life it was found that the magnitude of the loads remained very nearly constant.*

---

* For specimen 2802a, the maximum and minimum loads remained constant to at least 96.8 per cent of the life. For specimen 3202c, the maximum load dropped only 1.3 per cent at 99.8 per cent of the life.

V. RESULTS AND DISCUSSION

The experimental results and the analyses of data for all specimens are summarized in Tables 1 and 2. The specimens were numbered so that the first two digits indicate the maximum stress in thousands of psi. and the last two digits indicate the minimum stress. The stress range and mean stress are given also in Table 2a.

In Table 1, the crack lengths corresponding to various numbers of cycles of load are tabulated for each specimen. In Figs. 6 through 41, diagrams of the crack length, ℓ, plotted on a logarithmic ordinate scale and the number of cycles of load, N, plotted as the abscissa, are shown for each specimen. The data indicate that crack propagation can be divided into three periods: the initial, the middle, and the final.

The cracks propagated very irregularly in the initial period. This irregularity was probably caused by several factors including variations in the material introduced by machining the central hole, the slow propagation rate associated with a small crack length combined with microscopic inhomogeneities, and the difficulty of measuring the crack length when the crack was small. Actually irregular crack propagation was observed in each of the three periods, however it was considerably more sporadic during the initial period. In addition, the logarithmic ordinate employed in Figs. 6 through 41 tends to accentuate the irregularities of the short cracks and minimize the irregularities of the long cracks. The initial period occupied approximately one-quarter of the entire propagation cycle life, and ended as the crack length approached 0.07-in.

As the crack propagated into the middle period, the variation of ln ℓ with N was linear as predicted by Eq. (17). The crack configuration presumably reached a "stable" shape which was maintained until the assumption of semi-infinite sheet was no longer valid.

The propagation factor, C in Eq. (17), was evaluated from the slope of this straight line portion of the curve for each specimen. Values of C for individual specimens as well as the average values for specimens tested at the same stress range and mean stress are tabulated in Table 2a. It was pointed out earlier that the propagation factor C is related to the applied stresses. In Fig. 42, C is plotted as the ordinate, on a logarithmic scale, and the mean stress is shown as the abscissa. For each combination of mean stress and stress range, only the average values of C, from Table 2a, are shown. In Fig. 42, straight lines have been drawn through the points which represent the same stress ranges, the same maximum stresses, and the same minimum stresses. The three families of equally spaced lines thus formed, provide a very good representation of the trends exhibited by the data.

The qualitative variation of C, with respect to the influence of stress on the rate of crack propagation, as indicated by these three families of lines, forms a consistent pattern of behavior. For a constant mean stress, C increases with an increase in stress range which may be achieved by increasing the maximum stress or decreasing the minimum stress or both. Similarly if the stress range is maintained constant, C increases with an increase of mean stress, which may be achieved by increasing both the maximum stress and the minimum stress.

In Figure 42, the slope of the equi-stress-range lines is the smallest, while that of the equi-minimum-stress lines is the largest, and that of equi-maximum-stress lines is intermediate between the other two. These slopes provide a simple means of evaluating the significance of the various methods of specifying the stress conditions. Since only two of the four quantities, stress range, mean stress, maximum stress, and minimum stress, are independent, specification of any two of these quantities completely determines the other two quantities and the stress conditions. If the slope of the equi-stress-range lines in Fig. 42 were zero, the value of C would be dependent on stress range alone and independent of mean stress. However the slope of the equi-stress-range lines in Fig. 42 is relatively small, indicating that for a constant stress range, the value of C_o changes only a small amount for large changes of mean stress. Since the total range of variation of C_o is considerably larger, it may be concluded that the stress range, $\Delta\sigma$, has a greater influence on the value of C_o than mean stress. Comparing the influence of the other two quantities, the maximum stress and the minimum stress, with the mean stress, one at a time, the higher slopes of the equi-maximum stress lines and equi-minimum stress lines indicate that these two quantities have less influence on the value of C_o than the range of stress. From Fig. 42, three pairs of a possible six combinations of the four stress quantities have been compared; in each case the mean stress was used as a basis for comparison. It was shown that in the order of influence on C_o, the stress range was most important, followed by the maximum stress, and finally the minimum was least important.

To establish the position of the mean stress in this sequence, consider a similar diagram involving C_o as the ordinate and the stress range, $\Delta\sigma$, as the abscissa. In Fig. 43, average values of C_o from Table 2a are plotted on a logarithmic scale. The solid lines are equi-maximum-stress lines. With the maximum stress and stress range known at any point along the lines, the equi-minimum-stress and equi-mean-stress lines, although not shown, can be traced. It can be shown that the slope of equi-mean-stress lines is intermediate between that of equi-maximum-stress and equi-minimum-stress lines. The relative magnitude of these slopes indicates the relative influence of these three stress quantities on the propagation factor. Finally, arranged in the order of decreasing influence, they are: stress range, maximum stress, mean stress, and minimum stress.

The middle period of crack propagation covered about one half of the propagation life, and a range of crack lengths from approximately 0.07 in. to 0.16-in., or the range of values of ℓ/L from 0.0175 to 0.04.

The rate of crack propagation accelerated rapidly during the final period. This rapidly increasing rate of propagation was due to two factors: the increase in stress range as well as mean stress due to the reduction of cross-sectional area, and a change of stress distribution at the tip of the crack as the ratio of crack length to specimen width increased.

The effect of the increasing stress range and mean stress will now be analyzed in detail. In the discussion of the experimental investigation, it was pointed out that after initial adjustments the maximum and the minimum loads remained constant until the very last part of the test. Therefore, the stresses increased as the cross-sectional area reduced. The change of stress range and mean stress in a specimen due to reduced cross-section may be described by the following expressions,

$$\Delta\sigma = \frac{\Delta\sigma_o}{1 - \frac{\ell}{L}} \qquad (\underline{21})$$

$$\sigma_m = \frac{\sigma_{mo}}{1 - \frac{\ell}{L}} \qquad (\underline{22})$$

where $\Delta\sigma$ is the stress range, σ_m is the mean stress, and the subscript "o" denotes the initial condition, i.e., the condition before a crack was initiated.

With the aid of these two equations, the change of the propagation factor C due to an increase of crack length can be traced in Fig. 43. The solid lines in Fig. 43 are equi-maximum-stress lines, and the broken straight lines are the traces of the change of C due to reduction of cross-sectional area. The slopes of the broken lines are very nearly constant. Therefore using an average slope to represent all of the broken lines, the propagation factor C can be expressed at any stage of propagation, in terms of stress range by

$$C = C_o e^{s(\Delta\sigma - \Delta\sigma_o)} \qquad (\underline{23})$$

where s, the average slope of the broken lines in the semi-logarithmic diagram, Fig. 43, was equal to 0.000123. By using an average slope for the broken lines and describing C in terms of stress range only, the effect of the second stress parameter was neglected in Eq. (23).

Substituting Eq. (21) into Eq. (23), the expression for C becomes

$$C = \frac{C_o}{e^D} e^{\frac{D}{1-\frac{\ell}{L}}} \tag{24}$$

where

$$D = s \Delta\sigma_o$$

Substituting Eq. (24) into Eq. (17a) and rearranging terms gives

$$dN = \frac{e^D}{C_o} \frac{e^{-\frac{D}{1-\frac{\ell}{L}}}}{\ell} d\ell \tag{25}$$

Let

$$\rho = \frac{D}{1 - \frac{\ell}{L}} \tag{26a}$$

Rearranging Eq. (26a), gives

$$\ell = L \left(1 - \frac{D}{\rho}\right) \tag{26b}$$

Thus

$$d\ell = \frac{LD}{\rho^2} d\rho \tag{26c}$$

Substituting Eq. (26c) into Eq. (25) and simplifying

$$dN = \frac{e^D}{C_o} \left(\frac{1}{\rho - D} - \frac{1}{\rho}\right) e^{-\rho}\, d\rho \qquad (27)$$

Integrating Eq. (27)

$$(N-N_o) = \int_{\rho_o}^{\rho} \left(\frac{e^D}{C_o} \frac{e^{-\rho}}{\rho - D} - \frac{e^D}{C_o} \frac{e^{-\rho}}{\rho}\right) d\rho$$

$$= \frac{1}{C_o} \int_{\rho_o - D}^{\rho - D} \frac{e^{-\rho}}{\rho}\, d\rho - \frac{e^D}{C_o} \int_{\rho_o}^{\rho} \frac{e^{-\rho}}{\rho}\, d\rho$$

$$(N-N_o) = \frac{1}{C_o} \left\{ -E_i \left[-(\rho_o - D)\right] + E_i \left[-(\rho - D)\right] \right\}$$

$$- \frac{e^D}{C_o} \left\{ - E_i (-\rho_o) + E_i (-\rho) \right\} \qquad (28)$$

where

$$D = 0.000123\, \Delta\sigma$$

$$\rho = \frac{D}{1 - \frac{\ell}{L}}$$

and the subscript "o" indicates the initial condition. The term $-E_i(-x)$ in Eq. (28) is the exponential integral of argument x, and is defined as

$$-E_1(-x) = \int_x^{\infty} \frac{e^{-x}}{x}\, dx \qquad (\underline{29})$$

The values of this integral are tabulated.

Eq. (28) represents a modification of Eq. (17) for application to a specimen of finite width. The effect of the continuously changing stress range and mean stress caused by crack propagation are included, however, it does not account for a change in the stress distribution as the ratio, ℓ/L, becomes large.

The quantities N_o and C_o will now be evaluated for the purpose of comparing crack propagation as predicted by Eq. (28) with the experimental data. It is convenient to consider N_o first.

The initial condition in Eq. (28) is prescribed by ℓ_o which can be arbitrarily chosen. In this investigation, ℓ_o was the diameter of the hole and was equal to 0.033-in. An estimate of N_o may be obtained by extrapolating the straight line portion of the curves in Figs. 6 through 39 back to ℓ_o. This graphical method of determination of N_o is shown schematically in Fig. 6 and is equivalent to an algebraic solution for N_o using Eq. (17). The values of N_o obtained for each specimen are tabulated in Table 2b.

The calculation of the propagation factor C was based on the assumption that the specimen is infinitely wide. However, the specimen is of finite width, and the propagation of the crack is influenced by the increase in stress accompanying crack propagation. This effect is reflected in the values of C measured as the slope of the line representing the experimental data during the middle stage of propagation. Therefore this value of C is not the propagation constant for a given stress range and mean stress in a semi-infinite sheet. However, a first approximation to the propagation factor C_o for a semi-infinite sheet at the initial values of stress range and mean stress will be made. Eq. (28) may be rewritten solving for C_o, and evaluated for the fracture conditions, i.e., $\ell = L$, and $N = N_{ft}$, giving

$$C_o = \frac{\left\{-E_i\left[-(\rho_o - D)\right] + e^D E_i(-\rho_o)\right\}}{N_{ft} - N_o} \tag{30}$$

If N_{ft}, the theoretical number of cycles at fracture were known, C_o could be calculated. To determine N_{ft}, it is convenient to form the ratio, $(N - N_o)/(N_{ft} - N_o)$, which will be called the propagation cycle ratio. The relationship between two dimensionless quantities, the propagation cycle ratio, $(N - N_o)/(N_{ft} - N_o)$, and (ℓ/L) can be calculated using Eq. (28), since the quantity C_o does not appear in the expression for the propagation cycle ratio. From this relationship, N_{ft} can be calculated for each specimen using the previously determined values of N_o and one additional experimental point. The points used in this calculation were chosen from the linear portion of the curves because, in this region the assumption of semi-infinite sheet is still valid, and the effect of a change of stress distribution can still be neglected. The values of N_{ft} thus obtained, provide all of the necessary information to evaluate C_o using Eq. (30).

Before preceding with the calculation of C_o, it should be noted that based on the expression for the propagation cycle ratio, $(N - N_o)/(N_{ft} - N_o)$, the value of N can be calculated for various crack length ratios, ℓ/L. The results of this calculation are shown in Figs. 6 through 39 as broken lines. These theoretical curves coincide with the experimental results during the middle stage of crack propagation. In the final stage, the theoretical curves lie to the right of the experimental curves. This deviation was attributed to the changing stress distribution at the tip of the cracks during the final stage. However, the deviations are small and consistent. The ratio of the experimental to the theoretical propagation lives, $(N_{fe} - N_o)/(N_{ft} - N_o)$, are tabulated in Table 2b for each specimen. The values ranged from 0.69 to 0.84, and the average was 0.77.

The initial propagation factor C_o for every specimen and the average for specimens with same stress range and mean stress were calculated using Eq. (30) and are tabulated in Table 2a. The average values of C_o are plotted against the mean stress in Fig. 44. The experimental points are well represented by straight lines similar to Fig. 42. Based on this diagram, the value of C_o can be written in terms of $\Delta\sigma_o$ and σ_{mo} as

$$\ln C_o = 0.00009298\,\Delta\sigma_o + 0.00003914\,\sigma_{mo} - 12.61 \qquad (31)$$

Substituting Eq. (31) into Eq. (28), the crack propagation relation becomes

$$(N - N_o) = e^{Q}\left\{-E_i\left[-(\rho_o - D)\right] + E_i\left[-(\rho - D)\right] - e^{D}\left[-E_i(-\rho_o) + E_i(-\rho)\right]\right\} \qquad (32)$$

where

$$\varphi = 12.61 - 0.00009298\,\Delta\sigma_o - 0.00003914\,\sigma_{mo}$$

The results of the calculation of N for various values of ℓ using Eq. (32) are shown as dashed curves in Fig. 45, a through n. The solid curves represent the experimental data for various specimens denoted by the lower case letters. The agreement of the experimental data with the predicted curves is excellent during the middle stage of crack propagation. As in Fig. 6 through 39, the theoretical curves deviate from the experimental data during the final stage of propagation. However by forming the ratio, $(N_{fe} - N_o)/(N'_{ft} - N_o)$ it can be shown that the deviation is very consistent for all specimens. The ratios, $(N_{fe} - N_o)/(N'_{ft} - N_o)$, have an average value of 0.76 with a minimum to maximum range from 0.66 to 0.94. The maximum deviation from the mean value is 24%, however only two out of thirty-two values of the ratio are outside of the range 0.76 ± 0.10 or $\pm 13\%$ of the mean value. Therefore, the fatigue propagation life can be predicted very accurately using Eq. (32).

The crack propagation formula for a finite sheet, Eq. (28), was derived from the crack propagation formula for a semi-infinite sheet, Eq. (17), by assuming Eq. (24) for the expression of the change of the propagation factor with respect to an increase of crack length. From Eq. (28), Eq. (32) was derived by assuming Eq. (31) as the relation between the propagation factor and the stress range and mean stress. Therefore, Eqs. (28) and (32) are valid only for the material used in this investigation while Eq. (17) is valid for any material. Additional experimental investigations are needed to determine whether expressions similar to Eqs. (28) and (32) are applicable for other material. However, the general approach of adjusting C for change of stress as the crack propagates can be applied to other materials.

Irwin's critical crack extension force, $\mathcal{G}_c$,[29] was calculated for three specimens from measurements of the load on the last cycle and the crack length just prior to the last cycle. An average value of $\mathcal{G}_c$ of 231 lb/in was obtained from which the critical crack lengths for onset of rapid crack propagation were computed to be 0.96-in., 1.16-in., 1.42-in., and 1.73-in. for maximum stresses of 40,000 psi., 36,000 psi., 32,000 psi, and 28,000 psi, respectively. Based on these critical crack lengths and the corresponding maximum stresses the propagation life calculated by Eqs. (28) and (32) as the number of cycles for the onset of unstable fracture differed only 3 per cent from the life, N'_{ft}, predicted by Eqs. (28) and (32) alone. Therefore, the two methods gave essentially the same results for the cases considered.

The values of N_o, the number of cycles for crack initiation determined from the experimental data by extrapolation of the straight line to ℓ_o, as shown in Fig. 6, were tabulated in Table 2b. These values of N_o, because they are defined in an arbitrary manner, are fictitious, however they serve as a useful measure of the initiation period. The statistical scatter of the initiation period was investigated by determining the parameters of the statistical distribution of the ratio, $N_o/N_{o(mean)}$ assuming a normal distribution. The quantity, $N_{o(mean)}$, is the mean value of N_o for specimens subjected to the same stress range and mean stress. The standard deviation of the ratios was 0.127.

The propagation life can be specified in terms of $(N_{fe}-N_o)$. In a similar manner, the ratio, $(N_{fe}-N_o)/(N_{fe}-N_o)$mean, can be formed, where $(N_{fe}-N_o)_{mean}$ is the mean value for specimens subjected to the same stress range and mean stress. The standard deviation was computed as 0.052. As shown by the standard deviations, the scatter of the initiation period is more than twice as large as that of the propagation period. This is not unexpected since the phenomena of crack initiation is a more localized phenomenon than crack propagation.

As a measure of the crack length when the rate of propagation became fast, values of ℓ_f were determined by extrapolating the linear portions of the curves in the crack propagation diagrams, Figs. 6 through 39, to the fracture lives, N_{fe}, of the specimens. The determination of ℓ_f is shown schematically in Fig. 6. The values of ℓ_f were also tabulated in Table 2b. The length, ℓ_f, is also a fictitious value, but it serves as a measure of crack length for the transition from slow to very rapid crack propagation and eminent fracture of the specimen. The experimental data suggest that the value of ℓ_f depends on stress range as well as maximum stress.

Photomicrographs of the crack tips both before and after polishing and etching, are shown in Fig. (46) at a magnification of 200X. The over-all crack lengths are given below each picture. These pictures were taken from three specimens each subjected to the same stress range, 30,000 psi, and the same mean stress, 21,000 psi.

The same crack tip, both before and after polishing and etching, is shown in Fig. 46b and c, and the opposite tip of the same crack, after polishing and etching, is shown in Fig. 46a. The pictures in Figs. 46a, b, and c were taken after the same number of cycles of load. It may be observed that one side of the crack is longer than the other. In Fig. 46a, two small cracks were present at the same side of the hole. The stress at the tips of these two small cracks will be less than the stress at the opposite tip. Consequently, the crack will propagate faster on one side than the other. If the stress is sufficiently reduced, the two short cracks may become dormant until the other end of the crack has propagated enough to increase the stresses and cause one of these two small cracks to propagate further. Two such examples are shown in Figs. 40 and 41. For specimen 2802c, the crack propagated on only one side until 111,490 cycles were applied; for specimen 2806b, until 210,020 cycles were applied. This phenomenon produced two linear portions in each crack propagation curve. The intersection of these two lines indicates the beginning of crack propagation at the other side of the hole.

Occasionally the cracks split into several branches as shown in Fig. 46e and g. Branching has the effect of reducing the stress at the tip of crack. This may be the cause of the frequently observed hesitation periods. One such example of a hesitation period is shown in Fig. 38.

The size of the plastic zone at the crack tip increased with crack length as shown in Fig. 46b, d, and f by the slip lines. No visually detectable plastic deformation was present in Fig. 46a. However, the plastic zone in Fig. 46f is much larger than that shown in Fig. 46d. This observation is in qualitative agreement with the assumptions made in the derivation of Eq. (17).

In the development of Eq. (17), it was indicated that the validity of this relation was limited by the effect of stress history on the stress-strain relations. The significance of this limitation can be evaluated indirectly. The validity of Eq. (17) depends on the assumption that the mechanism of crack propagation is the same at each stage of the propagation life and thereby that homologous points experience identical stress histories prior to fracture. It was shown that prior to crack initiation the stress histories are identical. Following crack initiation, homologous points at two different stages of crack propagation experienced different stress histories. Point, P_2, corresponding to the later stage of propagation experienced a number of cycles of stress when the crack was not in close proximity that did not correspond to any period in the stress history of point P_1, corresponding to an earlier stage of propagation. If the stress-strain relations of point P_2 remained unchanged throughout this additional cyclic interval, it was shown that each increment of stress history experienced by point P_1 and P_2 preceding crack propagation could be claimed to be identical and the assumption of identical mechanisms of crack propagation in the vicinity of points P_1 and P_2 would be satisfied.

The good agreement of Eq. (17) with all of the experimental data in the second period of propagation justifies the use of this assumption for the range of stresses covered by this investigation. Of necessity the stresses used in this investigation were above the fatigue strength of the material; however the maximum nominal stress 40,000 psi. was below the yield strength at 0.03 per cent offset, 51,000 psi. It may be anticipated that at higher stresses the assumptions made in the analysis will provide a less accurate description of the crack propagation phenomena.

Head's Theory[22]

Utilizing Orowan's mechanism of fatigue fracture and a physical model of fatigue crack propagation, A. K. Head derived an expression for fatigue crack propagation in an infinite medium under completely reversed stress. The relation between the rate of propagation and crack length may be written as

$$\frac{d\ell}{dN} = k_1 \ell^{3/2} \tag{33a}$$

Upon integration, Eq. (33a) becomes

$$\ell^{-1/2} = k_2(N_\infty - N) \tag{33b}$$

where N_∞ corresponds to the number of cycles of loading at which the crack becomes infinitely long but for purposes of calculation is taken at fracture. k_1 and k_2 are parameters which depend on the applied stress and material properties.

Equation (33b) indicates that $\ell^{-1/2}$ varies linearly with N. In Fig. 47, a through n, the experimental data are shown on diagrams using $\ell^{-1/2}$ as the ordinate and N as the abscissa. Data for specimens subjected to the same stress range and mean stress are shown on the same diagram. For the range of crack lengths, ℓ, from 0.06-in. to 0.20-in. shown in Fig. 47, the experimental data of this investigation exhibit a linear relation as specified by Eq. (33). Since both Eqs. (17) and (33) agree vèry well with experimental results, it is of interest to compare these two relations. The form of (33a) is similar to Eq. (17) except that $\ell^{3/2}$ appears on the right hand side of Eq. (33a), in place of ℓ on the right hand side of Eq. (17). In Fig. 48 a diagram of $\ell^{3/2}$ versus ℓ is shown for the range of crack lengths, ℓ, from 0.06-in. to 0.20-in. In this range of crack lengths, $\ell^{3/2}$ is almost linearly proportional to ℓ, and Eqs. (17) and (33) predict essentially the same results. As indicated by Fig. 48, the curve of $\ell^{3/2}$ versus ℓ will deviate appreciably from a straight line only if the range of ℓ is extended. Therefore, to experimentally differentiate between Eqs. (17) and (33) it would be necessary to increase the width of the specimen.

Hypothesis Of Paris, Gomez, and Anderson(12)

Paris and others hypothesized that the fatigue crack propagation can be described in terms of elastic stresses at the tip of a crack. Based on the form of expression developed by Irwin,(23) the elastic stresses at the tip of a crack can be expressed in terms of a single elastic parameter K, the stress intensity factor.* K was defined as

$$K = \sigma_o \sqrt{\frac{\ell}{2}} \frac{\sqrt{4 + 2(\frac{\ell}{L})^4}}{2 - (\frac{\ell}{L})^2 - (\frac{\ell}{L})^4} \qquad (34a)$$

where

σ_o = nominal stress

ℓ = crack length

L = specimen width

For the ratio ℓ/L smaller than 0.1, K is approximately equal to

$$K = \sigma_o \sqrt{\frac{\ell}{2}} \qquad (34b)$$

---

* The stress components at a point P, which is defined by a vector $\bar{r}$ from the tip of a crack, are as follows:

$$\sigma_y = \frac{K}{\sqrt{2r}} \cos\frac{\theta}{2}\left[1 + \sin\frac{\theta}{2}\ \sin\frac{3\theta}{2}\right]$$

$$\sigma_x = \frac{K}{\sqrt{2r}} \cos\frac{\theta}{2}\left[1 - \sin\frac{\theta}{2}\ \sin\frac{3\theta}{2}\right]$$

$$\tau_{xy} = \frac{K}{\sqrt{2r}} \cos\frac{\theta}{2}\ \sin\frac{\theta}{2}\ \cos\frac{3\theta}{2}$$

$$\tau_{xz} = \tau_{yz} = 0$$

$$\sigma_z = 0 \qquad \text{for plane stress}$$

$$\sigma_z = \mu(\sigma_x + \sigma_y) \qquad \text{for plane strain}$$

where θ is the angle between the vector $\bar{r}$ and the x-axis, and μ is the Poisson's ratio. The axes are the same as in Fig. 1.

Under repeated loading, the elastic stresses at the tip of the crack can be specified by two quantities, K_{max} and the ratio, K_{min}/K_{max}, where K_{max} and K_{min} are stress intensity factors corresponding to the maximum and the minimum loads. If the maximum and the minimum loads are maintained constant, as in this investigation, the ratio K_{min}/K_{max} remains unchanged and is equal to the ratio between the maximum and the minimum loads. Therefore, the stresses throughout any one experiment can be specified by K_{max} alone, and the rate of crack propagation is a function of K_{max} only.

The logarithm of the rate of crack propagation is plotted against the stress intensity factor, K_{max}, in Fig. 49. Data for specimens subjected to the same stress range and mean stress are plotted on the same diagram. The data cover a range of crack lengths from 0.06 to 0.20, where accurate values of rate of propagation could be obtained. In each diagram, a straight line represents the experimental results very well over this range of crack lengths.

The crucial test of this hypothesis must be based on the coincidence of data for the same values of K_{max} and the ratio K_{min}/K_{max}. Consequently all of the lines from Fig. 49, a through n, are reproduced on one diagram in Fig. 50. The specimen numbers are indicated for each line in the legend along with the values of K_{min}/K_{max}. Since values of the ratio K_{min}/K_{max} are different for each specimen and cover a range of nearly one order of magnitude, a family of non-intersecting curves may be expected. In general the lines in Fig. 50 fit this description. The lines at the top of the group are for large values of K_{min}/K_{max} and similarly the lines at the bottom of the group are for small values of this ratio.

For curves numbered 11 through 14, the values of the ratio, K_{min}/K_{max}, are nearly the same, 0.05 to 0.0715, and it was expected that these lines would form a narrow band somewhat separated from the others. However, the experimental results show that the propagation rates of these four specimens differ by as much as 40 per cent. On the other hand lines numbered 9 and 10, with values of K_{min}/K_{max} of 0.167 and 0.150 respectively, intersect one or more of the lines numbered 11 through 14. Similar comparisons can be made for other lines, and in some cases the differences of crack propagation rates for lines with similar values of K_{min}/K_{max} are close to 50 per cent in the wrong direction.

Since the crack propagation rate, $d\ell/dN$, must be integrated to compute the crack length, ℓ, corresponding to a given number of cycles, N, it may be concluded that the predicted values of N corresponding to a critical value of ℓ will contain errors at least as large as those encountered with the propagation rate. Thus, in its present form, this hypothesis exhibits the proper trends; however the predictions appear to be less accurate than those given by Eq. (17).

Recently, the concepts leading to Eq. (34) have been modified empirically to include the influence of a small zone of plastic deformation at the tip of the crack. This modification may improve the accuracy of this hypothesis, but calculations were not made to investigate this possibility.

VI. CONCLUDING REMARKS

The major results of this investigation may be summarized as follows:

1. An expression of the crack length, ℓ, in a semi-infinite sheet under repeated loading in terms of number of cycles of loading, N, and a stress dependent propagation factor, C, was derived by dimensional analysis. The expression is

$$\frac{d\ell}{dN} = C\ell \qquad (\underline{17a})$$

$$\ln \frac{\ell}{\ell_o} = C\,(N-N_o) \qquad (\underline{17b})$$

In the derivation, no assumptions were made with regard to the mechanism of crack propagation, the stress or strain distribution, or the material properties. Therefore, the expression is general in these three respects.

2. In total, 36 specimens were tested covering various combinations of stress range and mean stress. The experimental results indicated that the propagation life can be divided into three periods: the initial, the middle, and the final. In the initial period, the crack propagated sporadically and slowly. In the middle period, measurements of crack propagation agreed with the prediction of Eq. (17); this period consumed 40 per cent to 50 per cent of the propagation life. In the final period, crack propagation was greatly accelerated due to two effects: an increase in stress range and mean stress as the net section was reduced and a disproportionate increase in the size of the plastic

zone which changed the stress distribution and the mechanism of fracture.

3. The crack propagation relation, Eq. (17) was modified to account for the effect of an increasing stress range and mean stress as the crack propagated in a finite specimen. The propagation life predicted by the modified equation was a constant proportion with the experimental propagation life. The ratios between the experimental and predicted propagation lives had an average value of 0.77 and ranged from 0.69 to 0.84. Therefore, accurate prediction of propagation life appears possible.

4. The propagation factor, C, in Eq. (17) was found to depend on the applied stresses. Arranged in the order of decreasing influence on the propagation factor, C, they are: stress range, maximum stress, mean stress, and minimum stress. However, only two of these four quantities are independent, and any two of these quantities are sufficient to specify completely the propagation factor.

The relationship between propagation factor and the stress range, $\Delta\sigma$, and mean stress, σ_m, was determined experimentally for 2024-T3 aluminum alloy to be

$$\ln C_o = 0.00009298\ \Delta\sigma + 0.00003914\ \sigma_m - 12.61 \qquad (31)$$

5. The scatter of the crack initiation period was found to be more than twice as large as that of propagation periods. This is reasonable in view of the fact that crack initiation is a more localized phenomenon than crack propagation.

6. The photomicrographs indicated that the size of the plastic zone at the tip of the crack increased as crack propagated.

7. Head's equation for crack propagation provided a good description of crack propagation. Although somewhat different in form, it gave results very similar to Eq. (17) for the range of crack lengths covered by this investigation. It would be necessary to increase the width of the specimen to differentiate experimentally between Eq. (17) and Head's equation.

8. The hypothesis used by Paris and others to predict fatigue crack propagation in terms of the elastic stresses at the tip of a crack neglects plastic deformation. In its present form, the hypothesis predicted the general trends observed experimentally. However, the accuracy was not as good as with Eq. (17).

BIBLIOGRAPHY

1. A. Wohler, "Über die Festigkeitsversuche mit Eisen und Stahl," z für Bauwesen, Vol. 8 (1858).

2. J. A. Ewing and J. C. W. Humphrey, "The Fracture of Metals Under Repeated Alternations of Stress," Philosophical Transactions, Roy. Soc., Series A., Vol. 200, p. 291 (1903).

3. R. A. MacGregor, W. S. Burn, and F. Bacon, "The Relation of Fatigue to Modern Engine Design," Transactions, N. E. Coast Instn. Engrs. and Shipbuilders, Vol. 51 (1935).

4. A. V. DeForest, "The Rate of Growth of Fatigue Cracks," Journal of Applied Mechanics, Vol. 3, No. 1, p. A23 (March 1936).

5. J. A. Bennett, "The Distinction Between Initiation and Propagation of a Fatigue Crack," International Conference on Fatigue of Metals, Session 6, Paper 8, 1956.

6. R. R. Shaw, "The Level of Safety Achieved by Periodic Inspection for Fatigue Cracks," Journal, Roy. Aero. Soc., Vol. 58, pp. 720-23 (October 1954).

7. W. Deck, "Crack Detection in Aircraft Structures," Journal, Roy. Aero. Soc., Vol. 60 (November 1956).

8. W. J. Conway, "Crack Propagation Tests Safeguard New Lockheed Structures," Aviation Age, December 1956.

9. N. Thompson, "Experiments Relating to the Basic Mechanism of Fatigue," International Conference on Fatigue of Metals, Session 6, Paper 3, Instn. Mech. Engrs. and Am. Soc. Mech. Engrs., London and New York, 1956.

10. W. J. Love, "Structural Changes in Ingot Iron Caused by Plastic and Repeated Stressing," Technical Report No. 33, Office of Naval Research, Department of Theoretical and Applied Mechanics, University of Illinois, Urbana, 1952.

11. A. K. Head, "The Growth of Fatigue Cracks," The Philosophical Magazine, Series 7, Vol. 44, p. 925 (1953).

12. P. C. Paris, M. P. Gomez, and W. E. Anderson, "A Rational Analytic Theory of Fatigue," report submitted for publication by the Institute of Aeronautical Sciences, 1959.

13. M. S. Hunter and W. G. Fricke Jr., "Effect of Alloy Content on the Metallographic Changes Accompanying Fatigue," Proceedings, Am. Soc. Test. Mats., Vol. 55, p. 942 (1955).

14. M. S. Hunter and W. G. Fricke Jr., "Cracking of Notch Fatigue Specimens," Proceedings, Am. Soc. Test. Mats., Vol. 57, p. 643 (1957).

15. W. Weibull, "The Propagation of Fatigue Cracks in Light-Alloy Plates," Saab Aircraft Co., TN 25, Linkoping, Sweden, 1954.

16. J. A. Bennett, and J. L. Baker, "Effect of Prior Static and Dynamic Stresses on the Fatigue Strength of Aluminum Alloys," Journal of Research, Vol. 45 (1950).

17. W. M. Wilson and J. L. Burke, "Rate of Propagation of Fatigue Cracks in 12 by 3/4 in. Steel Plates with Severe Geometrical Stress Raisers," Welding Research Supplement, p. 405 (August 1948).

18. D. E. Martin and G. M. Sinclair, "Crack Propagation Under Repeated Loading," Proceedings, Third U. S. Congress of Applied Mechanics, June 1958.

19. H. A. Lipsitt, F. W. Forbes, and R. B. Baird, "Anisotropy of Crack Propagation in Cold Rolled Aluminum Sheet," Proceedings, Am. Soc. Test. Mats., 1959.

20. A. J. McEvilly Jr. and W. Illg, "The Rate of Fatigue-Crack Propagation in Two Aluminum Alloys," Natl. Adv. Comm. Aero., TN 4394, September 1958.

21. W. Weibull, "Effect of Crack Length and Stress Amplitude on Growth of Fatigue Cracks," Aeronautical Research Institute of Sweden, Report 65, Stockholm, 1956.

22. N. E. Frost and D. S. Dugdale, "The Propagation of Fatigue Cracks in Sheet Specimens," Journal of the Mechanics and Physics of Solids, Vol. 6, No. 2 (1958).

23. G. R. Irwin, "Fracture Mechanics," Encyclopedia of Physics, Vol. 6, 1958.

24. G. R. Irwin, J. A. Kies, and H. L. Smith, "Fracture Strengths Relative to Onset and Arrest of Crack Propagation," Proceedings, Am. Soc. Test. Mats., 1958.

25. O. L. Bowie, "Analysis of an Infinite Plate Containing Radial Cracks Originating at the Boundary of an Internal Circular Hole," Journal of Mathematics and Physics, Vol. 35 (1956).

26. J. A. Bennett, "A Study of the Damaging Effect of Fatigue Stressing on X4130 Steel," Proceedings, Am. Soc. Test. Mats., 1946.

27. F. R. Shanley, "A Theory of Fatigue Based on Unbonding During Reversed Slip," Rand Corp., 1952, Santa Monica, Calif.

APPENDIX NOTATIONS

a, a_1, a_2	=	Constants
b	=	Side of a square material element
C	=	Crack propagation factor
C_o	=	Crack propagation factor in a semi-infinite sheet
D	=	$0.000123\,\Delta\sigma$
E	=	Tensile modulus of elasticity
$-E_1(-x)$	=	Exponential integral of argument x
f, f_1, f_2	=	Mathematical functions
F, F_1, F_2	=	Mathematical functions
G	=	Shearing modulus of elasticity
$\mathcal{G}_c$	=	Crack Extension Force
H'	=	Slope of an equivalent stress vs. plastic strain diagram
k, k_1, k_2	=	Constants
K	=	Stress intensity factor
K_N	=	Stress concentration factor
ℓ	=	Crack length
ℓ_o	=	Initial crack length
$\Delta\ell$	=	Incremental crack length
ℓ'	=	$\ell + \Delta\ell$
L	=	Width of specimen
N	=	Number of cycles of load
N_o	=	Number of cycles of load corresponding to ℓ_o
ΔN	=	Incremental number of cycles of load corresponding to $\Delta\ell$
N_{fe}	=	Experimental fatigue life

N_{ft} = Predicted fatigue life by Eq. (28)

N'_{ft} = Predicted fatigue life by Eq. (32)

t = Thickness of the specimen

$u_\theta(x,y)$ = Displacement at point P(x,y) in the direction of θ

z = $\dfrac{L - \ell}{L - \ell_o}$

ϵ'_{ij} = Deviatoric strain tensor

ϵ_{ii} = $\epsilon_{11} + \epsilon_{22} + \epsilon_{33}$

θ = Angle

μ = Poisson's ratio

ρ = $\dfrac{D}{1 - \frac{\ell}{L}}$

φ = $12.61 - 0.00009298\ \Delta\sigma_o - 0.00003914\ \sigma_{mo}$

σ = Unit stress

$\sigma_\theta(x,y)$ = Stress at point P(x,y) in the direction of θ

$\Delta\sigma$ = Stress range

σ_m = Mean stress

σ_n = Nominal stress across the net cross sectional area

σ_o = Initial nominal stress

σ_t = Stress at the tip of the crack

σ'_{ij} = Deviatoric stress tensor

σ_{ii} = $\sigma_{11} + \sigma_{22} + \sigma_{33}$

$\bar{\sigma}$ = Equivalent stress

σ_e = Endurance limit

TABLE 1 FATIGUE CRACK PROPAGATION DATA FOR 2024-T3 ALUMINUM ALLOY

Spec. No. 4002a $\Delta\sigma$ = 38,000 psi σ_m = 21,000 psi		Spec. No. 4002b $\Delta\sigma$ = 38,000 psi σ_m = 21,000 psi		Spec. No. 4002c $\Delta\sigma$ = 38,000 psi σ_m = 21,000 psi		Spec. No. 4002c continued		Spec. No. 4006a $\Delta\sigma$ = 34,000 psi σ_m = 23,000 psi	
N cycles	ℓ inches	N cycles	ℓ inches	N cycles	ℓ inches	N cycles	ℓ inches	N cycles	ℓ inches
15350	0.084	11780	0.037	11210	0.0424	17510	rupt.	13460	0.047
15550	0.093	11980	0.037	11410	0.0514			13760	0.045
15750	0.099	12180	0.037	11610	0.0519			14060	0.052
15950	0.101	12380	0.057	11810	0.0527			14360	0.050
16150	0.110	12580	0.077	12010	0.0553			14660	0.052
16350	0.125	12780	0.082	12410	0.0627			14960	0.055
16550	0.128	12980	0.090	12610	0.0668			15260	0.054
16750	0.132	13180	0.077	12810	0.0685			15560	
16950	0.142	13380	0.092	13010	0.0705			15860	0.056
17150	0.151	13580	0.099	13210	0.0739			16160	0.059
17350	0.159	13780	0.101	13410	0.0797			16460	
17550	0.170	13980	0.104	13610	0.0841			16760	0.071
17750	0.181	14180	0.111	13810	0.0851			17060	0.074
17950	0.196	14380	0.118	14010	0.0936			17360	0.082
18150	0.207	14580	0.128	14210	0.0980			17660	0.084
18350	0.227	14780	0.134	14410	0.102			17960	0.088
18550	0.254	14980	0.144	14610	0.108			18260	0.097
18750	0.269	15180	0.150	14810	0.111			18560	0.106
18950	0.325	15380	0.160	15010	0.118			18860	0.110
19150	0.403	15580	0.172	15210	0.125			19160	0.120
19350	0.779	15780	0.179	15410	0.134			19460	0.127
19450	rupt.	15980	0.192	15610	0.141			19760	0.140
		16180	0.212	15810	0.151			20060	0.152
		16380	0.234	16010	0.164			20360	0.166
		16580	0.273	16210	0.176			20660	0.186
		16780	0.333	16410	0.192			20960	0.210
		16980	0.477	16610	0.219			21260	0.243
		17080	0.647	16810	0.249			21500	0.297
		17180	rupt.	17010	0.296			21860	0.394
				17210	0.403			22160	0.718
				17410	0.750			22260	rupt.

TABLE 1 (Continued)

Spec. No. 4006b $\Delta\sigma$ = 34,000 psi σ_m = 23,000 psi		Spec. No. 4006c $\Delta\sigma$ = 34,000 psi σ_m = 23,000 psi		Spec. No. 4006c continued		Spec. No. 4010a $\Delta\sigma$ = 30,000 psi σ_m = 25,000 psi		Spec. No. 4010a continued	
N cycles	ℓ inches	N cycles	ℓ inches	N cycles	ℓ inches	N cycles	ℓ inches	N cycles	ℓ inches
13690	0.043	11840	0.041	21140	0.707	21810	0.054	31110	0.455
13990	0.048	12140	0.042	21240	rupt.	22110	0.063	31410	0.660
14290	0.049	12440	0.046			22410	0.069	31630	rupt.
14590	0.051	12740	0.045			22710	0.071		
14890	0.056	13040	0.048			23010	0.076		
15190	0.057	13340	0.050			23310	0.081		
15490	0.058	13640	0.053			23610	0.084		
15790	0.059	13940	0.054			23910	0.086		
16090	0.064	14240	0.058			24210	0.087		
16390	0.067	14540	0.062			24510	0.094		
16690	0.070	14840	0.066			24810	0.101		
16990	0.073	15140	0.068			25110	0.104		
17290	0.076	15440	0.073			25410	0.109		
17590	0.083	15740	0.076			25710	0.114		
17890	0.086	16040	0.078			26010	0.118		
18190	0.094	16340	0.083			26310	0.123		
18490	0.100	16640	0.091			26610	0.129		
18790	0.105	16940	0.097			26910	0.136		
19090	0.111	17240	0.103			27210	0.143		
19390	0.116	17540	0.114			27510	0.149		
19690	0.128	17840	0.118			27810	0.160		
19990	0.137	18140	0.125			28110	0.165		
20290	0.143	18440	0.131			28410	0.176		
20590	0.157	18740	0.144			28710	0.193		
20890	0.171	19040	0.157			29010	0.206		
21190	0.187	19340	0.172			29310	0.220		
23050	rupt.	19640	0.193			29610	0.238		
		19940	0.217			29910	0.259		
		20240	0.252			30210	0.287		
		20540	0.309			30510	0.321		
		20840	0.402			30810	0.371		

TABLE 1 (Continued)

Spec. No. 4010b		Spec. No. 4014a		Spec. No. 4014b		Spec. No. 4014c		Spec. No. 4014d	
$\Delta\sigma$ = 30,000 psi		$\Delta\sigma$ = 26,000 psi		$\Delta\sigma$ = 26,000 psi		$\Delta\sigma$ = 26,000 psi		$\Delta\sigma$ = 26,000 psi	
σ_m = 25,000 psi		σ_m = 27,000 psi		σ_m = 27,000 psi		σ_m = 27,000 psi		σ_m = 27,000 psi	
N cycles	ℓ inches	N cycles	ℓ inches	N cycles	ℓ inches	N cycles	ℓ inches	N cycles	ℓ inches
24380	0.069	33830	0.073	30190	0.048	22390	0.054	31380	0.047
24680	0.073	34430	0.073	30790	0.051	22990	0.058	31980	0.049
24980	0.076	35030	0.076	31390	0.051	23590	0.069	32580	0.054
25280	0.080	35630	0.080	31990	0.056	24190	0.076	33180	0.057
25580	0.082	36230	0.082	32590	0.058	24790	0.081	33780	0.059
25880	0.085	36830	0.086	33190	0.064	25390	0.085	34380	0.063
26180	0.087	37430	0.093	33790	0.070	25990	0.093	34980	0.065
26480	0.093	38030	0.100	34390	0.078	26590	0.101	35580	0.070
26780	0.095	38630	0.107	34990	0.080	27190	0.105	36180	0.079
27080	0.100	39230	0.114	35590	0.086	27790	0.114	36780	0.085
27380	0.104	39830	0.120	36190	0.094	28390	0.124	37380	0.091
27680	0.109	40430	0.131	36790	0.099	28990	0.139	37980	0.100
27980	0.114	41030	0.141	37390	0.103	29590	0.151	38580	0.105
28280	0.122	41630	0.153	37990	0.114	30190	0.156	39180	0.114
28580	0.128	42230	0.167	38590	0.119	30790	0.174	39780	0.121
28880	0.131	42530	0.168	39190	0.125	31390	0.187	40380	0.131
29180	0.140	42830	0.179	39790	0.138	31990	0.204	40980	0.139
29480	0.147	43130	0.184	40390	0.142	32590	0.233	41580	0.156
29780	0.155	43430	0.197	40990	0.151	33190	0.262	42180	0.171
30080	0.165	44030	0.218	41590	0.163	33790	0.315	42780	0.190
30380	0.176	44630	0.235	42190	0.177	34390	0.399	43380	0.205
30680	0.190	45230	0.274	42790	0.198	34990	0.611	43980	0.227
30980	0.205	45830	0.313	43390	0.213	35290	rupt.	44580	0.254
31280	0.216	46430	0.386	43990	0.236			45180	0.287
31580	0.237	47030	0.494	44590	0.260			45780	0.328
31880	0.259	47630	0.605	45190	0.295			46380	0.383
32180	0.293	47730	rupt.	45790	0.334			46980	0.498
32480	0.339			46390	0.395			47670	rupt.
32780	0.402			46990	0.555				
33080	0.526			47590	0.698				
33440	rupt.			47870	rupt.				

TABLE 1 (Continued)

Spec. No. 4018a $\Delta\sigma$ = 22,000 psi σ_m = 29,000 psi		Spec. No. 4018a continued		Spec. No. 4018b $\Delta\sigma$ = 22,000 psi σ_m = 29,000 psi		Spec. No. 3602a $\Delta\sigma$ = 34,000 psi σ_m = 19,000 psi		Spec. No. 3602b $\Delta\sigma$ = 34,000 psi σ_m = 19,000 psi	
N cycles	ℓ inches	N cycles	ℓ inches	N cycles	ℓ inches	N cycles	ℓ inches	N cycles	ℓ inches
41600	0.063	60200	0.501	43550	0.044	23400	0.049	22430	0.049
42200	0.064	60800	0.628	44450	0.046	24000	0.048	22730	0.049
42800	0.069	61400	1.082	45350	0.049	24600	0.048	23030	0.049
43400	0.074	61500	rupt.	46250	0.051	25200	0.053	23330	0.053
44000	0.077			47150	0.055	25500	0.062	23630	0.055
44600	0.084			48050	0.058	25800	0.062	23930	0.057
45200	0.088			48950	0.061	26100	0.064	24230	0.073
45800	0.090			49850	0.063	26400	0.064	24530	0.077
46400	0.095			50750	0.068	26700	0.072	25730	0.090
47000	0.100			51650	0.071	27000	0.074	26030	0.098
47600	0.103			52550	0.079	27300	0.072	26330	0.101
48200	0.108			53450	0.083	27600	0.077	26630	0.103
48800	0.115			54350	0.092	28200	0.079	26930	0.112
49400	0.119			55250	0.096	28800	0.087	27230	0.113
50000	0.127			56150	0.105	29400	0.097	27530	0.125
50600	0.134			57050	0.112	30000	0.105	27830	0.134
51200	0.144			57950	0.119	30600	0.118	28130	0.138
51800	0.151			58850	0.131	31200	0.129	28430	0.141
52400	0.164			59750	0.141	31800	0.141	28730	0.146
53000	0.170			60650	0.154	32400	0.157	29030	0.158
53600	0.176			61550	0.163	33000	0.178	29630	0.175
54200	0.190			62450	0.175	33600	0.197	30230	0.197
54800	0.204			63350	0.193	34200	0.219	30530	0.207
55400	0.217			64250	0.213	34800	0.253	30830	0.226
56000	0.235			65150	0.235	35100	0.264	31130	0.247
56600	0.256			66050	0.267	35400	0.289	31430	0.270
57200	0.274			66950	0.301	35700	0.322	33150	rupt.
57800	0.298			67850	0.358	36000	0.360		
58400	0.327			68750	0.428	36300	0.415		
59000	0.372			69650	0.533	36600	0.523		
59600	0.431			70740	rupt.	36980	rupt.		

TABLE 1 (Continued)

Spec. No. 3606a $\Delta\sigma$ = 30,000 psi σ_m = 21,000 psi		Spec. No. 3606b $\Delta\sigma$ = 30,000 psi σ_m = 21,000 psi		Spec. No. 3606b continued		Spec. No. 3606c $\Delta\sigma$ = 30,000 psi σ_m = 21,000 psi		Spec. No. 3606c continued	
N cycles	ℓ inches	N cycles	ℓ inches	N cycles	ℓ inches	N cycles	ℓ inches	N cycles	ℓ inches
26420	0.054	34680	0.092	43980	0.631	26390	0.057	38790	0.440
27020	0.054	34980	0.096	44280	1.692	26790	0.060		no
27620	0.059	35280	0.102	44330	rupt.	27190	0.061		rupt.
28220	0.059	35580	0.105			27590	0.064		
28820	0.064	35880	0.108			27990	0.064		
29420	0.066	36180	0.109			28390	0.068		
30020	0.071	36480	0.118			28790	0.071		
30620	0.072	36780	0.117			29190	0.074		
31220	0.078	37080	0.119			29590	0.077		
31820	0.084	37380	0.124			29990	0.084		
32420	0.095	37680	0.129			30390	0.085		
33020	0.100	37980	0.136			30790	0.091		
33620	0.108	38280	0.141			31190	0.097		
34220	0.116	38580	0.147			31590	0.102		
34820	0.128	38880	0.150			31990	0.106		
35430	0.138	39180	0.160			32390	0.111		
36020	0.153	39480	0.168			32790	0.118		
36620	0.163	39780	0.177			33190	0.124		
37220	0.188	40080	0.181			33590	0.131		
37820	0.203	40380	0.191			33990	0.136		
38420	0.232	40680	0.203			34390	0.144		
39020	0.271	40980	0.212			34790	0.151		
39620	0.338	41280	0.227			35190	0.164		
40220	0.465	41580	0.241			35590	0.176		
40900	rupt.	41880	0.254			35990	0.187		
		42180	0.280			36390	0.202		
		42480	0.302			36790	0.220		
		42780	0.325			37190	0.242		
		43080	0.354			37590	0.270		
		43380	0.402			37990	0.305		
		43680	0.479			38390	0.361		

TABLE 1 (Continued)

Spec. No. 3610a $\Delta\sigma$ = 26,000 psi σ_m = 23,000 psi		Spec. No. 3610b $\Delta\sigma$ = 26,000 psi σ_m = 23,000 psi		Spec. No. 3614a $\Delta\sigma$ = 22,000 psi σ_m = 25,000 psi		Spec. No. 3614a continued		Spec. No. 3614b $\Delta\sigma$ = 22,000 psi σ_m = 25,000 psi	
N cycles	ℓ inches	N cycles	ℓ inches	N cycles	ℓ inches	N cycles	ℓ inches	N cycles	ℓ inches
40940	0.063	29270	0.059	76910	0.046	104810	0.437	50020	0.047
41540	0.068	29870	0.063	77810	0.051	105710	0.530	51220	0.051
42140	0.067	30470	0.065	78710	0.053	106610	0.718	52420	0.056
42740	0.077	31070	0.066	79610	0.055	107360	rupt.	53620	0.060
43340	0.073	31670	0.070	80510	0.056			54820	0.061
43940	0.072	32270	0.071	81410	0.064			56020	0.062
44540	0.081	32870	0.077	82310	0.065			57220	0.070
45140	0.092	33470	0.083	83210	0.066			58420	0.072
45740	0.094	34070	0.089	84110	0.069			59620	0.078
46340	0.097	34670	0.095	85010	0.074			60820	0.084
46940	0.103	35270	0.101	85910	0.080			62020	0.090
47540	0.111	35870	0.108	86810	0.085			63220	0.098
48140	0.123	36470	0.113	87710	0.091			64420	0.107
48440	0.131	37070	0.120	88610	0.096			65620	0.117
48740	0.143	37670	0.133	89510	0.102			66820	0.130
49040	0.140	38270	0.143	90410	0.111			68020	0.147
49340	0.147	38870	0.150	91310	0.119			69220	0.160
49940	0.156	39470	0.160	92210	0.129			70420	0.175
50540	0.172	40070	0.173	93110	0.133			71620	0.188
51140	0.179	40670	0.188	94010	0.143			72820	0.209
51740	0.192	41270	0.206	94910	0.155			74020	0.230
52340	0.206	41870	0.229	95810	0.165			75220	0.255
52940	0.223	42470	0.253	96710	0.179			76420	0.283
53540	0.244	43070	0.289	97610	0.192			77620	0.320
54140	0.265	43670	0.333	98510	0.210			78820	0.367
54740	0.282	44270	0.406	99410	0.227			80020	0.439
55340	0.323	44870	0.530	100310	0.246			81220	0.560
55940	0.369	45470	0.910	101210	0.270			82420	0.944
56540	0.438	45630	rupt.	102110	0.297			82590	rupt.
57140	0.569			103010	0.327				
57830	rupt.			103910	0.374				

TABLE 1 (Continued)

Spec. No. 3202a $\Delta\sigma$ = 30,000 psi σ_m = 17,000 psi		Spec. No. 3202b $\Delta\sigma$ = 30,000 psi σ_m = 17,000 psi		Spec. No. 3202c $\Delta\sigma$ = 30,000 psi σ_m = 17,000 psi		Spec. No. 3206a $\Delta\sigma$ = 26,000 psi σ_m = 19,000 psi		Spec. No. 3206a continued	
N cycles	ℓ inches	N cycles	ℓ inches	N cycles	ℓ inches	N cycles	ℓ inches	N cycles	ℓ inches
29530	0.061	33970	0.052	39770	0.050	41010	0.058	58410	0.230
30130	0.060	34570	0.054	40370	0.054	41610	0.059	59010	0.249
30730	0.061	35170	0.055	40970	0.059	42210	0.061	59610	0.269
31330	0.065	35770	0.058	41570	0.063	42810	0.063	60210	0.298
31930	0.069	36370	0.064	42170	0.072	43410	0.066	60810	0.324
32530	0.074	36970	0.065	42770	0.078	44010	0.067	61410	0.369
33130	0.078	37570	0.071	43370	0.082	44610	0.069	62010	0.419
33730	0.085	38170	0.076	43970	0.088	45210	0.071	62610	0.555
34330	0.085	38770	0.083	44570	0.093	45810	0.076	63210	0.635
34930	0.093	39370	0.087	45170	0.100	46410	0.079	63810	0.776
35530	0.100	39970	0.093	45770	0.107	47010	0.082	63910	rupt.
36130	0.105	40570	0.100	46370	0.113	47610	0.087		
36730	0.111	41170	0.106	46970	0.120	48210	0.088		
37330	0.118	41770	0.115	47570	0.127	48810	0.096		
37930	0.125	42370	0.120	48170	0.135	49410	0.101		
38530	0.139	42970	0.126	48770	0.145	50010	0.106		
39130	0.147	43570	0.136	49370	0.154	50610	0.111		
39730	0.154	44170	0.148	49970	0.166	51210	0.114		
40330	0.165	44770	0.153	50570	0.178	51810	0.124		
40930	0.177	45370	0.166	51170	0.193	52410	0.133		
41530	0.195	45970	0.176	51770	0.209	53010	0.139		
42130	0.214	46570	0.190	52370	0.226	53610	0.145		
42730	0.237	47170	0.203	52970	0.254	54210	0.150		
43330	0.263	47770	0.218	53570	0.288	54510	0.156		
43930	0.299	48370	0.237	54170	0.320	54810	0.159		
44530	0.345	48970	0.262	54770	0.379	55110	0.161		
45130	0.439	49570	0.290	55370	0.469	55410	0.167		
45730	0.682	50170	0.339	55970	0.690	56010	0.175		
46030	rupt.	50770	0.415	56350	rupt.	56610	0.186		
		51370	0.538			57210	0.206		
		52100	rupt.			57810	0.214		

TABLE 1 (Continued)

Spec. No. 3206b $\Delta\sigma$ = 26,000 psi σ_m = 19,000 psi		Spec. No. 3206c $\Delta\sigma$ = 26,000 psi σ_m = 19,000 psi		Spec. No. 3210a $\Delta\sigma$ = 22,000 psi σ_m = 21,000 psi		Spec. No. 3210b $\Delta\sigma$ = 22,000 psi σ_m = 21,000 psi		Spec. No. 2802a $\Delta\sigma$ = 26,000 psi σ_m = 15,000 psi	
N cycles	ℓ inches	N cycles	ℓ inches	N cycles	ℓ inches	N cycles	ℓ inches	N cycles	ℓ inches
41950	0.048	49190	0.065	72230	0.063	64610	0.042	73770	0.070
42850	0.052	50090	0.068	73730	0.058	66110	0.050	74670	0.074
43750	0.051	50990	0.072	75230	0.059	67610	0.056	75570	0.078
44650	0.057	51890	0.076	76730	0.063	69110	0.059	76470	0.084
45550	0.061	52790	0.083	78230	0.065	72110	0.062	77370	0.088
46450	0.063	53690	0.088	79730	0.071	73610	0.065	78270	0.091
47350	0.069	54590	0.093	81230	0.068	75110	0.064	79170	0.101
48250	0.075	55490	0.103	82730	0.073	76610	0.071	80070	0.105
49150	0.082	56390	0.110	84230	0.074	78110	0.074	80970	0.112
49750	0.086	57290	0.117	85730	0.079	79610	0.079	81870	0.116
50050	0.092	58190	0.127	87230	0.082	81110	0.088	82770	0.126
50350	0.095	59090	0.133	88730	0.089	82610	0.097	83670	0.132
50950	0.102	60890	0.153	90230	0.101	84110	0.107	84570	0.141
51850	0.113	61790	0.169	91730	0.114	85610	0.117	85420	0.149
52750	0.120	62690	0.181	93230	0.123	87110	0.130	86370	0.154
53650	0.134	63590	0.197	94730	0.138	88610	0.140	87270	0.166
54550	0.146	64490	0.220	96230	0.154	90110	0.155	88170	0.175
55450	0.160	65390	0.244	97730	0.170	91610	0.171	89070	0.186
56350	0.179	66290	0.274	99230	0.192	93110	0.190	89970	0.197
57250	0.194	67190	0.308	100730	0.217	94610	0.214	90870	0.215
58150	0.218	68090	0.356	102230	0.238	96110	0.241	91770	0.226
59050	0.246	68990	0.436	103730	0.289	97610	0.277	92670	0.245
59950	0.283	69890	0.575	105230	0.339	99110	0.329	93570	0.268
60850	0.328		no	106730	0.424	100610	0.410	99470	0.289
61750	0.393		rupt.	108230	0.563	102110	0.546	95370	0.317
62650	0.504			109920	rupt.	103610	0.965	96270	0.346
63550	0.799					103880	rupt.	97170	0.384
63850	rupt.							98070	0.445
								98970	0.521
								99870	0.684
								100880	rupt.

TABLE 1 (Continued)

Spec. No. 2802b $\Delta\sigma$ = 26,000 psi σ_m = 15,000 psi		Spec. No. 2802b continued		Spec. No. 2806a $\Delta\sigma$ = 22,000 psi σ_m = 17,000 psi		Spec. No. 2802c $\Delta\sigma$ = 26,000 psi σ_m = 15,000 psi		Spec. No. 2806b $\Delta\sigma$ = 22,000 psi σ_m = 17,000 psi	
N cycles	ℓ inches	N cycles	ℓ inches	N cycles	ℓ inches	N cycles	ℓ inches	N cycles	ℓ inches
53680	0.080	71080	0.350	116400	0.074	88990	0.052	162020	0.042
54280	0.080	71680	0.378	117600	0.077	90490	0.054	164420	0.046
54880	0.085	72280	0.415	118800	0.080	91990	0.054	166820	0.048
55480	0.088	72880	0.463	120000	0.082	93490	0.056	169220	0.048
56080	0.094	73480	0.545	121200	0.082	94990	0.058	171620	0.048
56680	0.097	74080	0.673	122400	0.086	96490	0.061	174020	0.050
57280	0.103	74680	0.901	123600	0.094	97990	0.064	176420	0.053
57880	0.107	75280	rupt.	124800	0.100	99490	0.065	178820	0.056
58480	0.105			126000	0.107	100990	0.069	181220	0.060
59080	0.112			127200	0.111	102490	0.071	183620	0.063
59380	0.115			128400	0.119	103990	0.074	186020	0.067
59680	0.119			129600	0.124	105490	0.076	188420	0.069
59980	0.121			130800	0.131	106990	0.078	190820	0.071
60280	0.122			132000	0.141	108490	0.083	193220	0.075
60880	0.130			133200	0.151	109990	0.085	195620	0.082
61480	0.138			134400	0.158	111490	0.101	198020	0.087
62080	0.143			135600	0.173	112990	0.107	200420	0.093
62680	0.148			136800	0.188	114490	0.115	202820	0.097
63280	0.159			138000	0.206	115990	0.124	205220	0.102
63880	0.167			139200	0.221	117490	0.140	207620	0.108
64480	0.173			140400	0.242	118990	0.149	210020	0.127
65080	0.181			141600	0.263	120490	0.163	212420	0.140
65680	0.200			142800	0.289	121990	0.185	214820	0.161
66280	0.209			144000	0.318	123490	0.205	217220	0.187
66880	0.220			145200	0.356	124990	0.237	219620	0.220
67480	0.232			146400	0.401	126490	0.277	222020	0.256
68080	0.241			147600	0.470	127990	0.327	224420	0.311
68680	0.260			148800	0.561	129490	0.408	226820	0.386
69280	0.271			150000	0.726	130990	0.555	229220	0.540
69880	0.291			151290	rupt.	132490	1.084	231620	1.082
70480	0.318						no rupt.	231910	rupt.

TABLE 2a ANALYSES OF FATIGUE CRACK PROPAGATION DATA FOR 2024-T3 ALUMINUM ALLOY*

Specimen Number	$\Delta\sigma$ psi	σ_m psi	Propagation Factor C	C_{ave}	C_o	$C_{o(ave)}$
4002a	38,000	21,000	.000313	.000289	.000285	.000264
4002b	38,000	21,000	.000305		.000278	
4002c	38,000	21,000	.000250		.000230	
4006a	34,000	23,000	.000221	.000203	.000208	.000191
4006b	34,000	23,000	.000191		.000180	
4006c	34,000	23,000	.000197		.000185	
4010a	30,000	25,000	.000151	.000149	.000147	.000143
4010b	30,000	25,000	.000147		.000138	
4014a	26,000	27,000	.000129	.000120	.000120	.000111
4014b	26,000	27,000	.000108		.0000988	
4014c	26,000	27,000	.000124		.000116	
4014d	26,000	27,000	.000120		.000110	
4018a	22,000	29,000	.0000899	.0000860	.0000855	.0000815
4018b	22,000	29,000	.0000820		.0000774	
3602a	34,000	19,000	.000167	.000167	.000151	.000154
3602b	34,000	19,000	.000166		.000157	
3606a	30,000	21,000	.000138	.000133	.000127	.000123
3606b	30,000	21,000	.000135		.000125	
3606c	30,000	21,000	.000125		.000118	
3610a	26,000	23,000	.000124	.000118	.000114	.000109
3610b	26,000	23,000	.000112		.000104	
3614a	22,000	25,000	.0000754	.0000776	.0000720	.000737
3614b	22,000	25,000	.0000798		.0000754	
3202a	30,000	17,000	.000102	.000105	.0000969	.0000995
3202b	30,000	17,000	.000108		.0001036	
3202c	30,000	17,000	.000104		.0000979	

* Terms used in Table 2a are defined in Appendix.

TABLE 2a (Continued)

Specimen Number	$\Delta\sigma$ psi	σ_m psi	Propagation Factor C	C_{ave}	C_o	$C_{o(ave)}$
3206a	26,000	19,000	.0000857	.0000898	.0000784	.0000829
3206b	26,000	19,000	.0001046		.0000968	
3206c	26,000	19,000	.0000792		.0000736	
3210a	22,000	21,000	.0000702	.0000666	.000067	.0000634
3210b	22,000	21,000	.0000630		.0000597	
2802a	26,000	15,000	.0000631	.0000725	.0000586	.0000672
2802b	26,000	15,000	.0000818		.0000757	
2806a	22,000	17,000	.0000512	.0000512	.0000486	.0000486

TABLE 2b ANALYSIS OF FATIGUE CRACK PROPAGATION DATA FOR 2024-T3 ALUMINUM ALLOY*

Specimen Number	N_o cycles	N_{fe} cycles	$(N_{fe}-N_o)$ cycles	N_{ft} cycles	$(N_{ft}-N_o)$ cycles	$\frac{N_{fe}-N_o}{N_{ft}-N_o}$	ℓ_o inches
4002a	12,310	19,450	7,140	21,200	8,890	0.803	0.309
4002b	10,170	17,180	7,010	19,300	9,130	0.768	0.279
4002c	9,890	17,510	7,620	20,920	11,030	0.691	0.221
4006a	13,390	22,260	8,870	26,040	12,650	0.701	0.237
4006b	12,790	23,050	10,260	27,390	14,600	0.703	0.236
4006c	11,440	21,240	9,800	25,650	14,210	0.690	0.231
4010a	17,760	31,630	13,870	36,340	18,580	0.747	0.278
4010b	19,400	33,440	14,040	39,090	19,690	0.713	0.260
4014a	29,610	47,730	18,120	53,070	23,460	0.772	0.344
4014b	26,560	47,870	21,310	55,060	28,500	0.748	0.326
4014c	17,610	35,290	17,680	41,910	24,300	0.728	0.305
4014d	28,930	47,670	18,740	54,430	25,500	0.735	0.311
4018a	34,800	61,500	26,700	69,450	34,650	0.771	0.366
4018b	41,850	70,740	28,890	80,120	38,270	0.755	0.352
3602a	22,760	36,980	14,220	40,190	17,430	0.816	0.341
3602b	19,600	33,150	13,550	36,370	16,770	0.808	0.314
3606a	24,700	40,900	16,200	46,210	21,510	0.753	0.288
3606b	27,500	44,330	16,830	49,240	21,740	0.774	0.346
3606c	22,600			45,660	23,060		
3610a	37,390	57,830	20.440	62,090	24,700	0.827	0.418
3610b	25,370	45,630	20,260	52,470	27,100	0.748	0.322
3614a	74,300	107,360	33,060	115,470	41,170	0.803	0.398
3614b	49,450	82,590	33,140	88,760	39,310	0.843	0.470
3202a	24,700	46,030	21,330	52,820	28,120	0.759	0.301
3202b	30,400	52,100	21,700	56,700	26,300	0.825	0.347
3202c	34,520	56,350	21,830	62,330	27,810	0.785	0.316

* Terms used in Table 2b are defined in Appendix.

TABLE 2b (Continued)

Specimen Number	N_o cycles	N_{fe} cycles	$(N_{fe}-N_o)$ cycles	N_{ft} cycles	$(N_{ft}-N_o)$ cycles	$\frac{N_{fe}-N_o}{N_{ft}-N_o}$	ℓ_o inches
3206a	36,300	63,910	27,610	72,190	35,890	0.769	0.349
3206b	40,400	63,850	23,450	69,470	29,070	0.807	0.386
3206c	79,570			79,570	38,250		
3210a	74,150	109,920	35,770	118,625	44,475	0.804	0.409
3210b	65,500	103,880	38,380	115,148	49,648	0.773	0.377
2802a	61,750	100,880	39,130	109,770	48,020	0.815	0.388
2802b	44,140	75,280	31,140	81,310	37,170	0.838	0.420
2806a	103,550	151,290	47,740	164,470	60,920	0.784	0.381

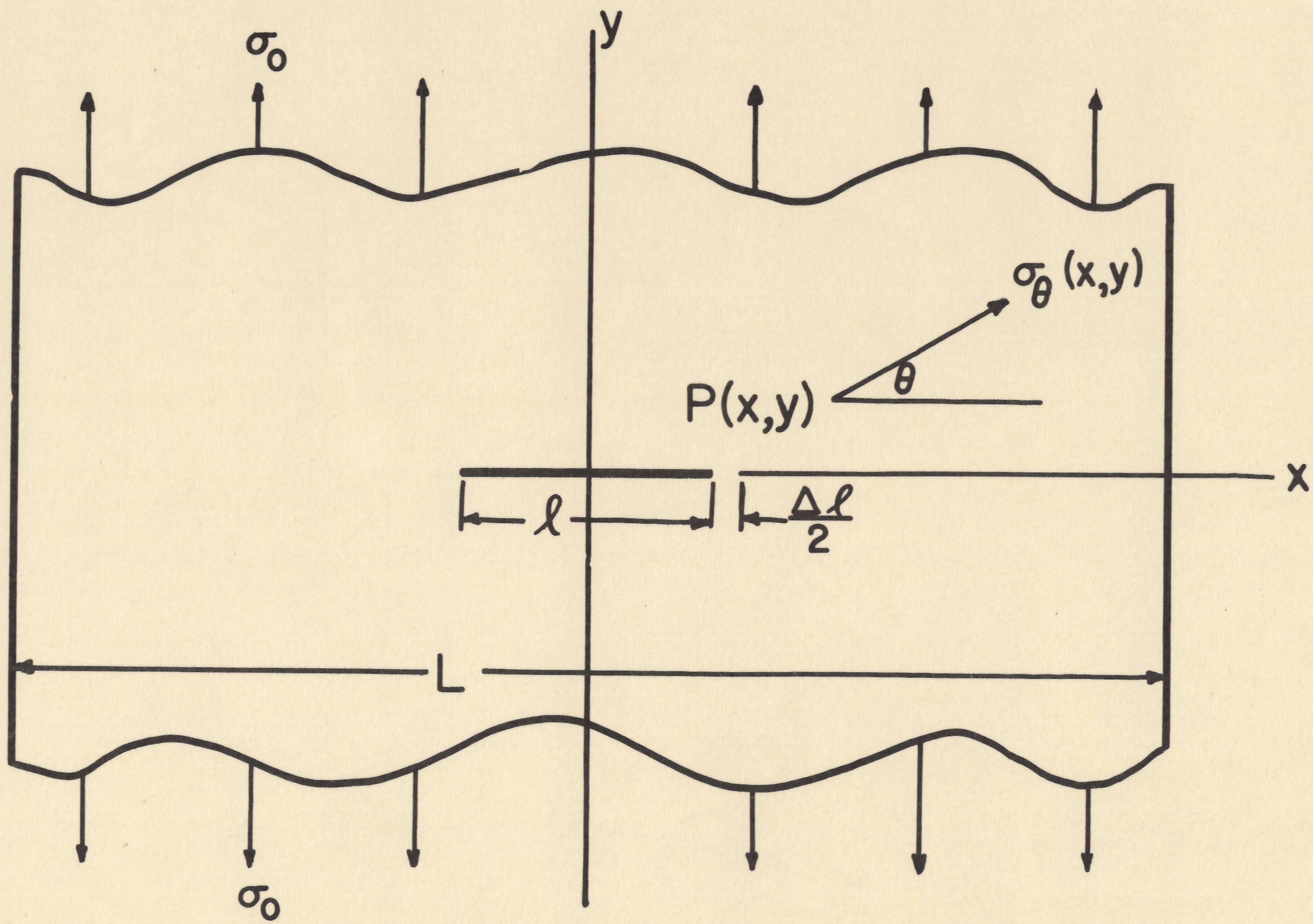

Fig. I Schematic Diagram of a Section of an Axially Loaded Sheet Specimen with a Central Crack

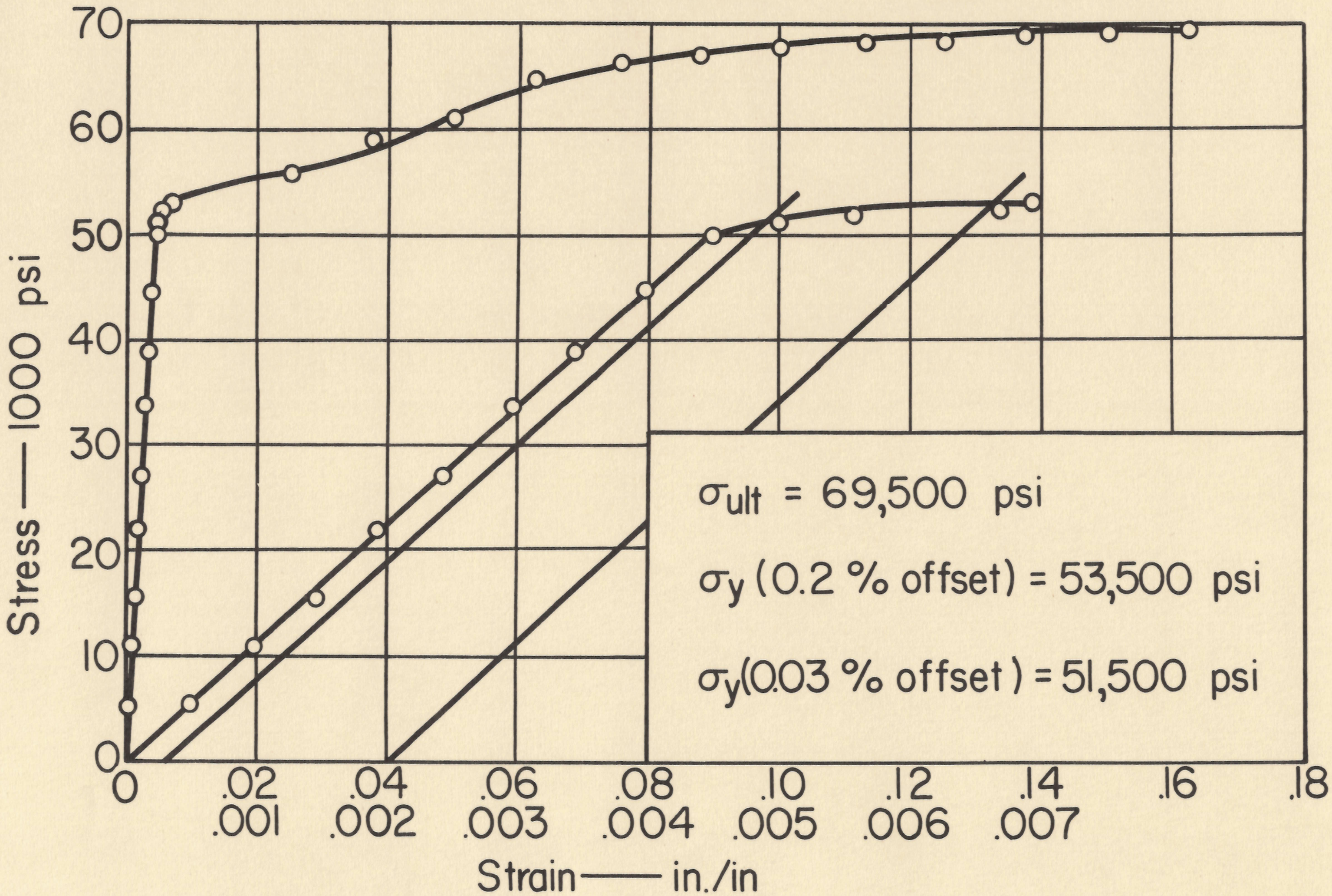

Fig. 2 Stress—Strain Diagram for 2024-T3 Aluminum Alloy

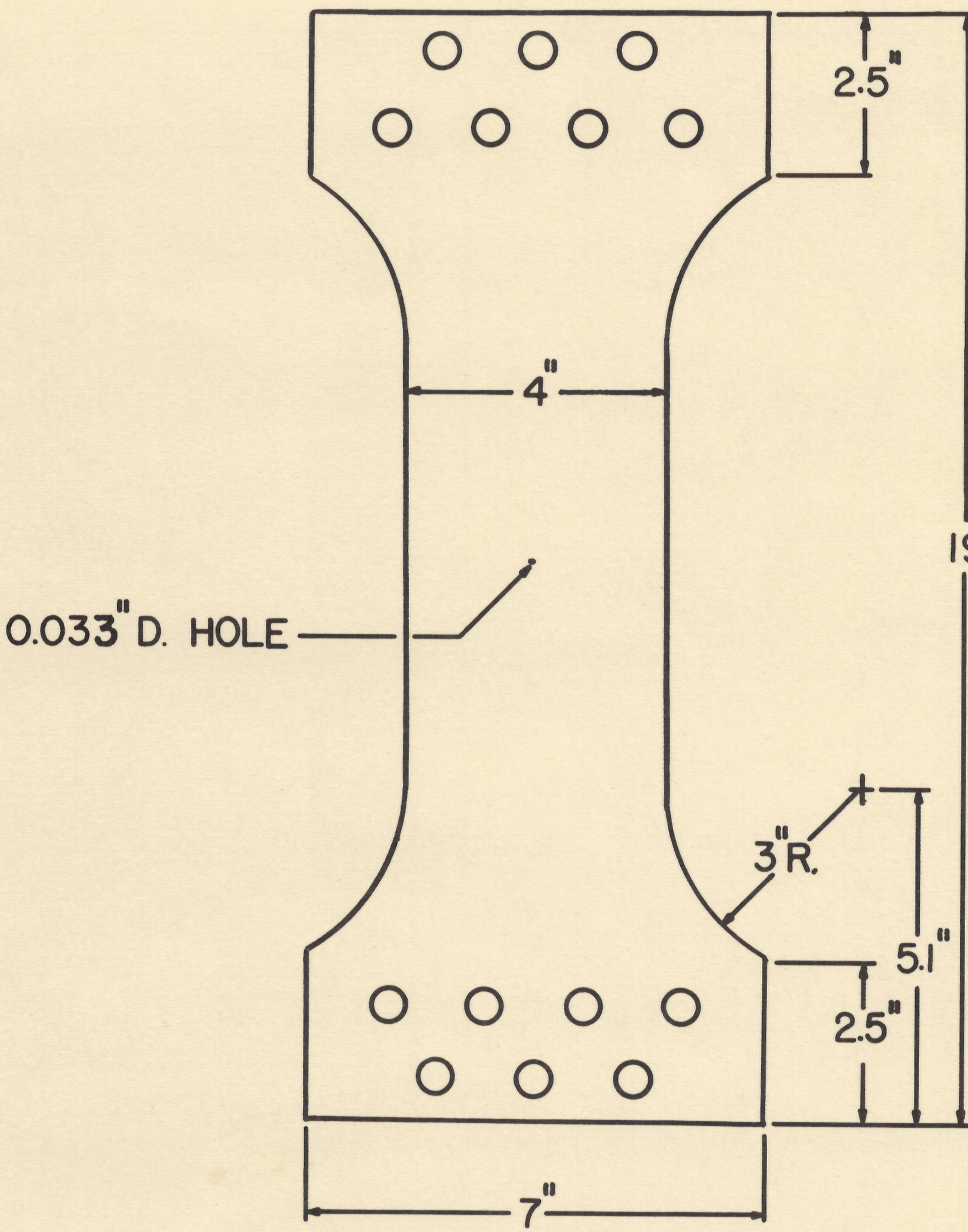

Fig. 3 Critical Dimensions of Fatigue Specimen

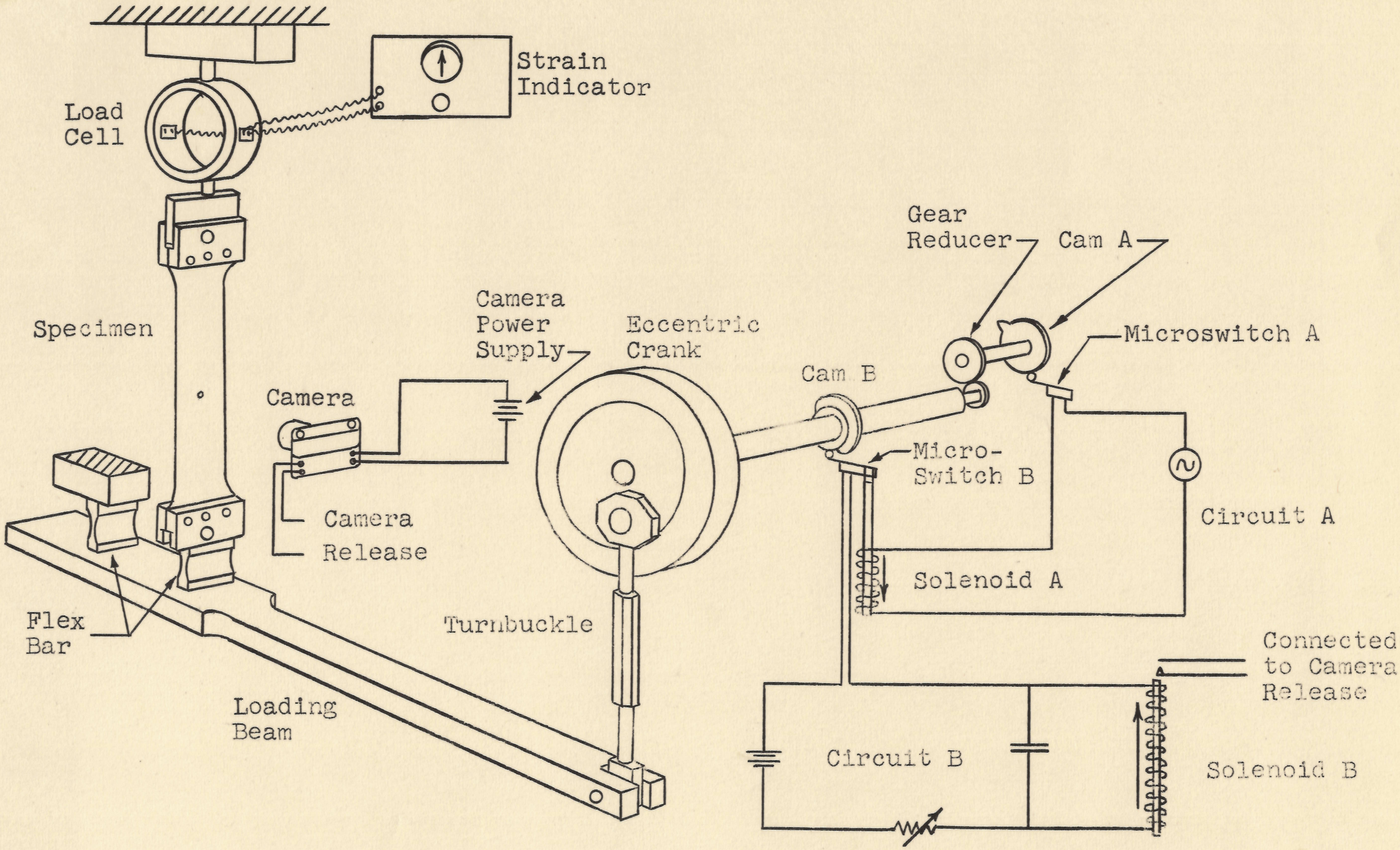

FIG. 4a SCHEMATIC DIAGRAM OF TEST APPARATUS

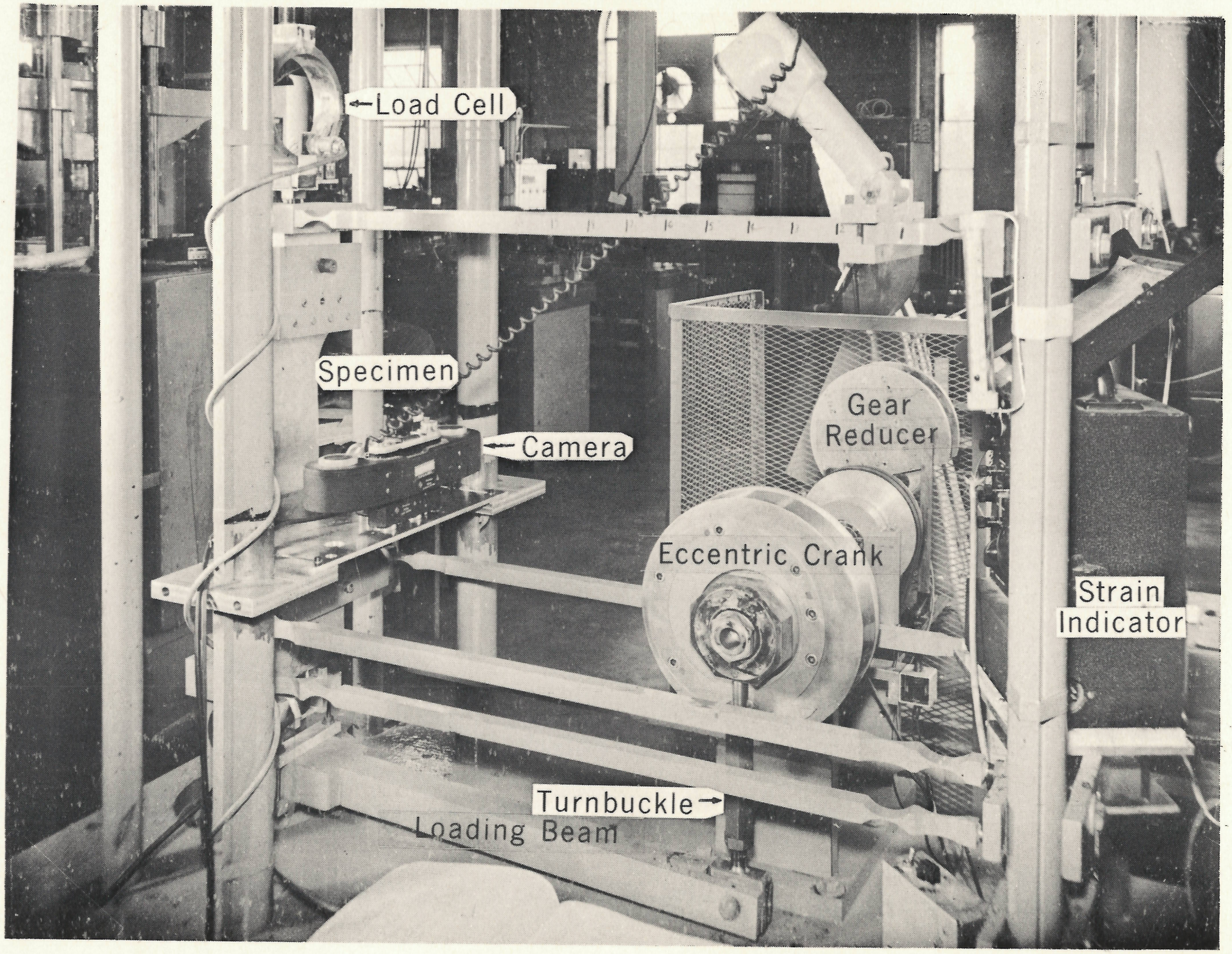

Fig. 4b Photograph of Test Apparatus

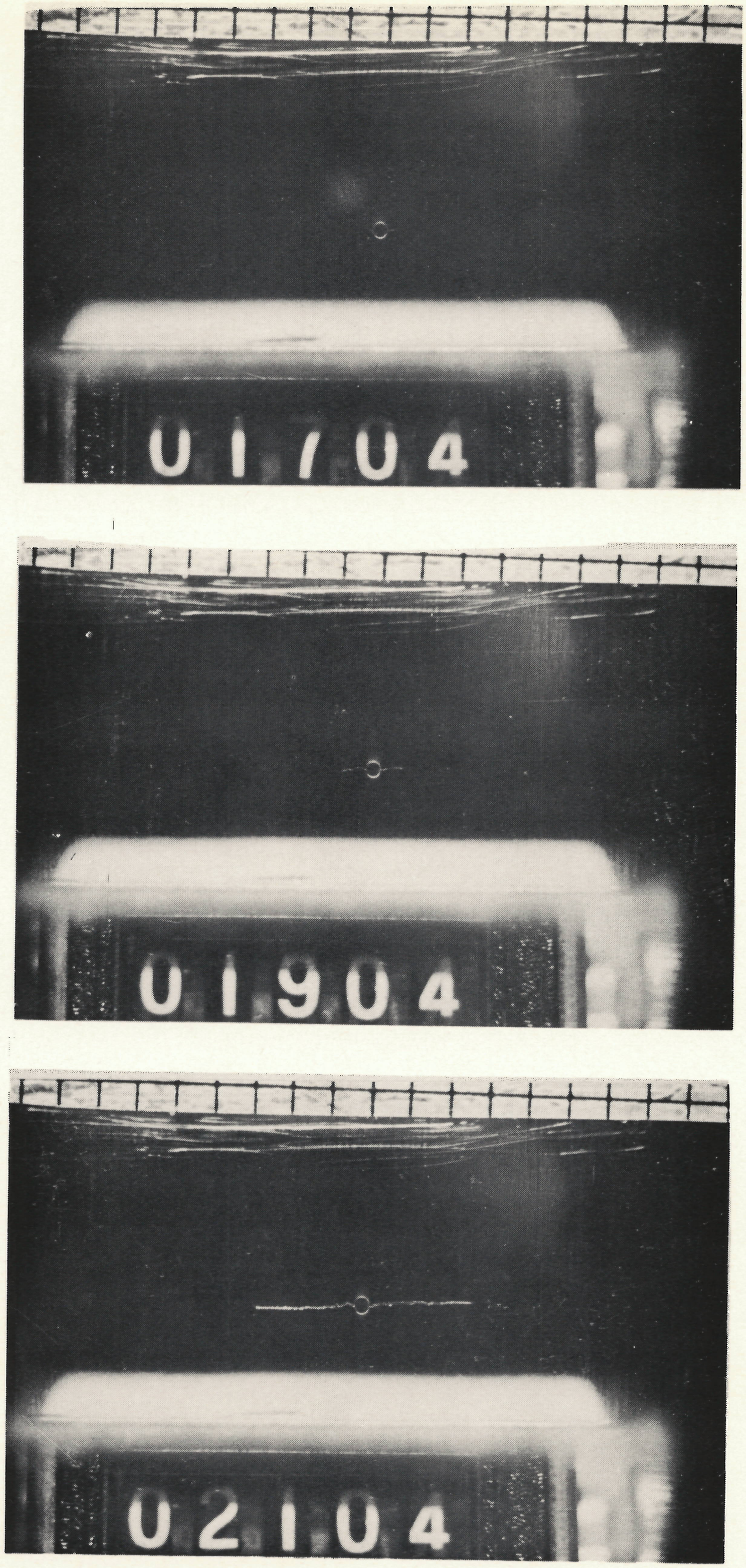

Fig. 5 Fatigue Cracks at Three Different Stages Reproduced from Recording Film

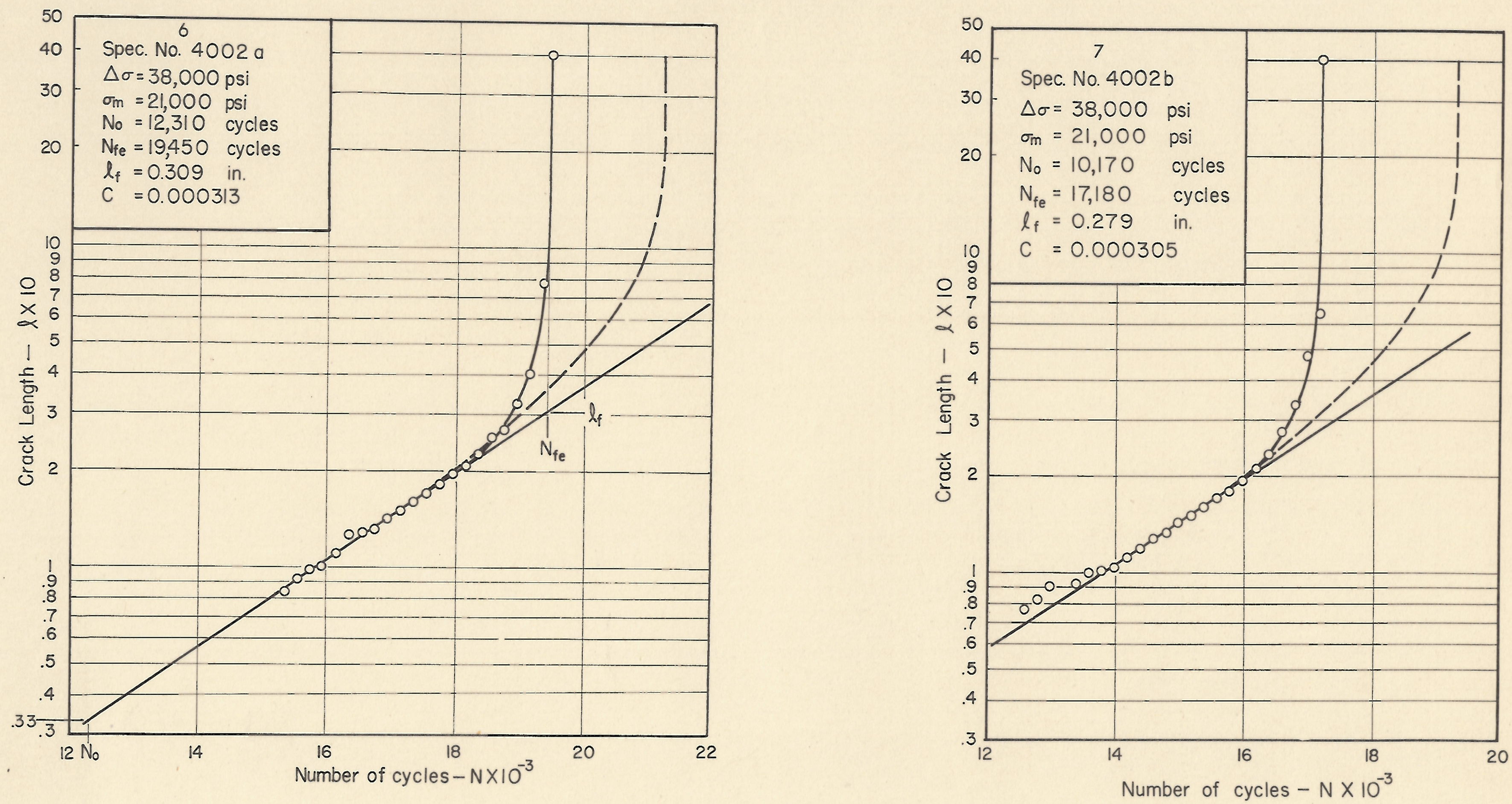

Figs. 6 & 7 Fatigue Crack Propagation Diagram, 2024–T3 Aluminum Alloy

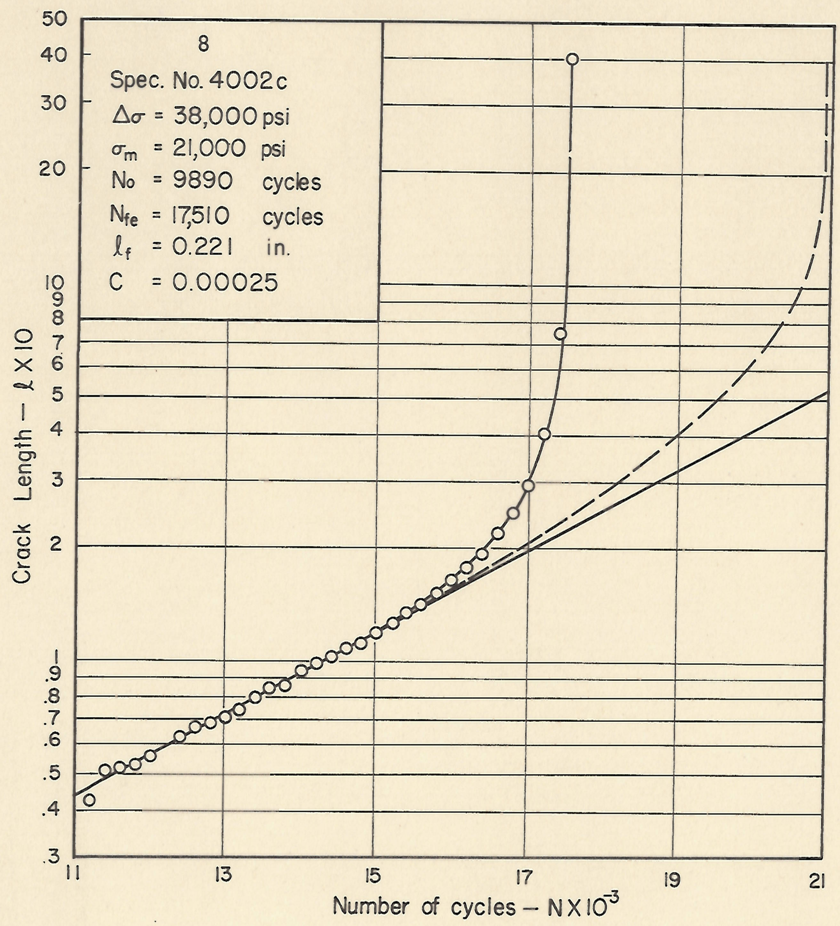

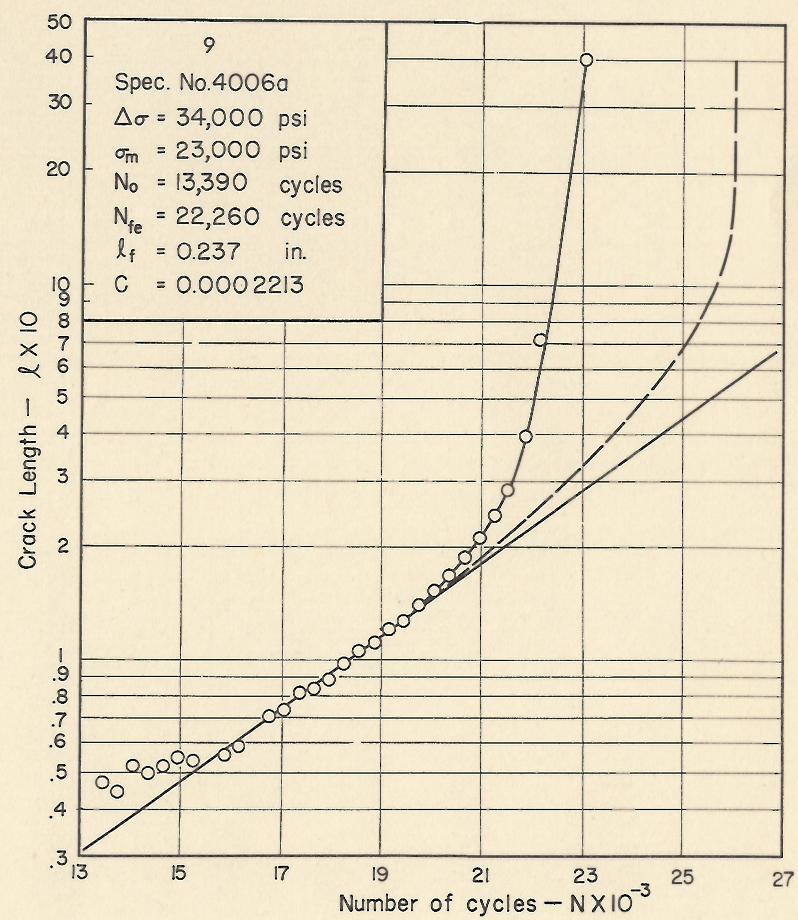

Figs. 8 & 9 Fatigue Crack Propagation Diagram, 2024—T3 Aluminum Alloy

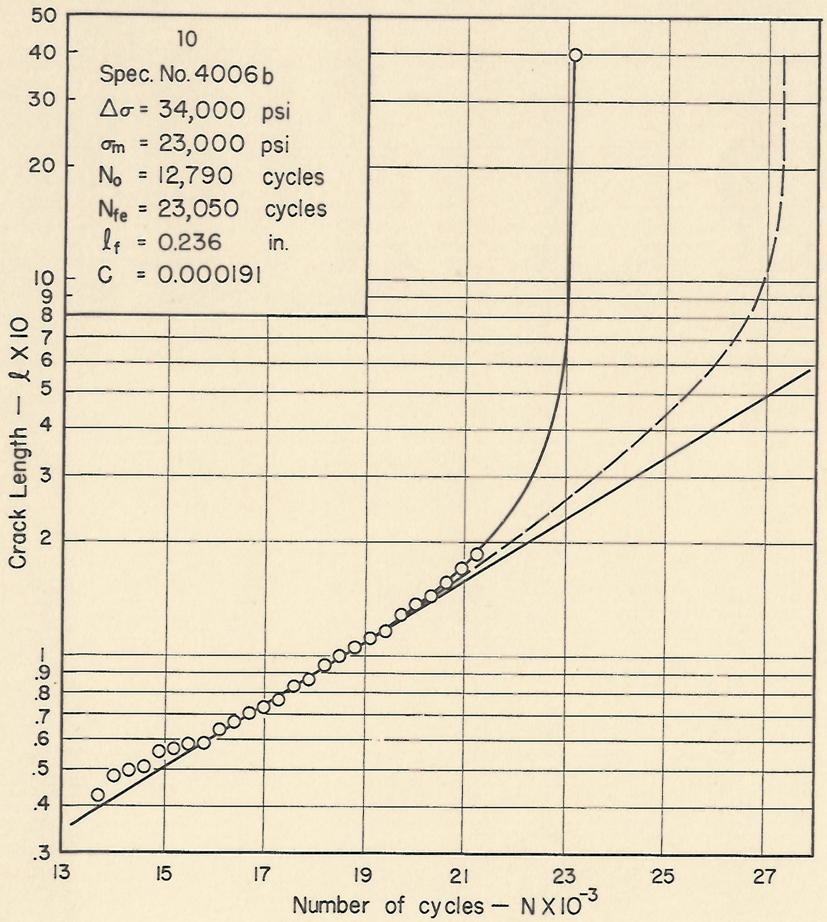

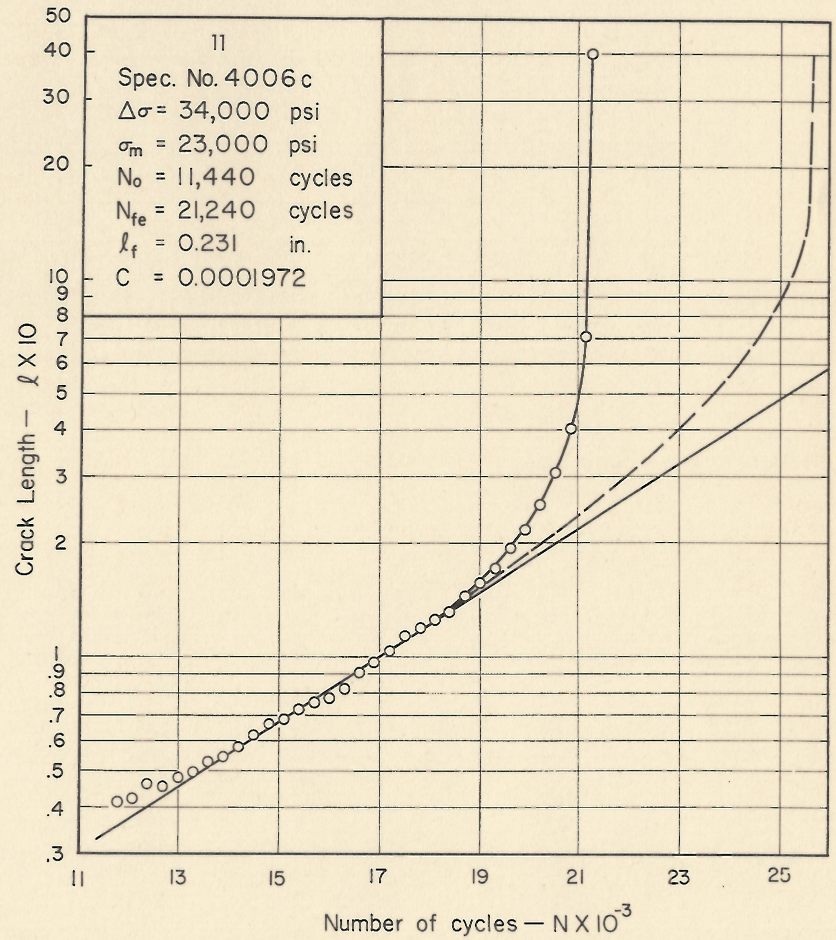

Figs. 10 & 11 Fatigue Crack Propagation Diagram, 2024—T3 Aluminum Alloy

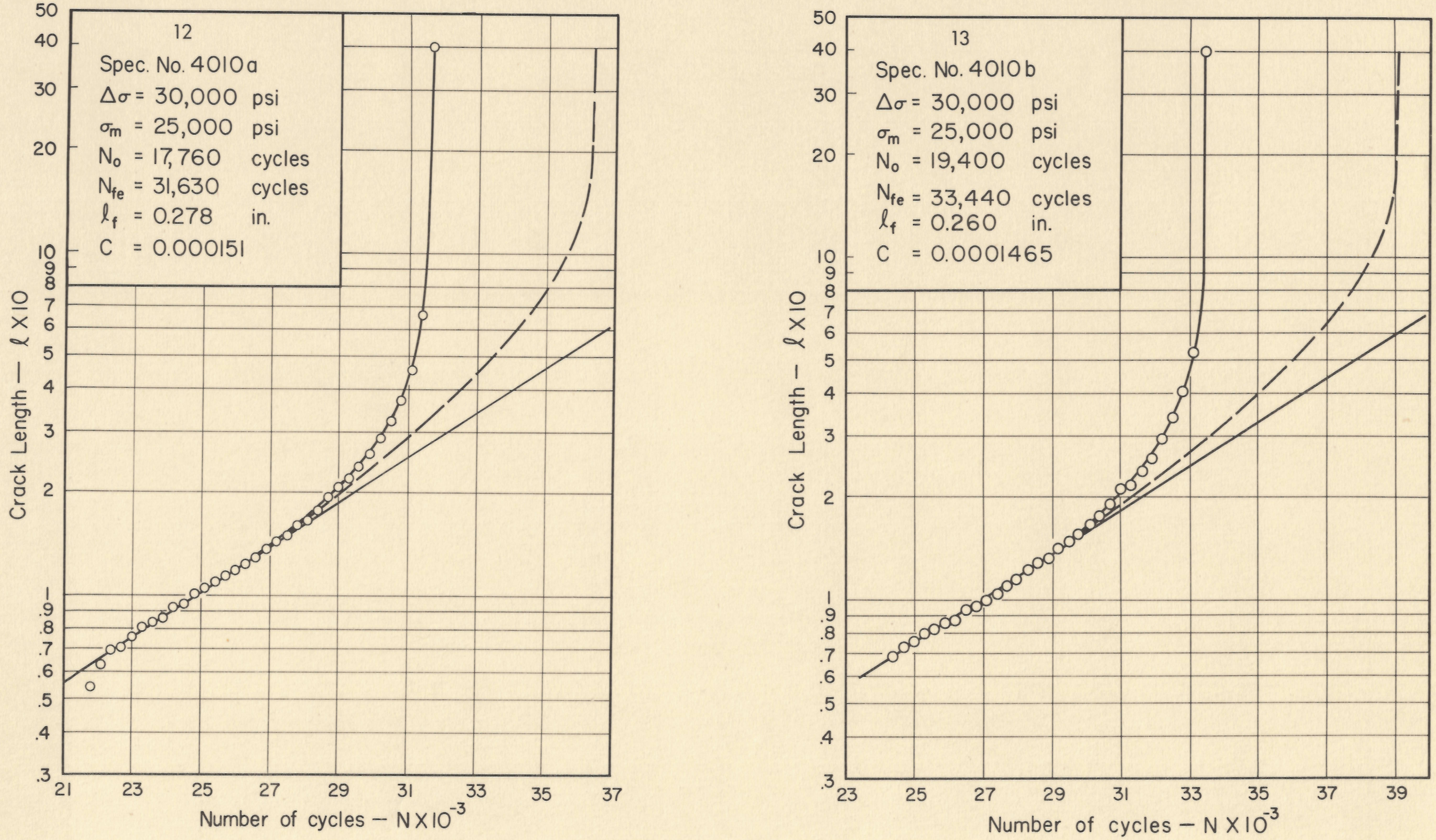

Figs. 12 & 13 Fatigue Crack Propagation Diagram, 2024—T3 Aluminum Alloy

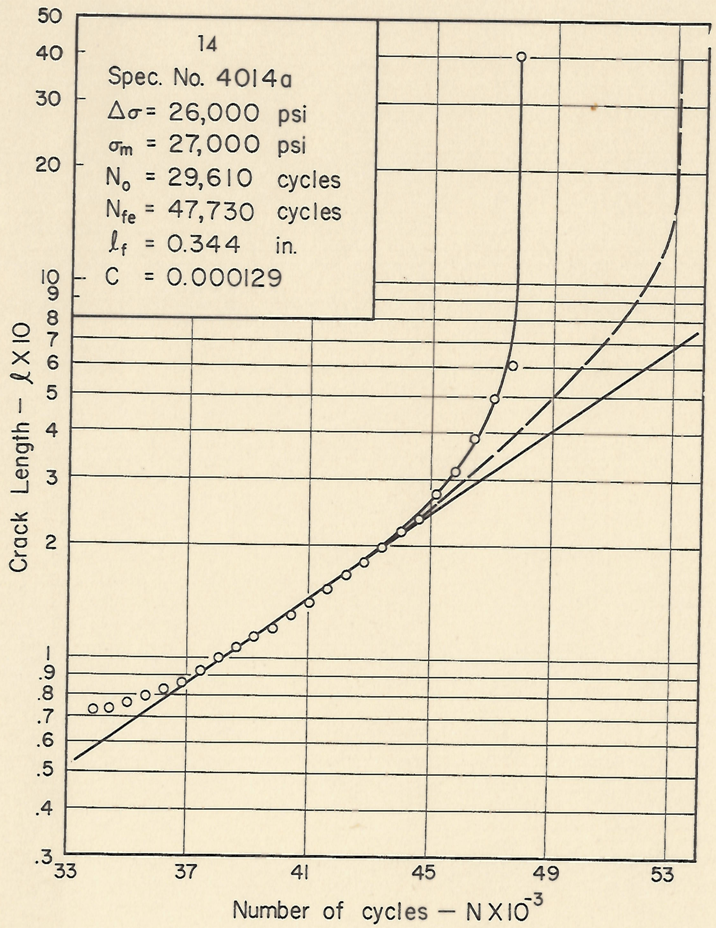

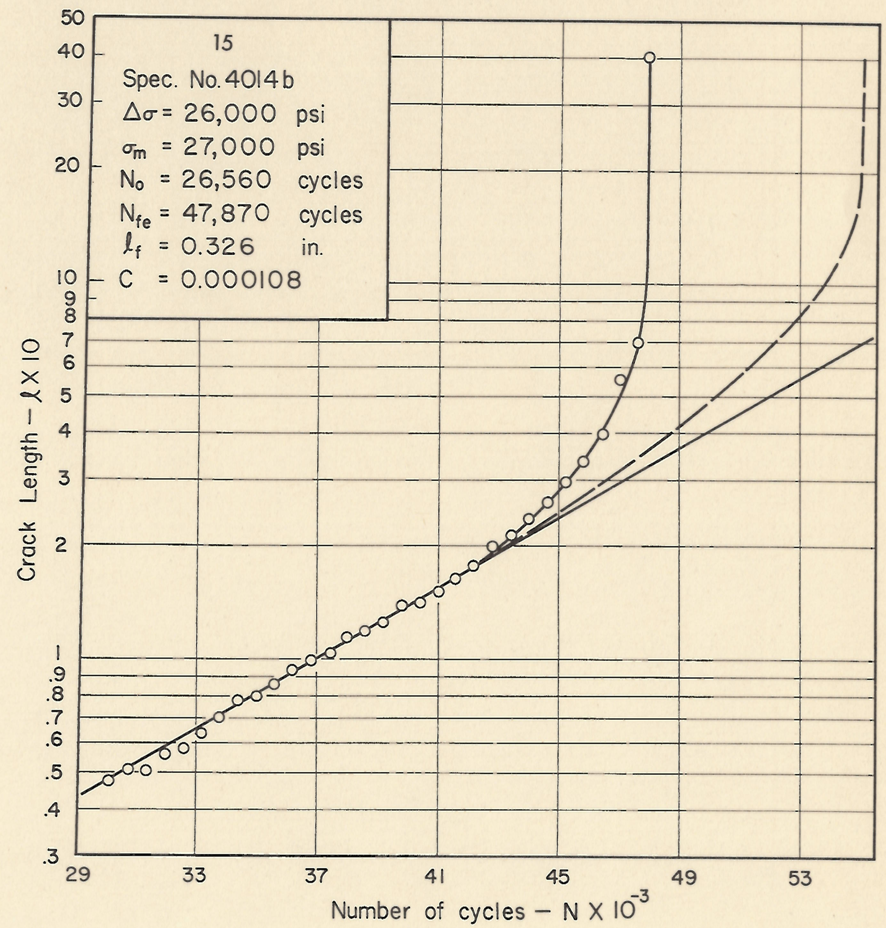

Figs. 14 & 15 Fatigue Crack Propagation Diagram, 2024—T3 Aluminum Alloy

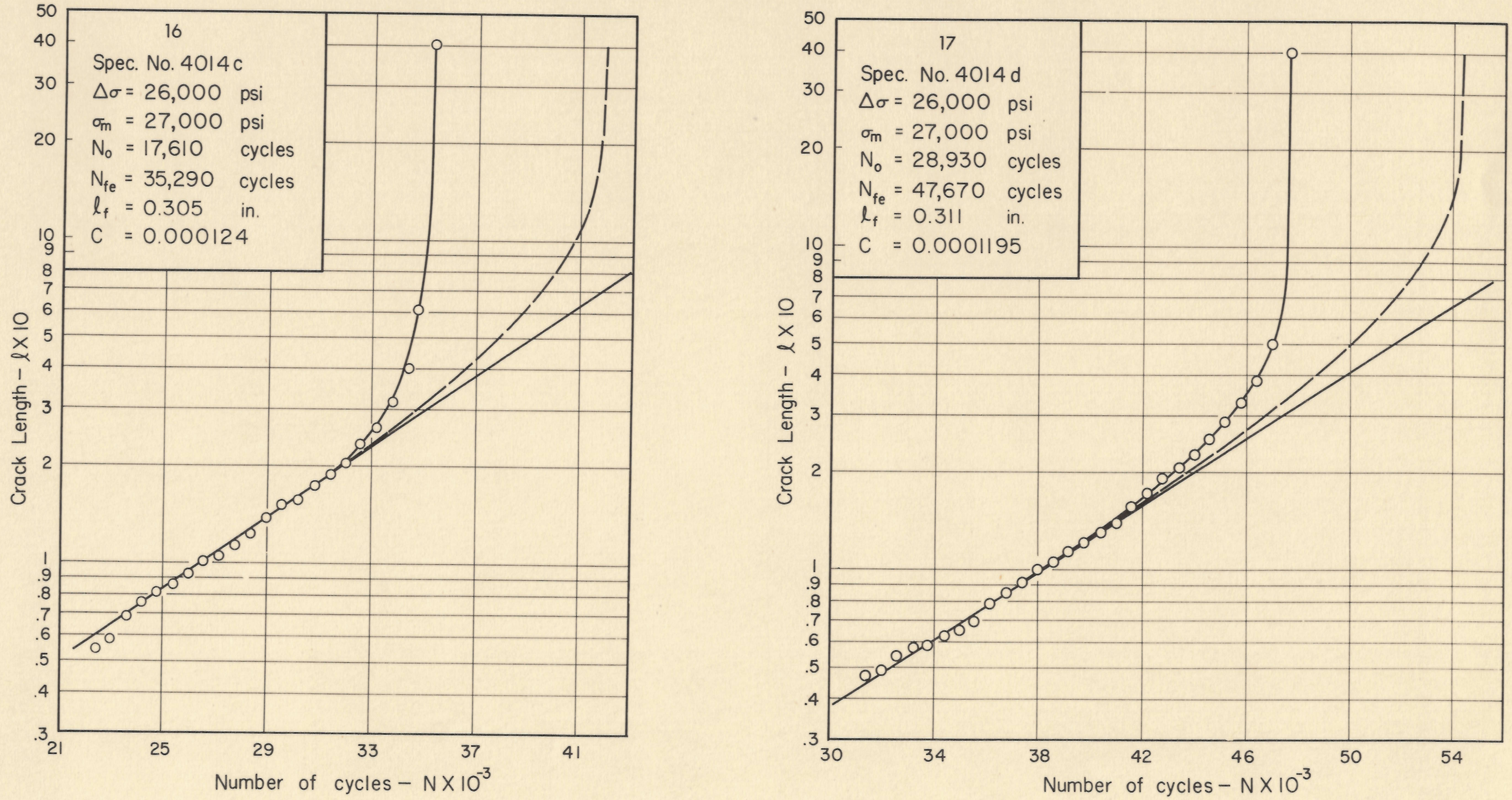

Figs. 16 & 17 Fatigue Crack Propagation Diagram, 2024–T3 Aluminum Alloy

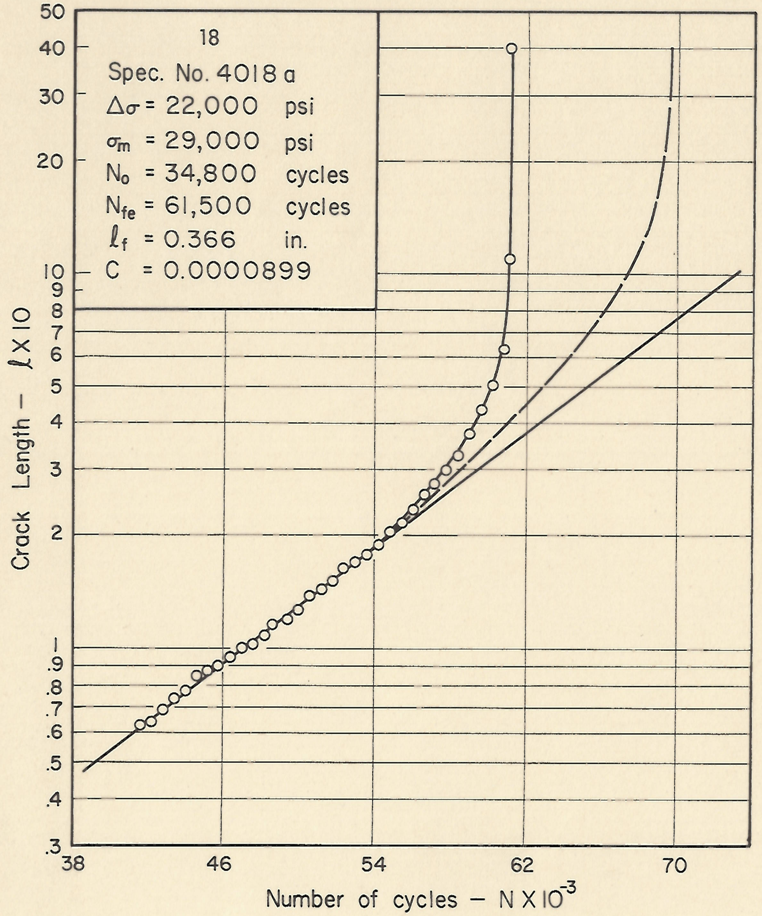

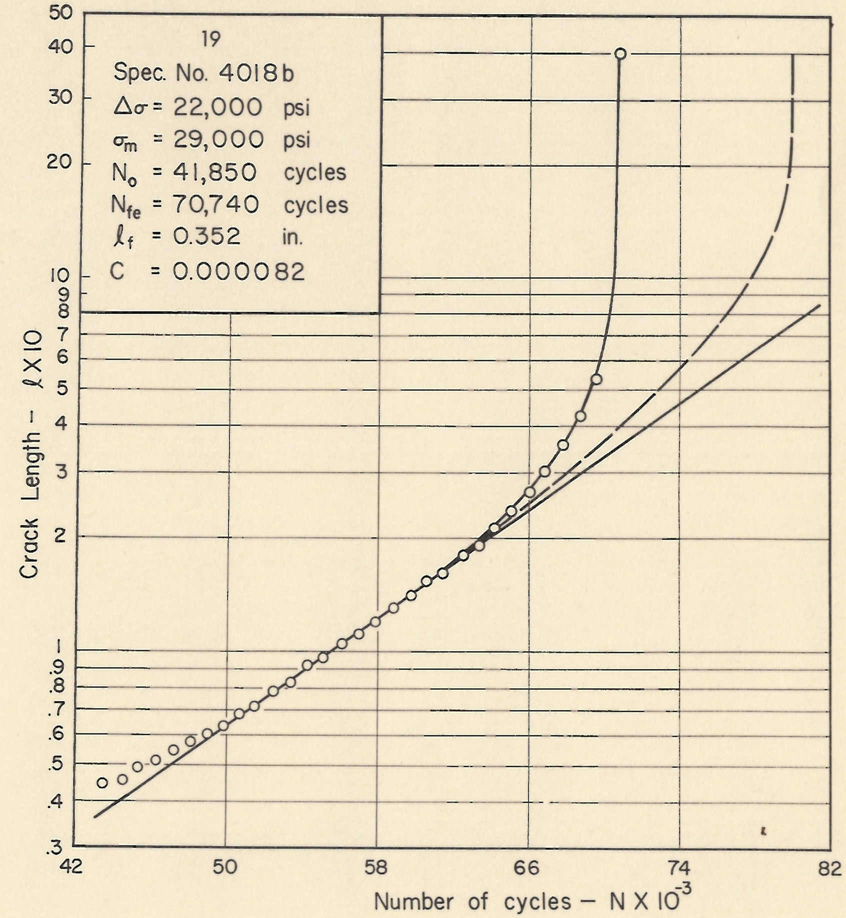

Figs. 18 & 19 Fatigue Crack Propagation Diagram, 2024–T3 Aluminum Alloy

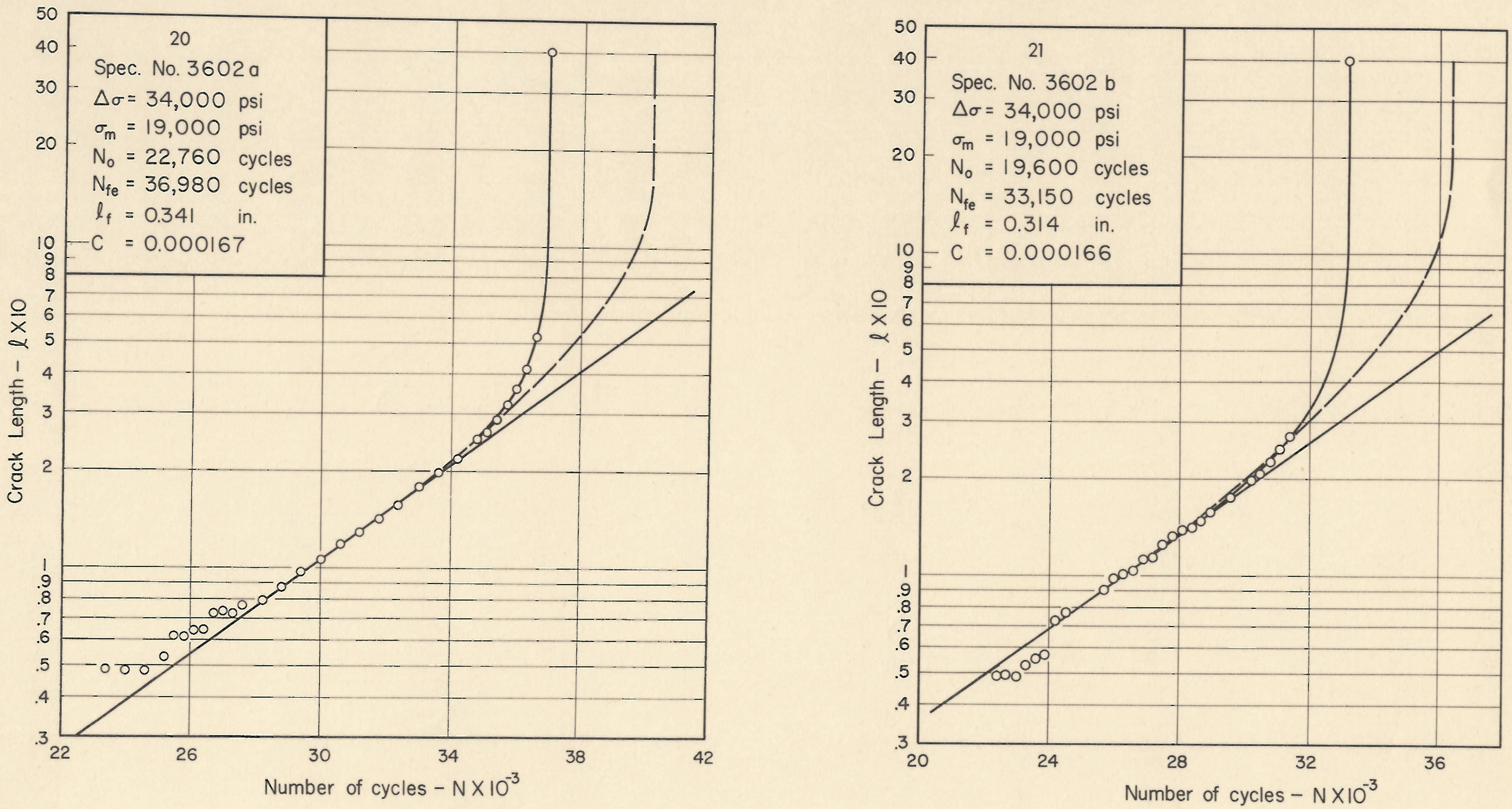

Figs. 20 & 21 Fatigue Crack Propagation Diagram, 2024—T3 Aluminum Alloy

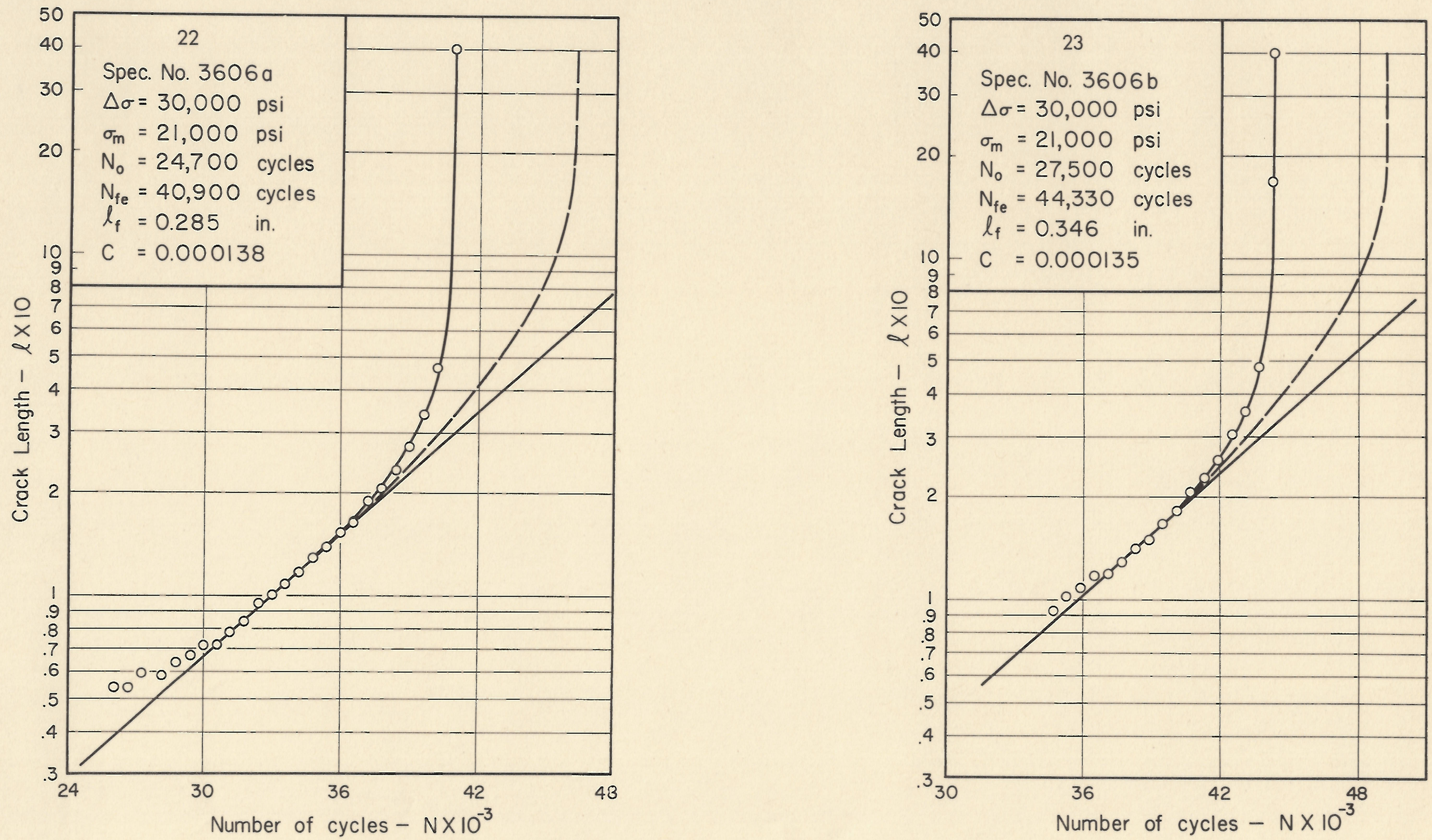

Figs. 22 & 23 Fatigue Crack Propagation Diagram, 2024–T3 Aluminum Alloy

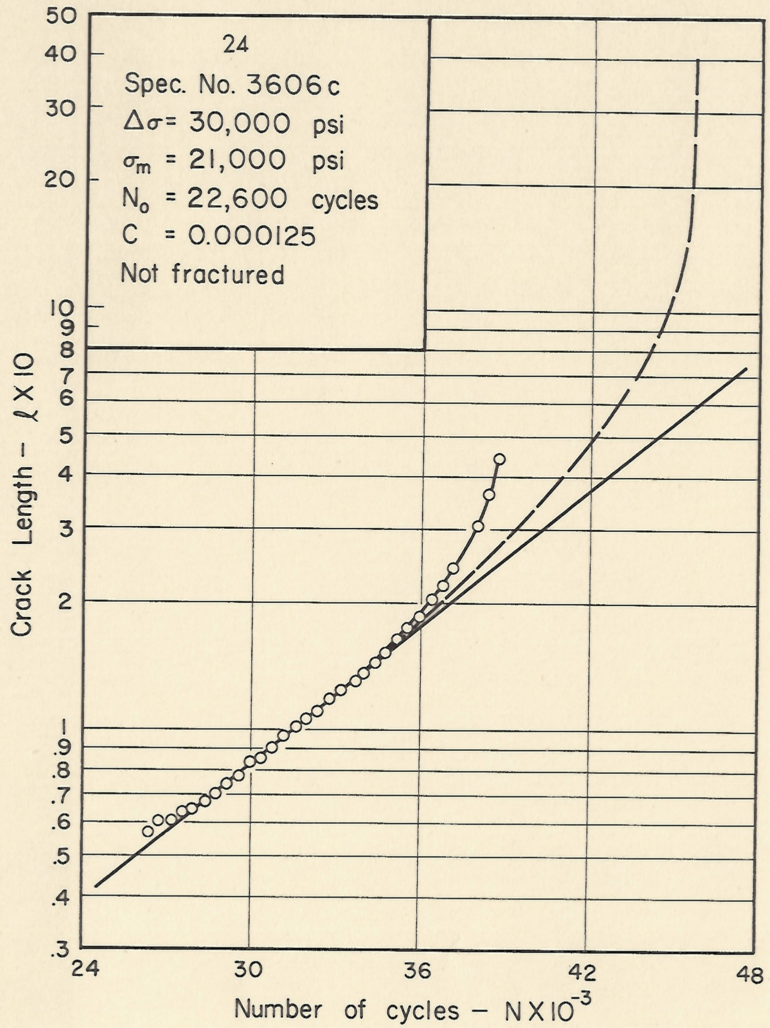

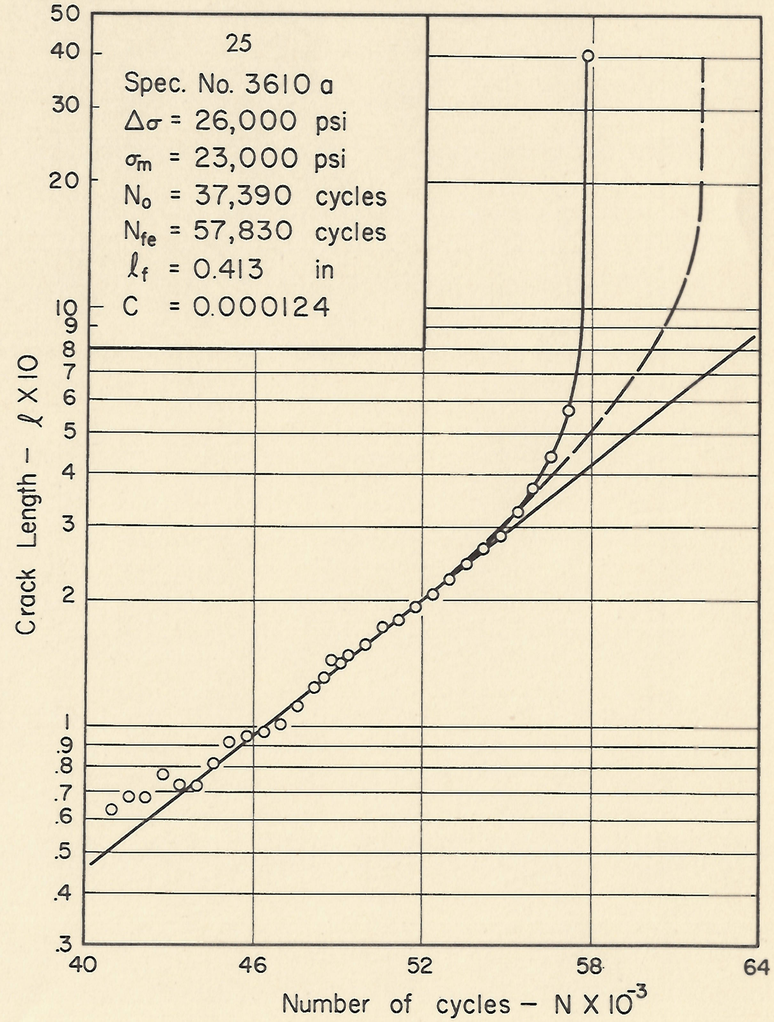

Figs. 24 & 25 Crack Propagation Diagram, 2024–T3 Aluminum Alloy

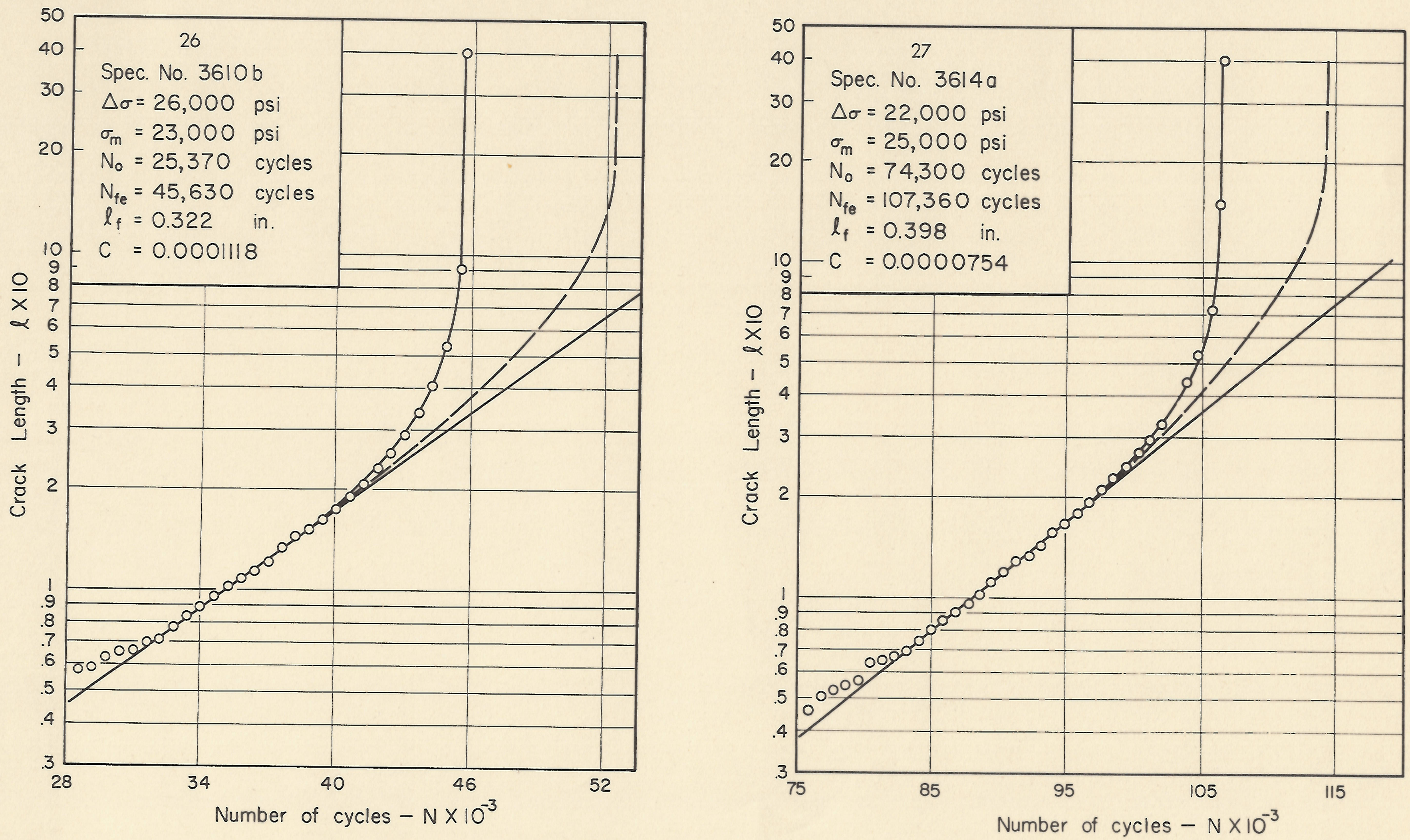

Figs. 26 & 27 Fatigue Crack Propagation Diagram, 2024 –T3 Aluminum Alloy

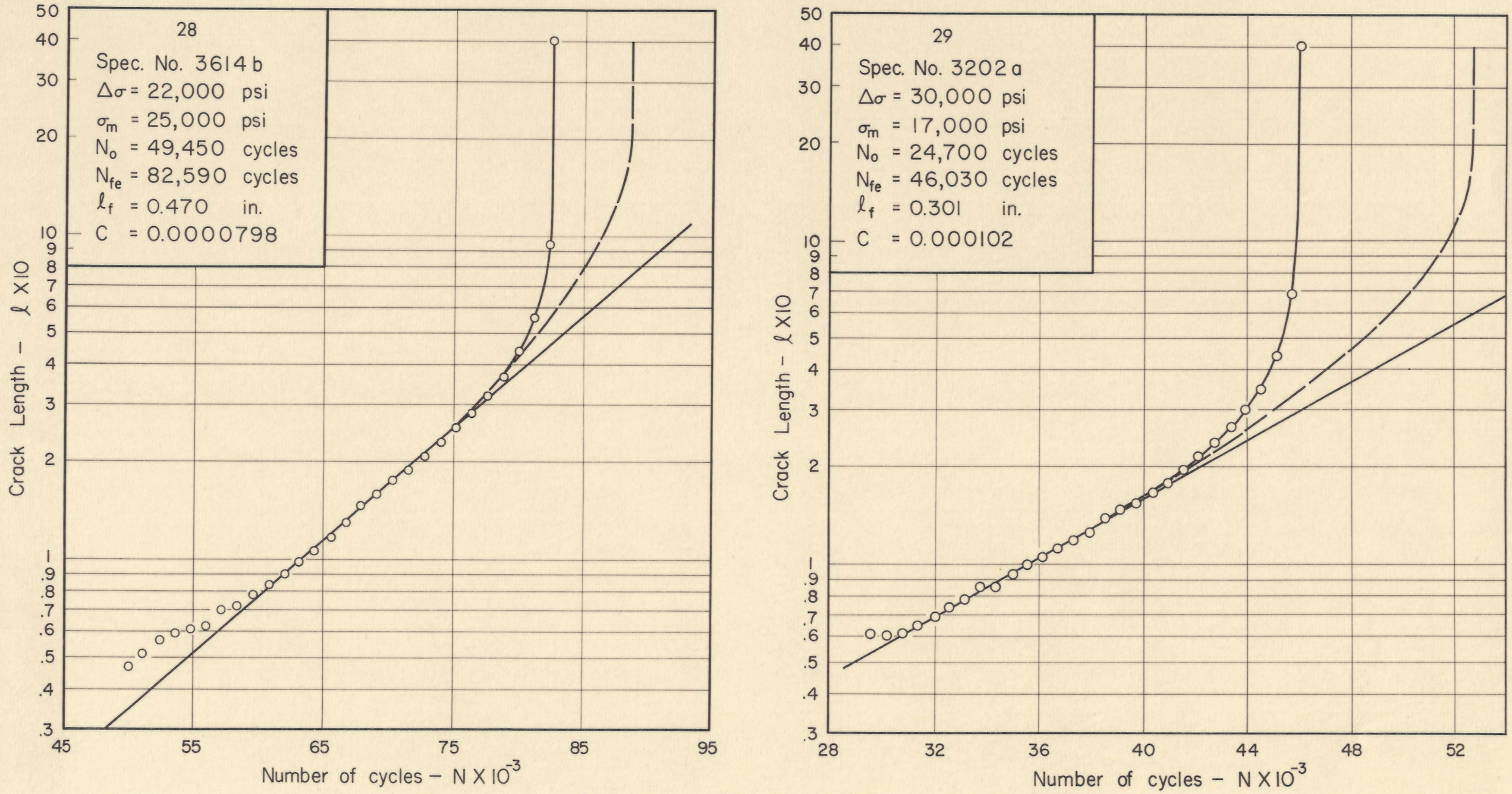

Figs. 28 & 29 Fatigue Crack Propagation Diagram, 2024–T3 Aluminum Alloy

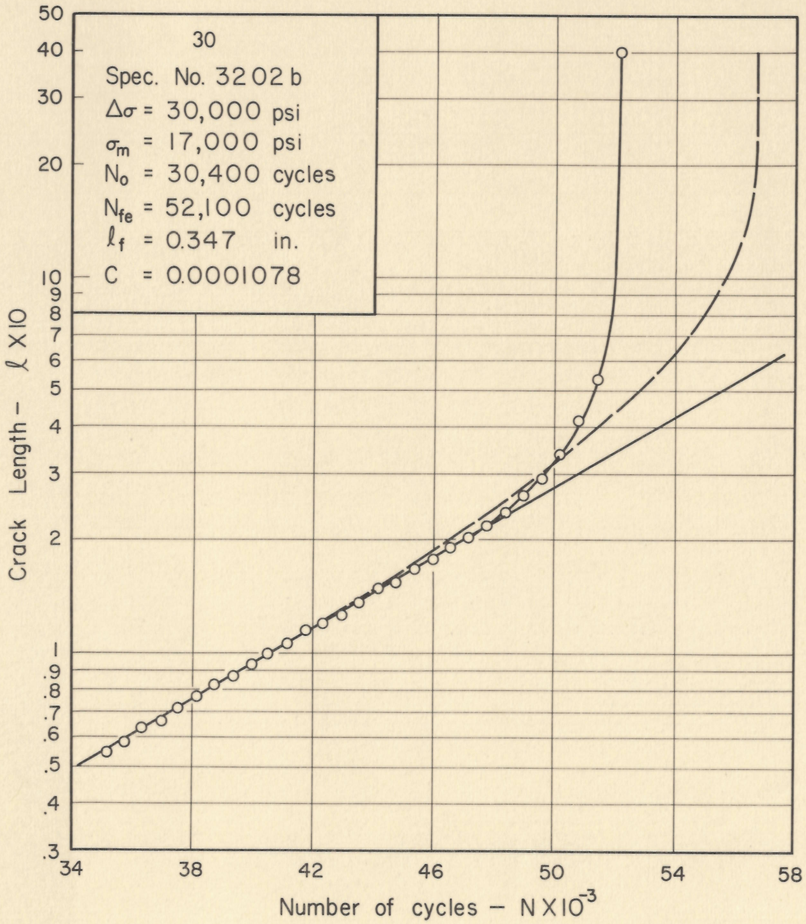

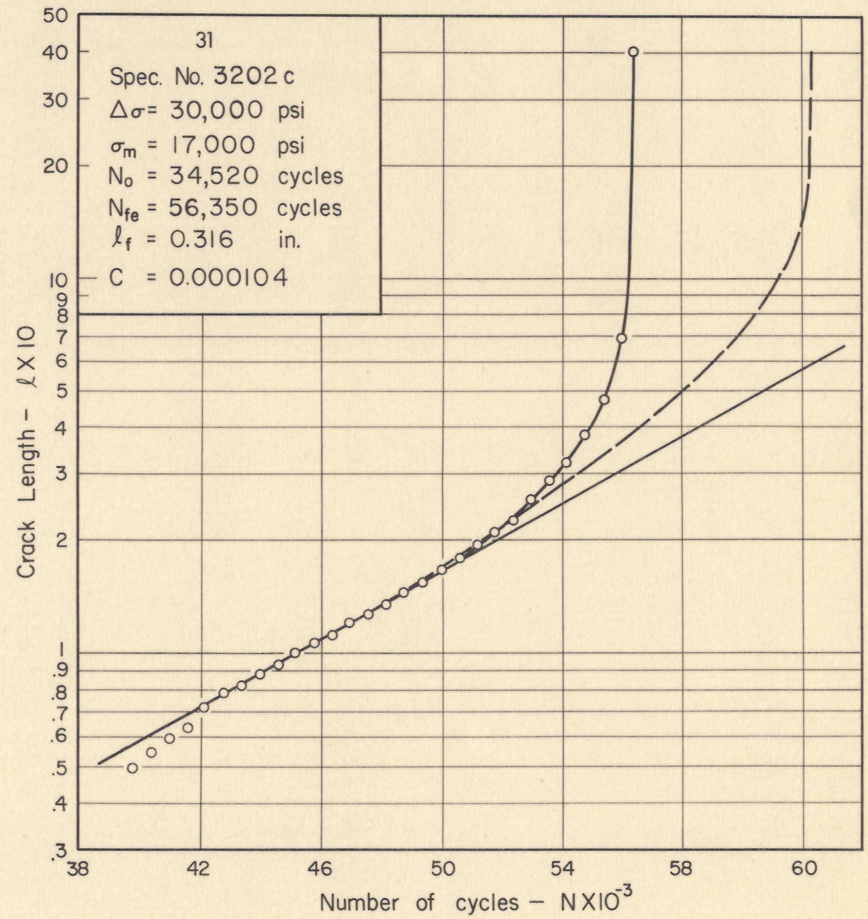

Figs. 30 & 31 Fatigue Crack Propagation Diagram, 2024–T3 Aluminum Alloy

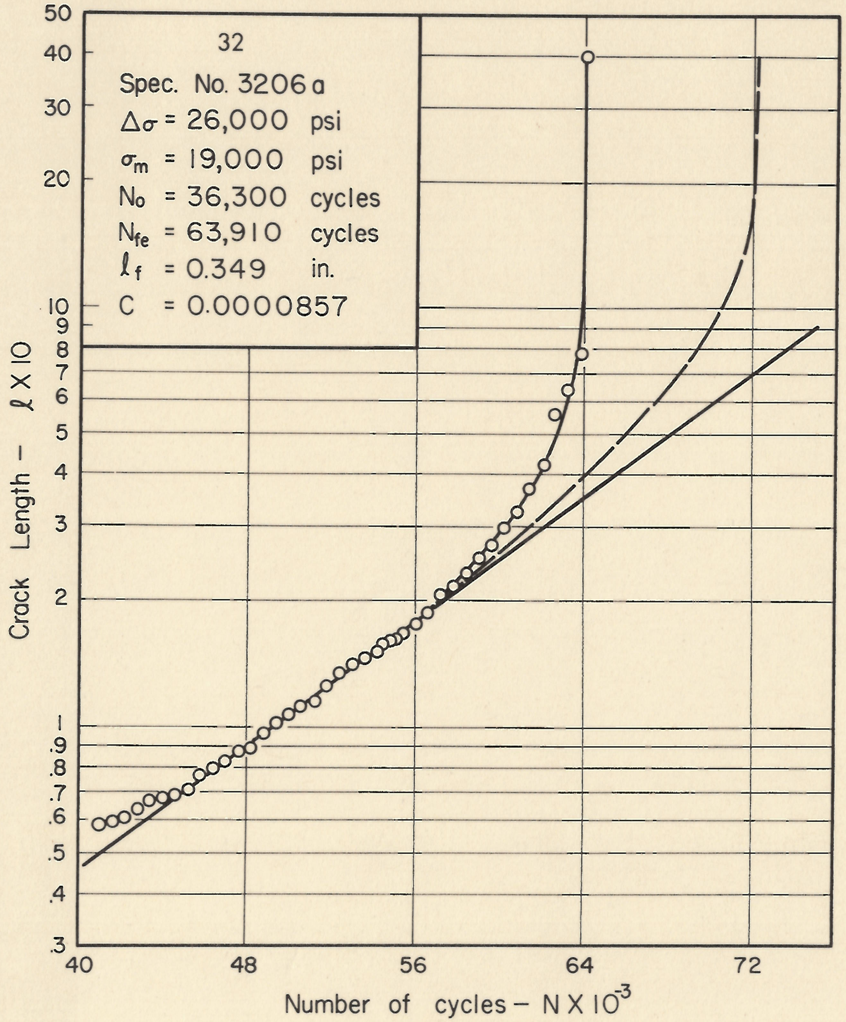

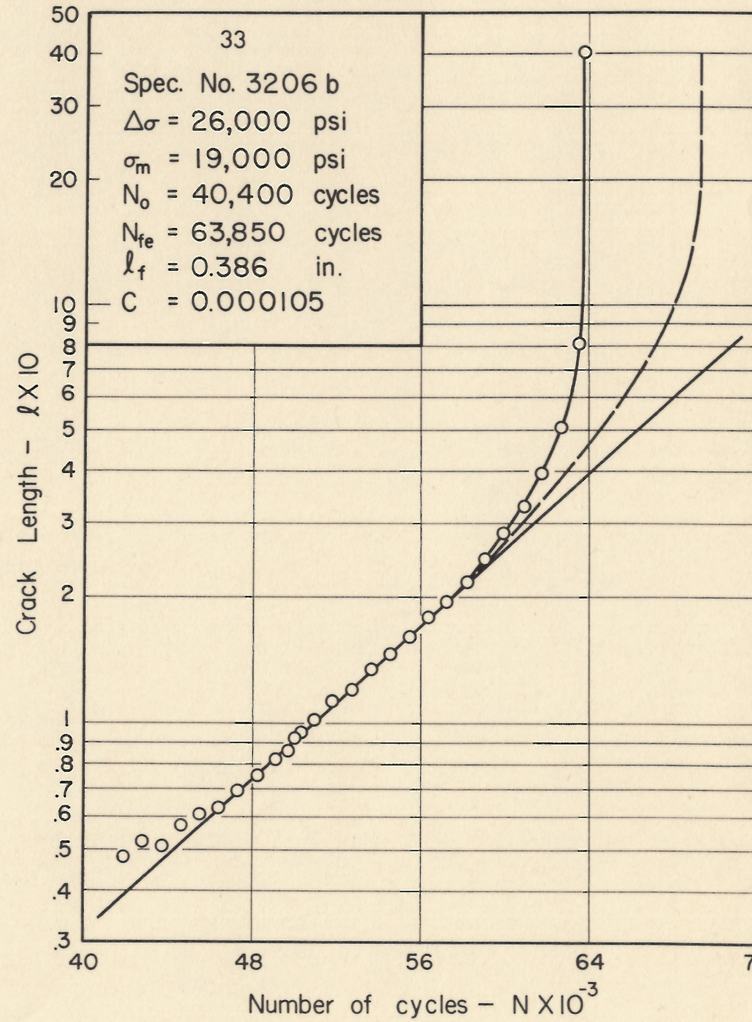

Figs. 32 & 33 Fatigue Crack Propagation Diagram, 2024–T3 Aluminum Alloy

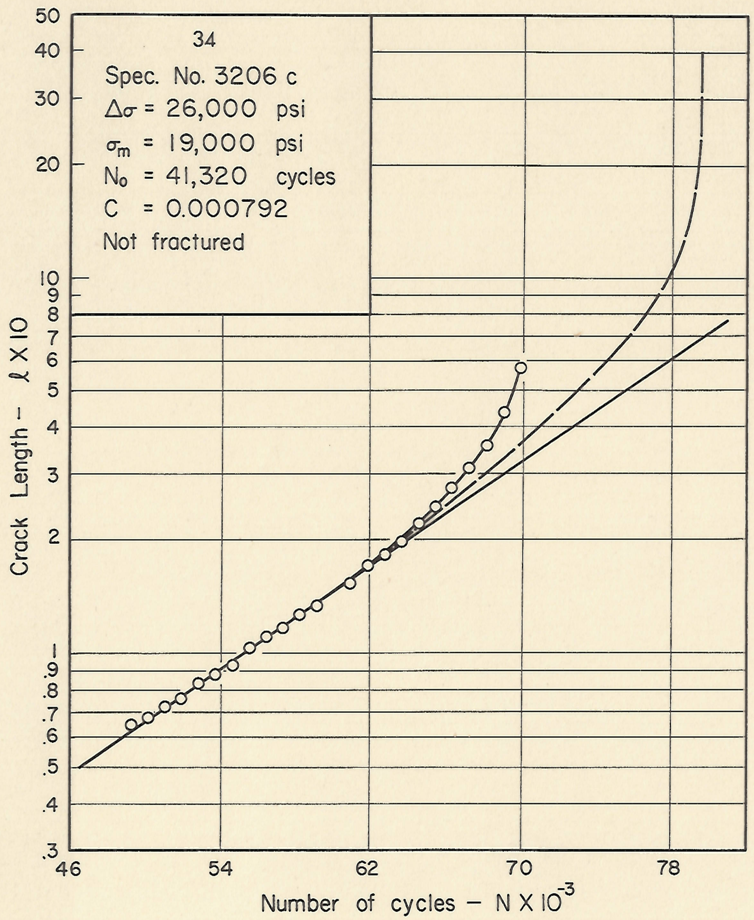

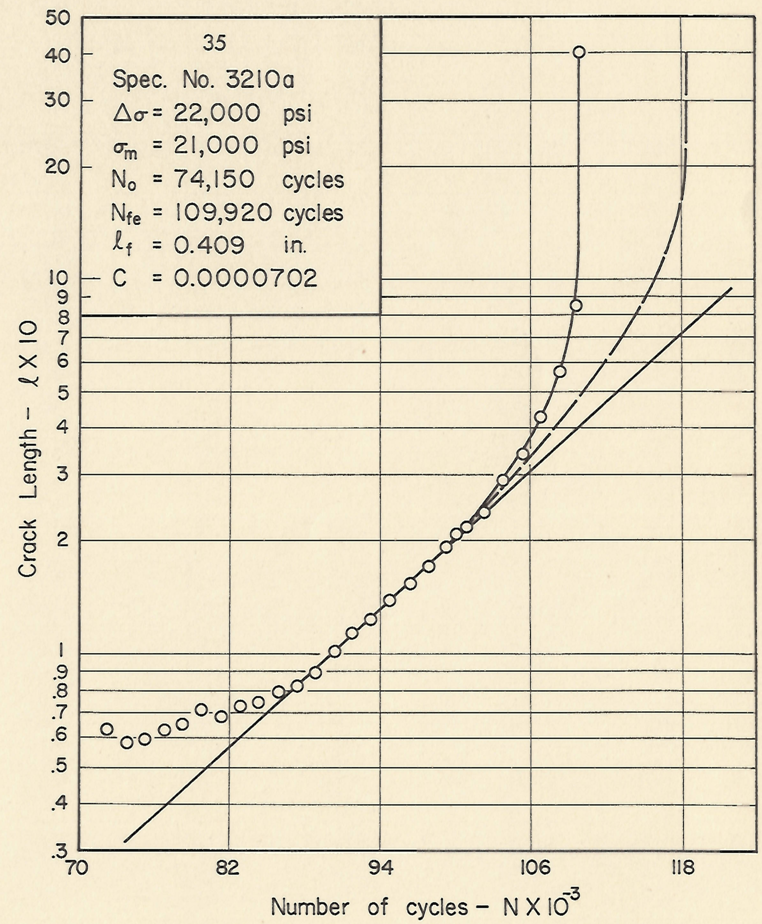

Figs. 34 & 35 Fatigue Crack Propagation Diagram, 2024—T3 Aluminum Alloy

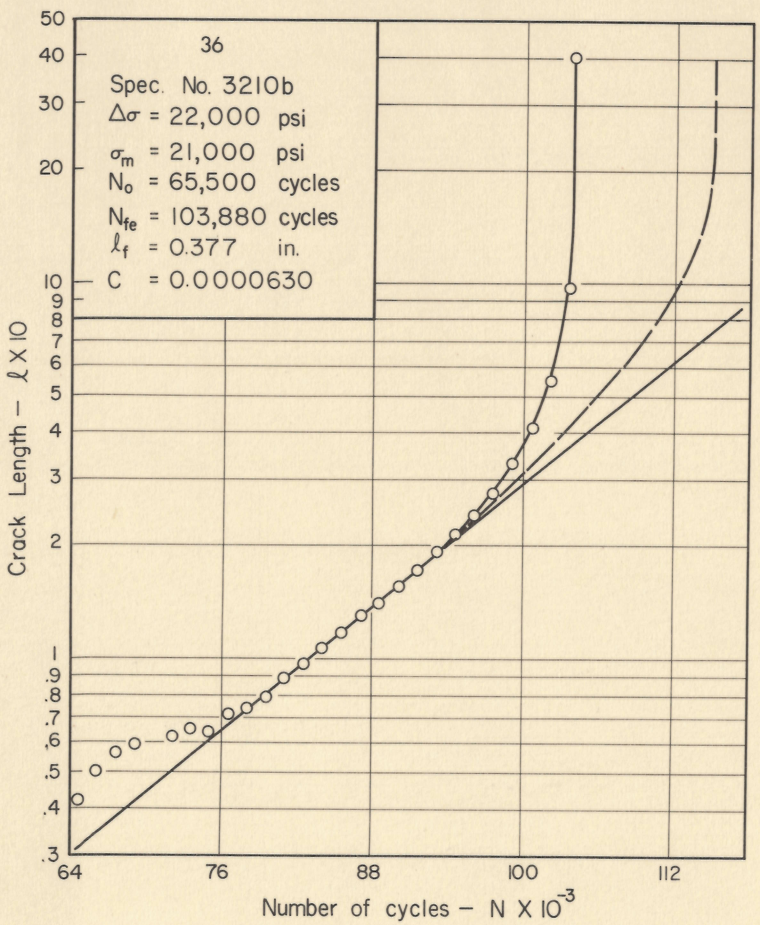

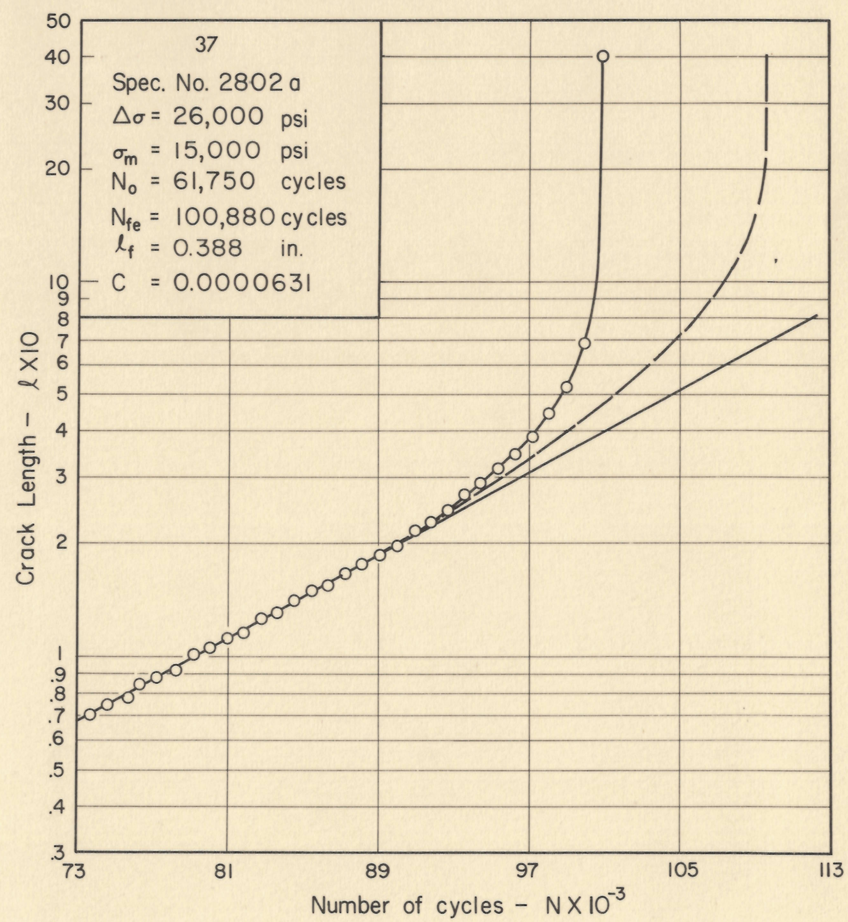

Figs. 36 & 37 Fatigue Crack Propagation Diagram, 2024–T3 Aluminum Alloy

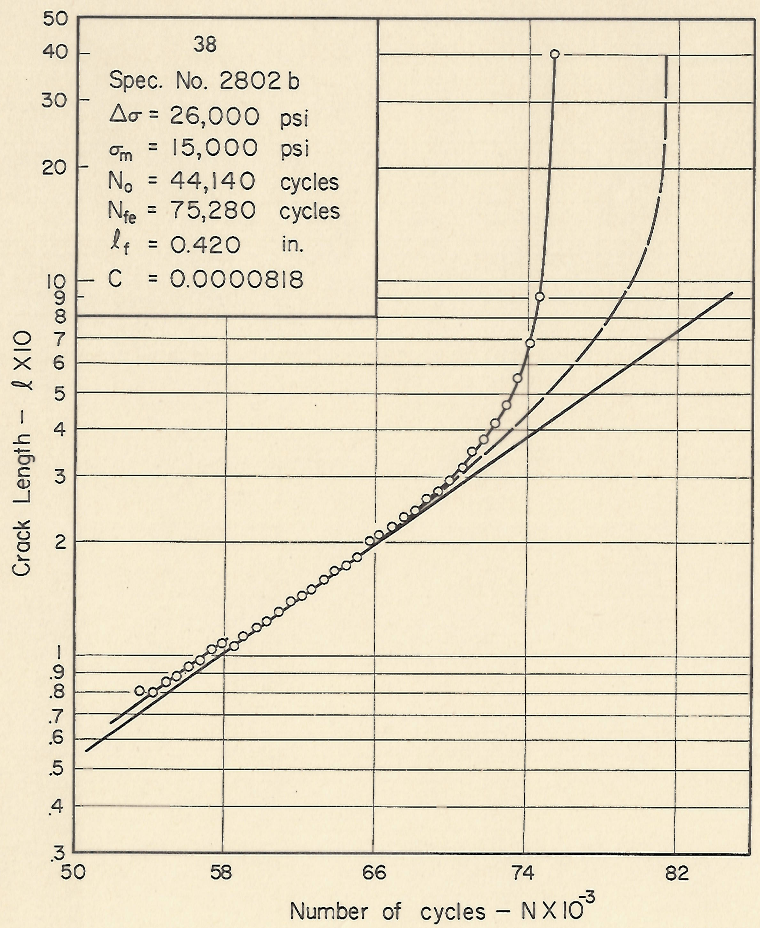

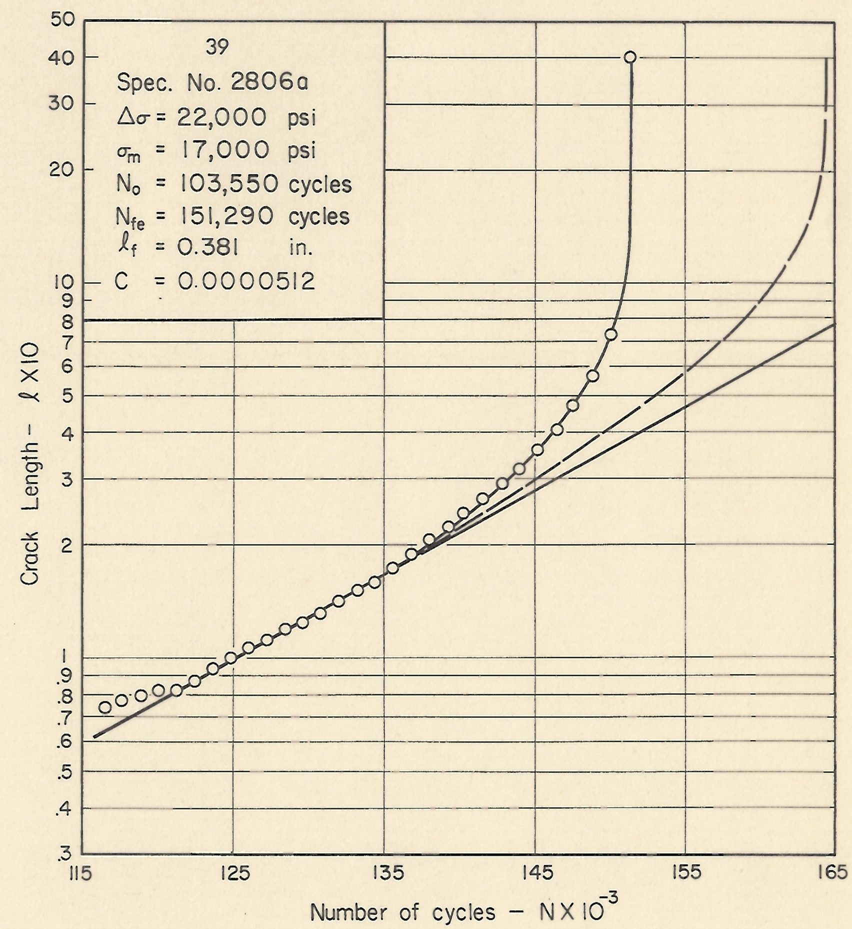

Figs. 38 & 39 Fatigue Crack Propagation Diagram, 2024–T3 Aluminum Alloy

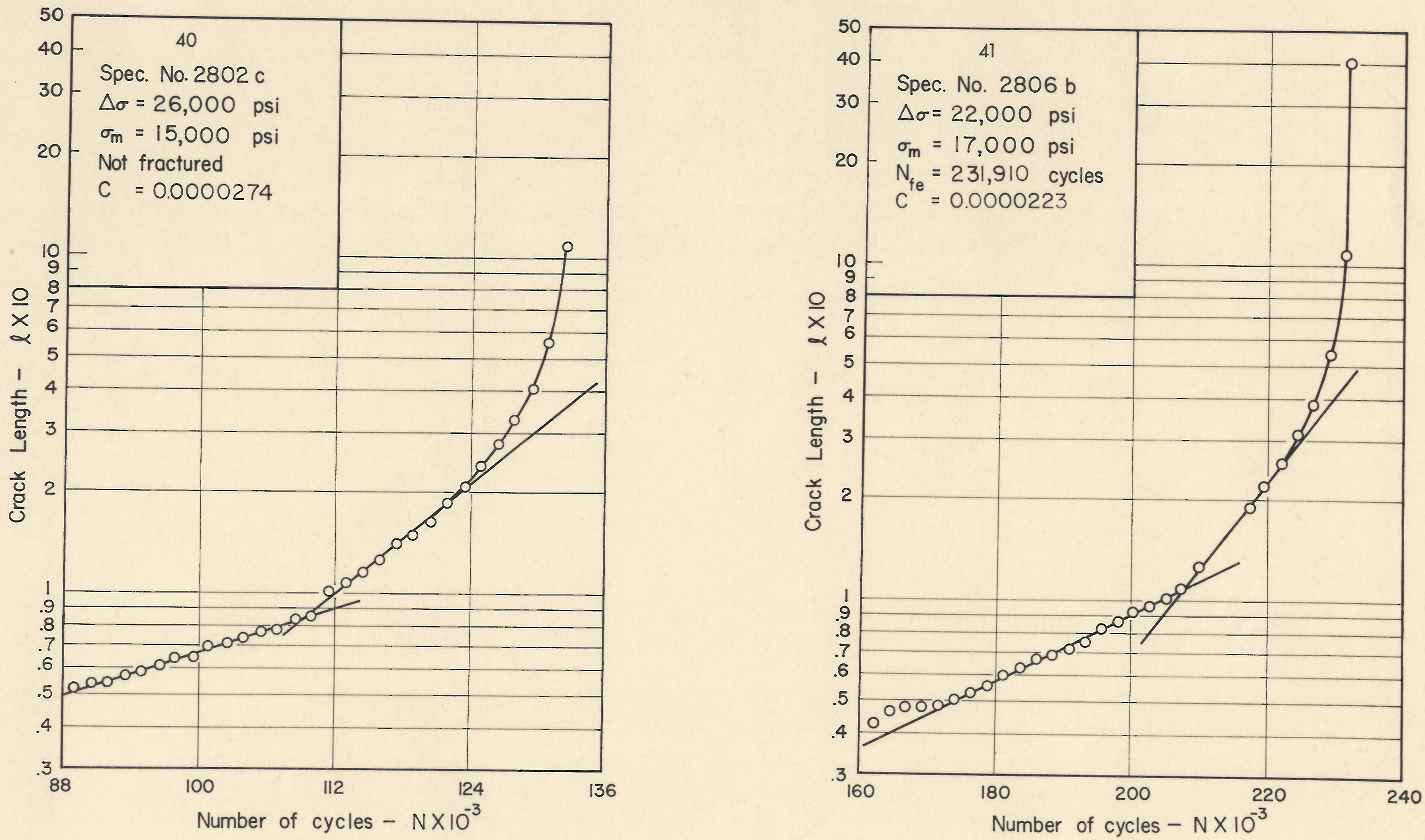

Figs. 40 & 41 Fatigue Crack Propagation Diagram, 2024—T3 Aluminum Alloy

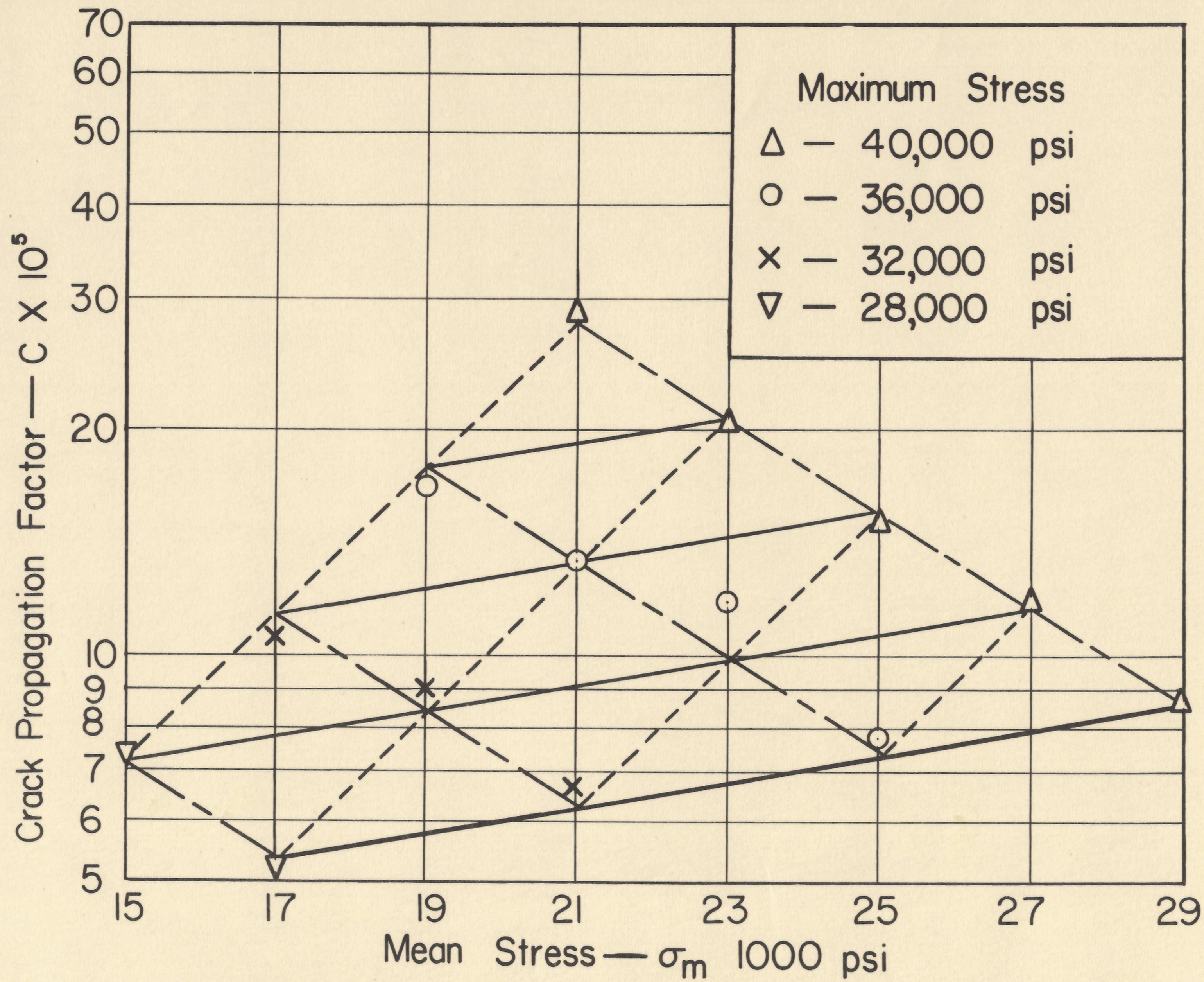

Fig. 42 Correlation between Propagation Factor and Mean Stress

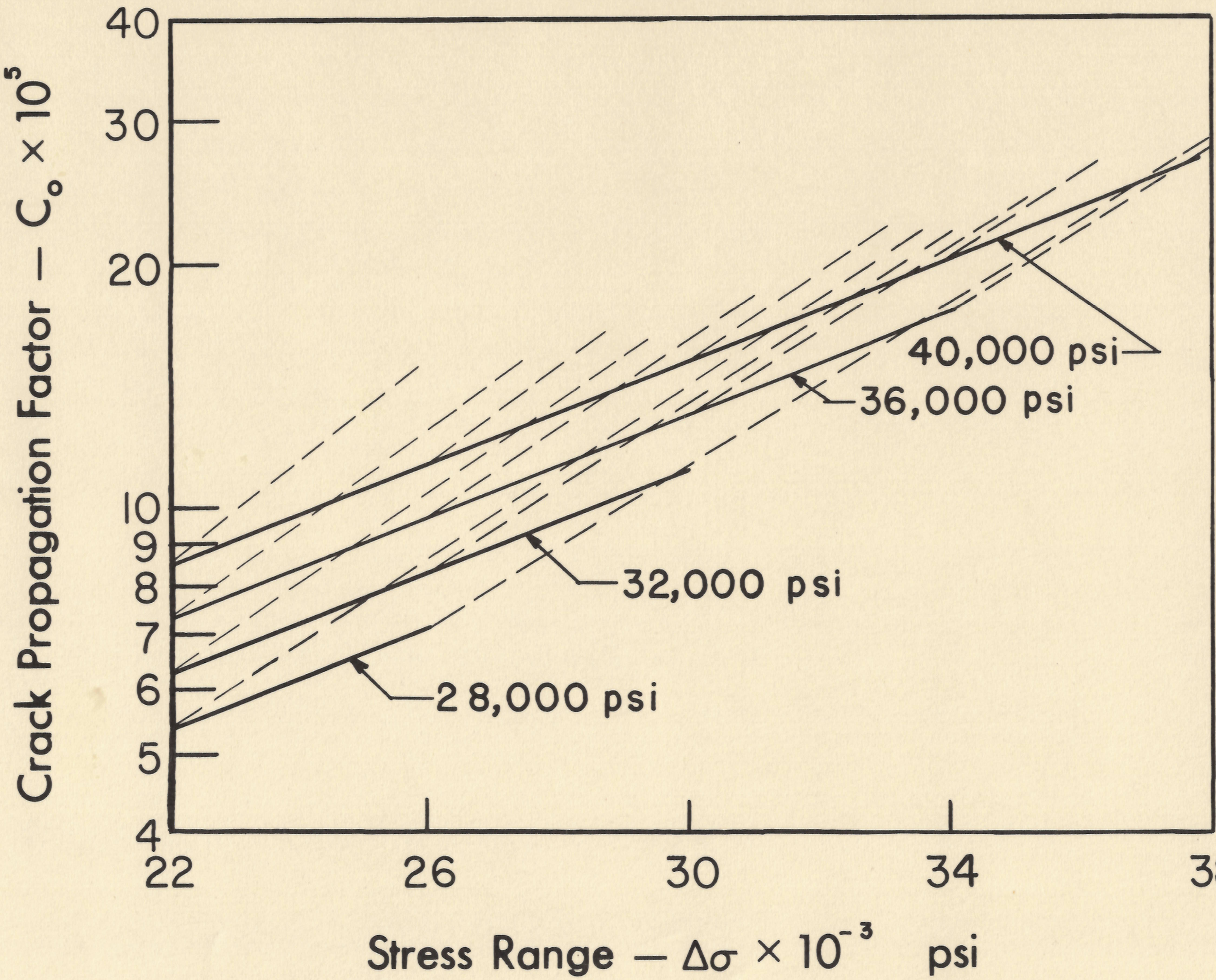

Fig. 43 Correlation between Crack Propagation Factor and Stress Range

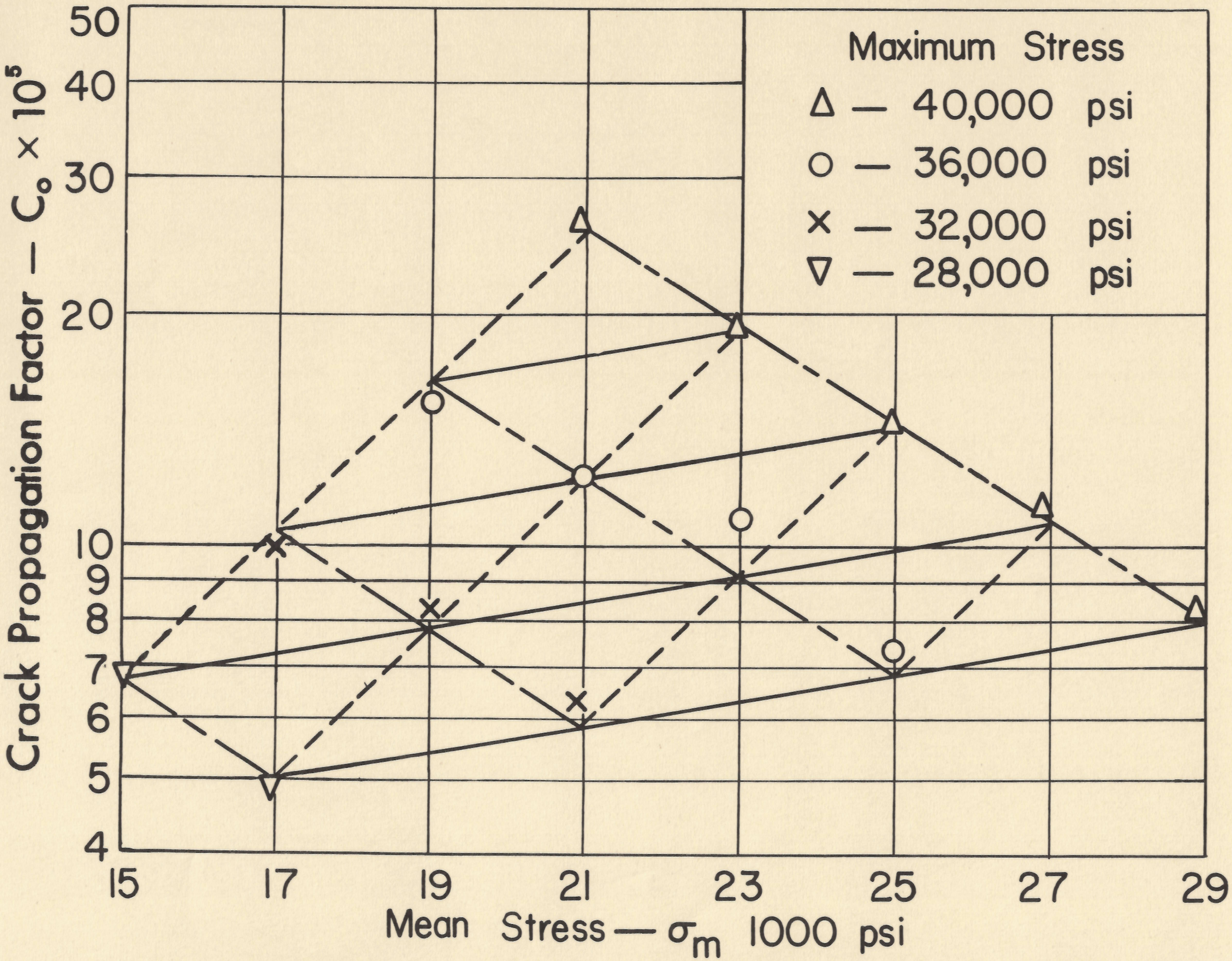

Fig. 44 Correlation between Initial Propagation Factor and Mean Stress

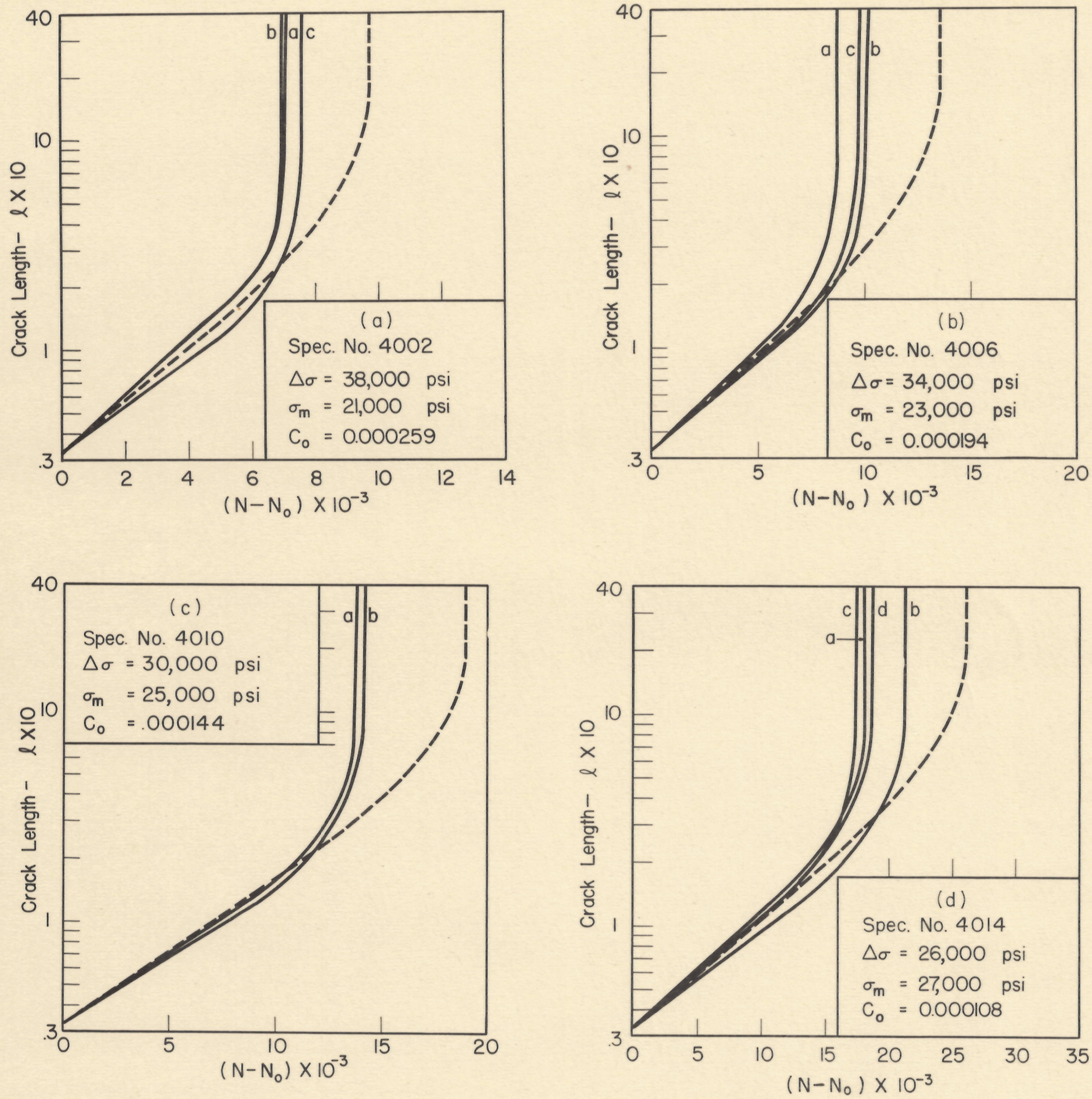

Fig. 45(a,b,c,d) Combined Fatigue Crack Propagation Diagram

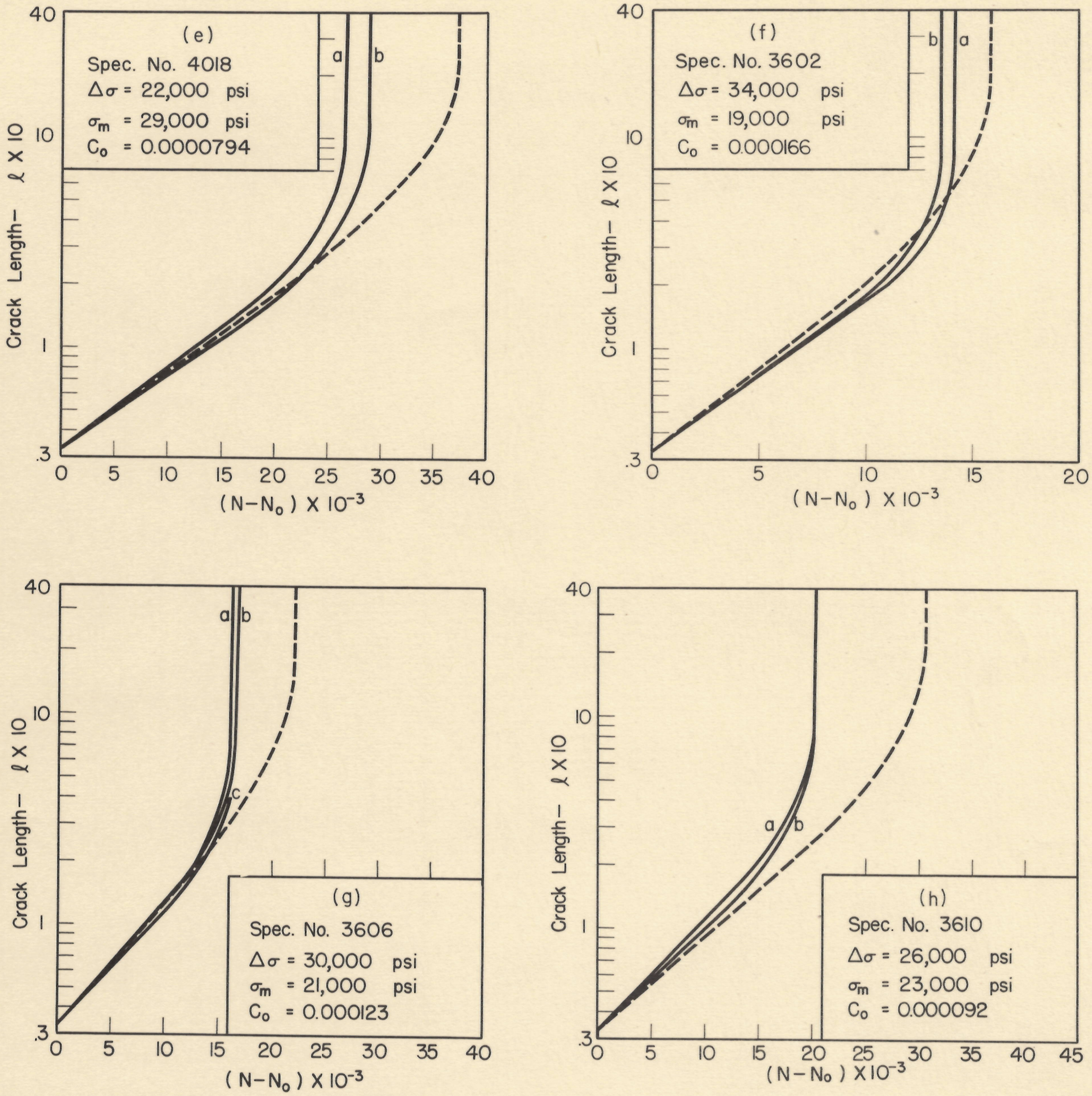

Fig. 45(e,f,g,h) Combined Fatigue Crack Propagation Diagram

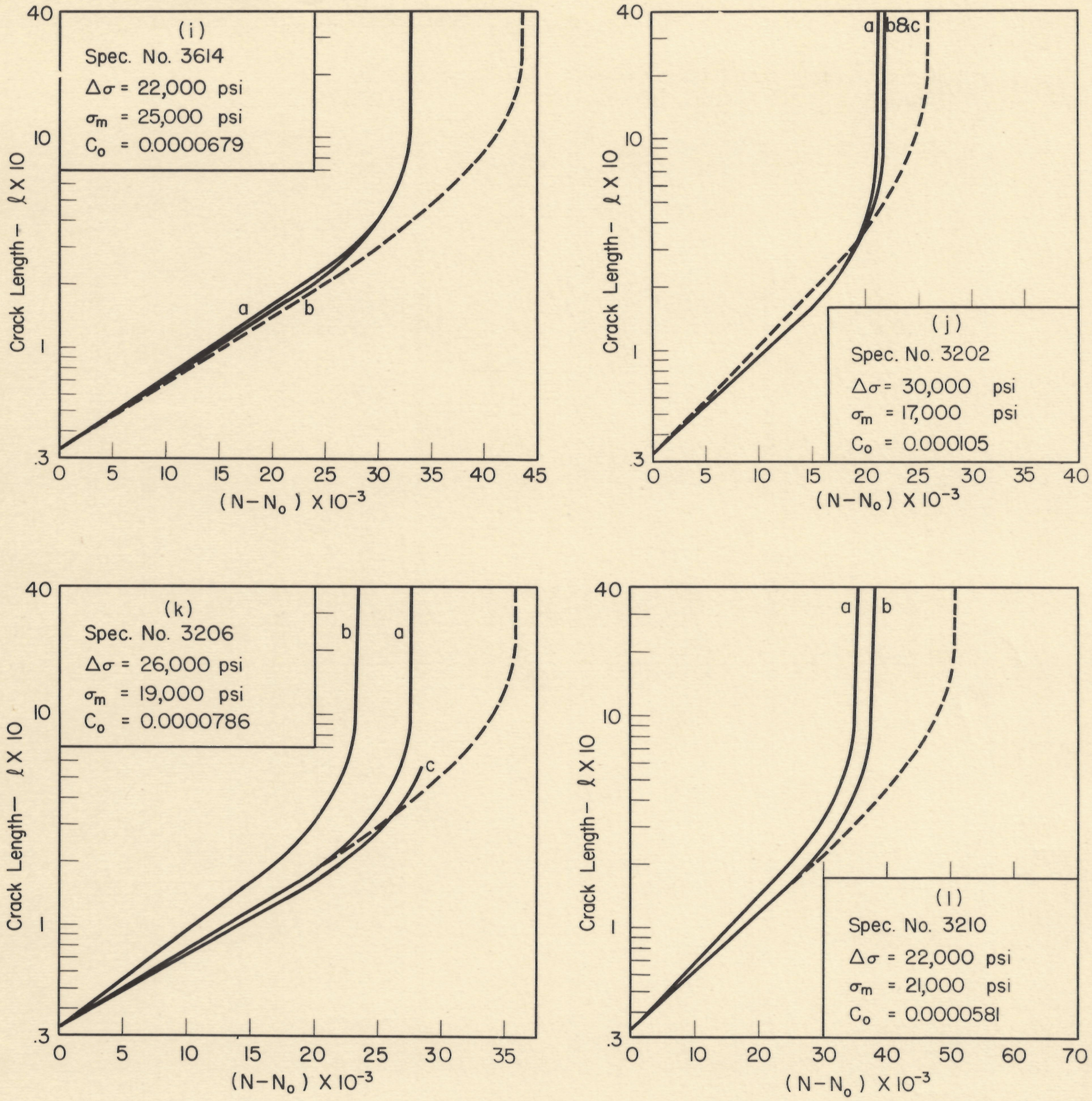

Fig. 45(i,j,k,l) Combined Fatigue Crack Propagation Diagram

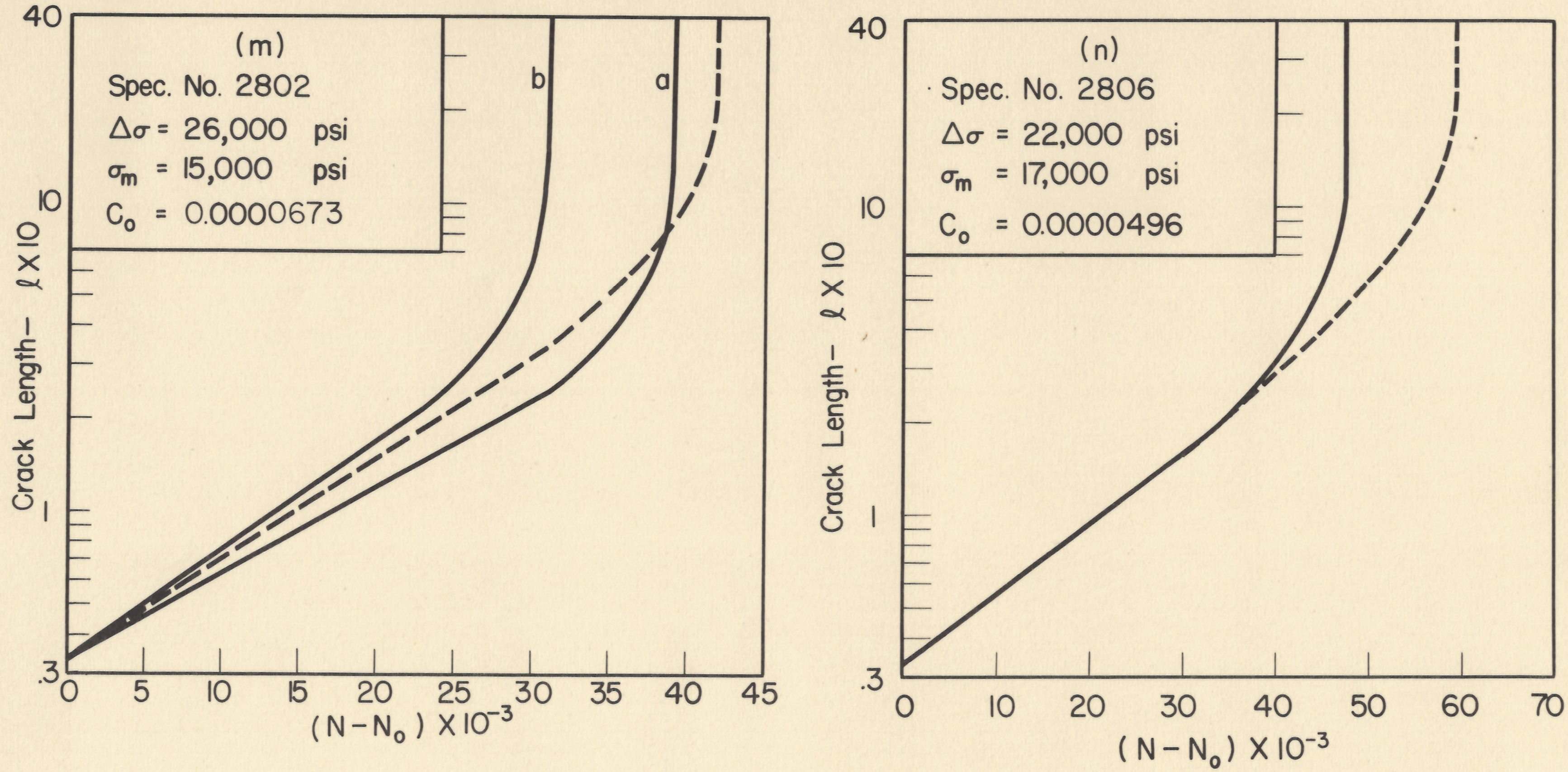

Fig. 45(m,n) Combined Fatigue Crack Propagation Diagram

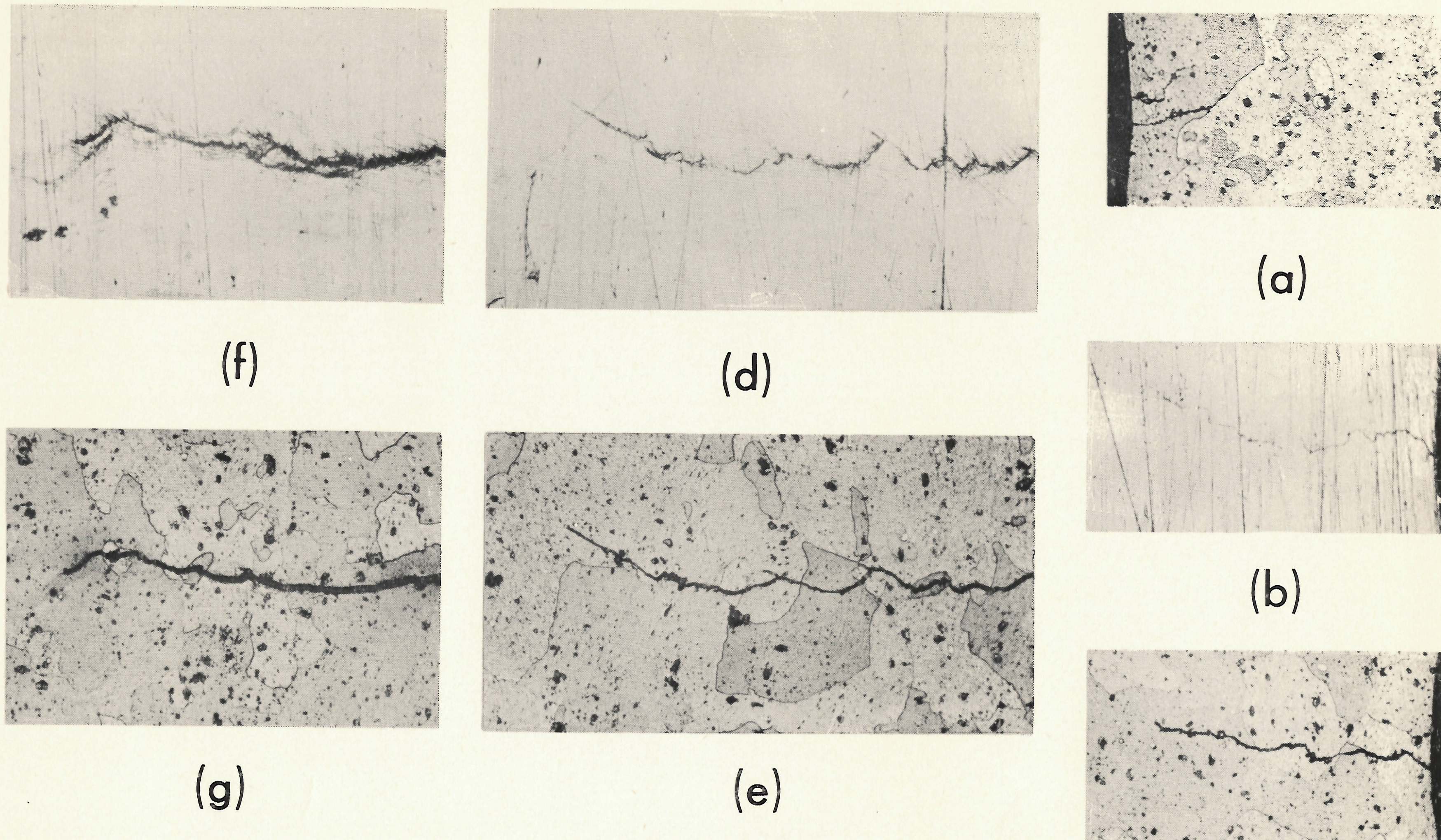

(f) (d) (a)

(b)

(g) (e)

(c)

$\ell = 0.446$ in. $\ell = 0.188$ in. $\ell = 0.046$ in.

Fig. 46 Photomicrograph of Fatigue Crack Tips (×200)

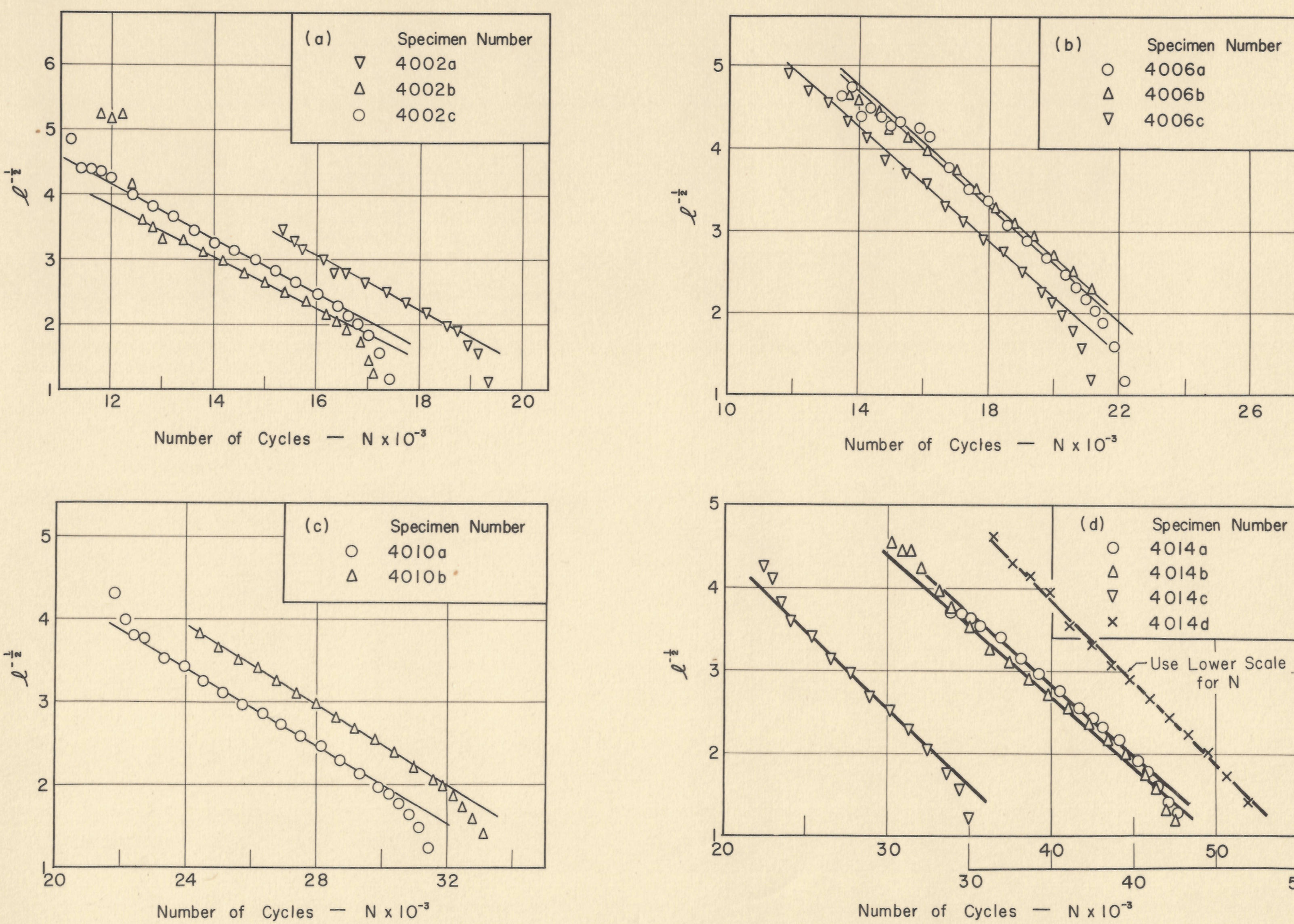

Fig. 47(a,b,c,d) Correlation According to Head's Equation of $\ell^{-\frac{1}{2}}$ with Number of Cycles of Load

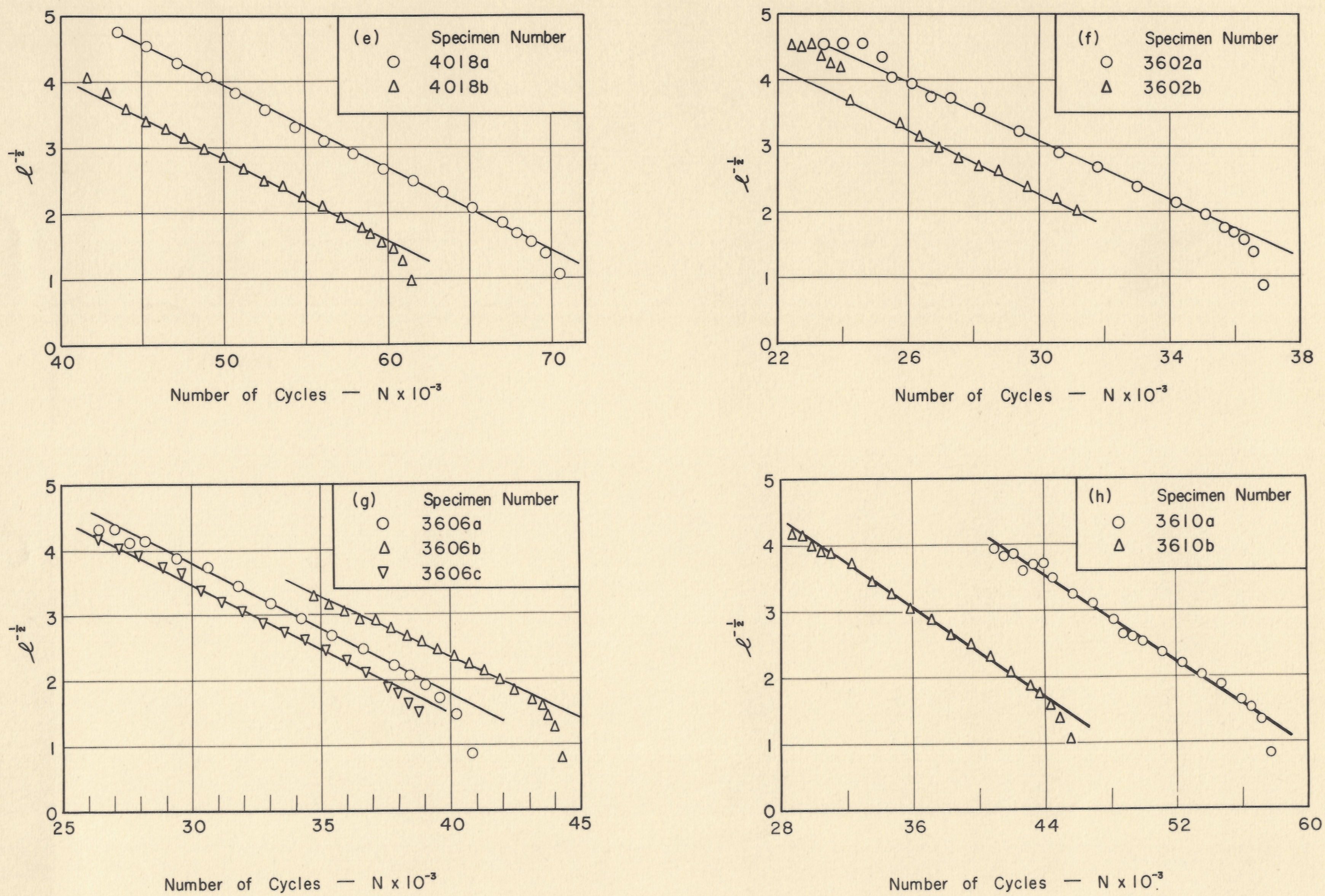

Fig. 47(e,f,g,h) Correlation According to Head's Equation of $\ell^{-\frac{1}{2}}$ with Number of Cycles of Load

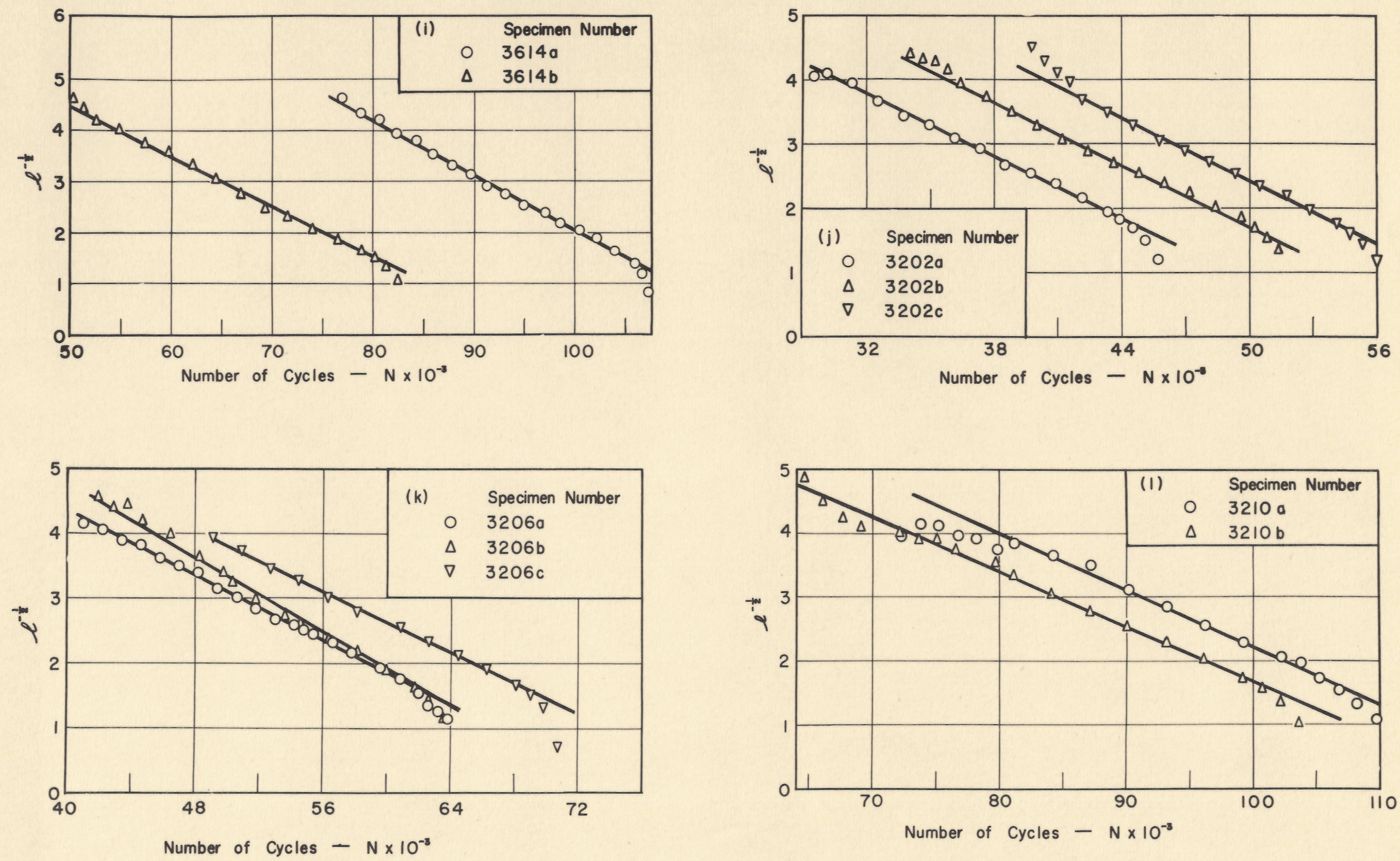

Fig. 47(i,j,k,l) Correlation According to Head's Equation of $\ell^{-\frac{1}{2}}$ with Number of Cycles of Load

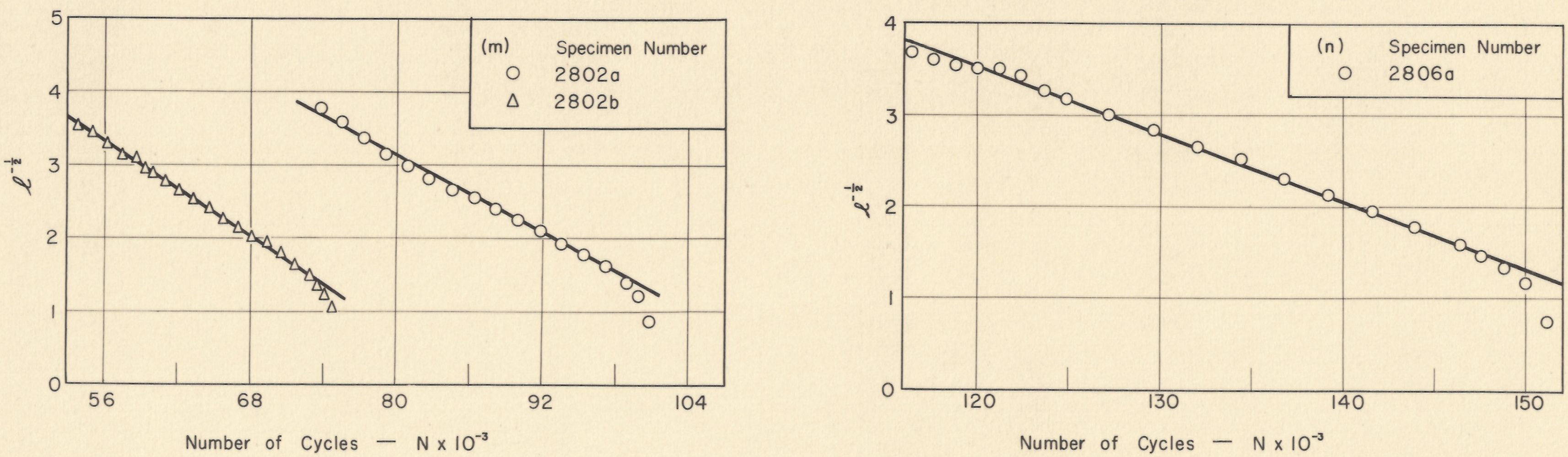

Fig. 47(m,n) Correlation According to Head's Equation of $\ell^{-\frac{1}{2}}$ with Number of Cycles of Load

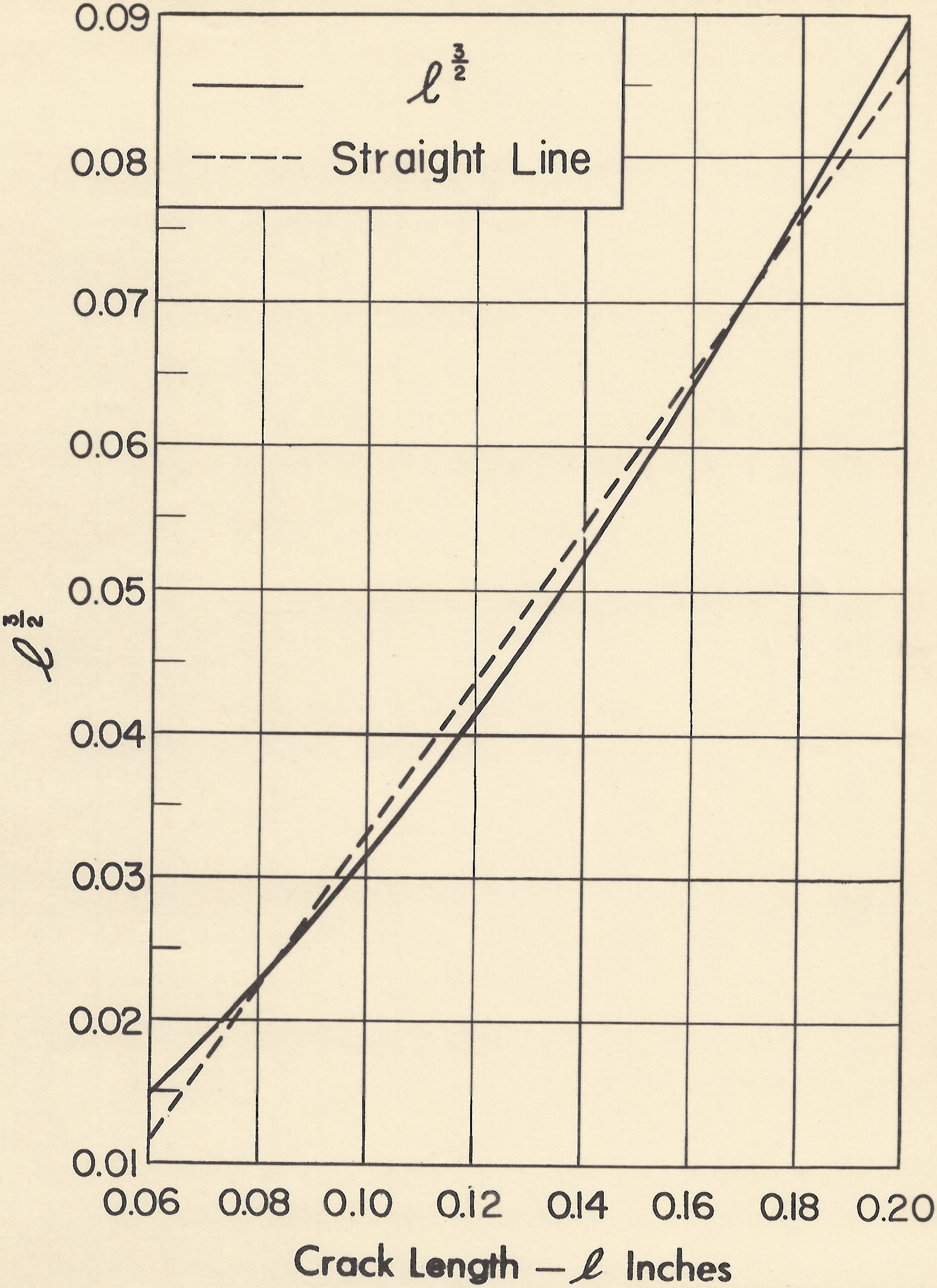

Fig. 48 $l^{\frac{3}{2}}$ versus l

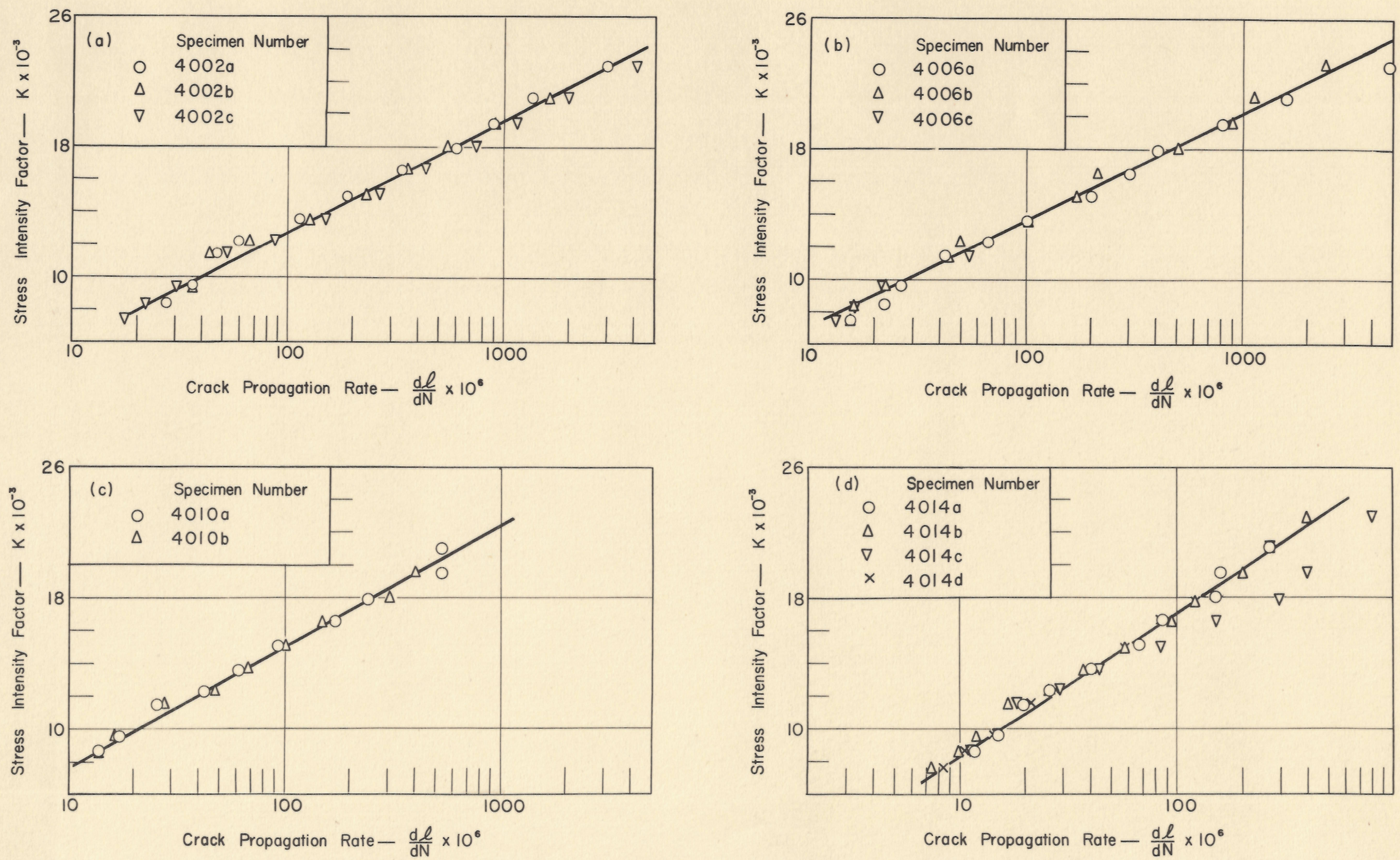

Fig. 49(a,b,c,d) Correlation of Crack Propagation Rate with Stress Intensity Factor

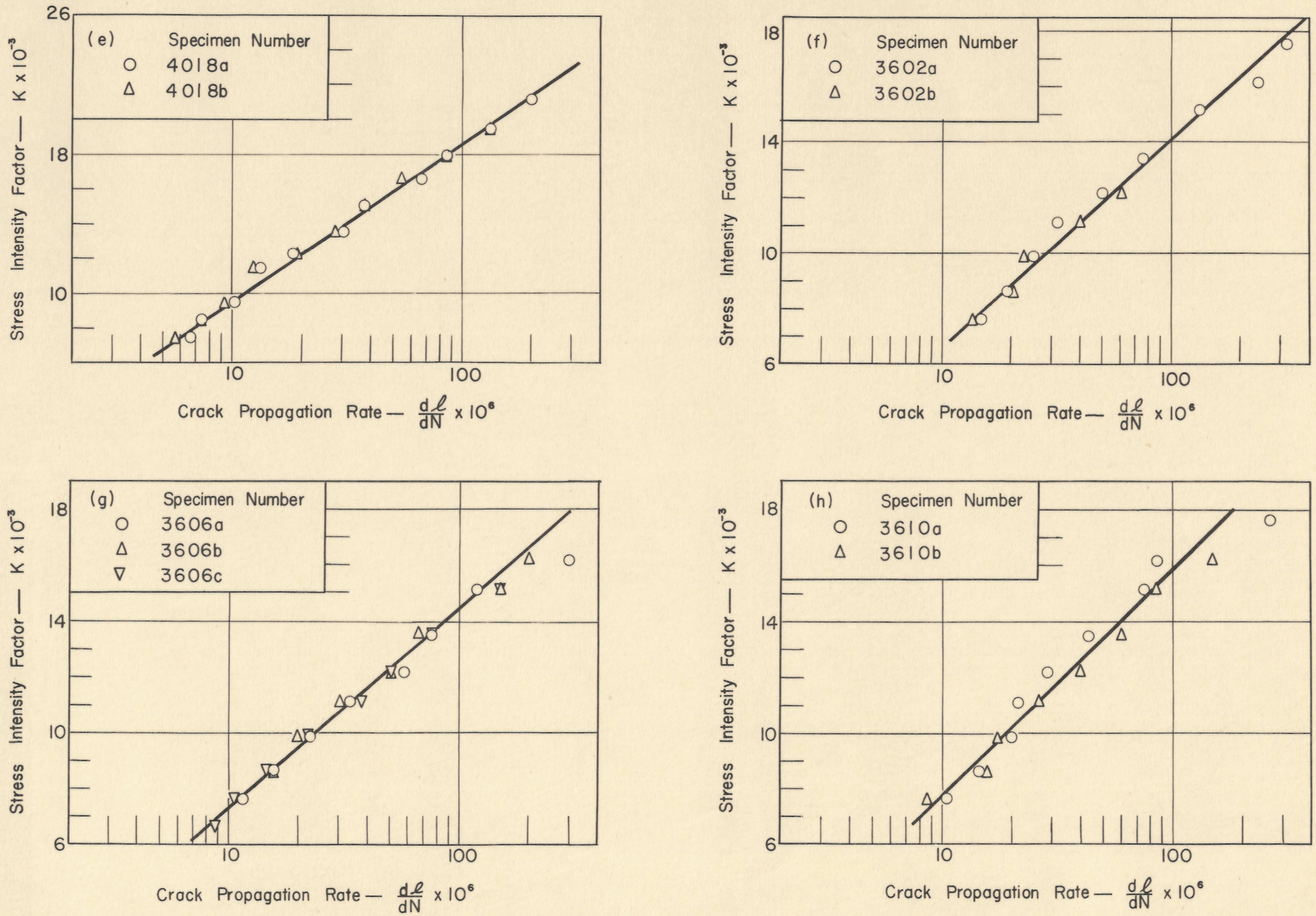

Fig. 49(e,f,g,h) Correlation of Crack Propagation Rate with Stress Intensity Factor

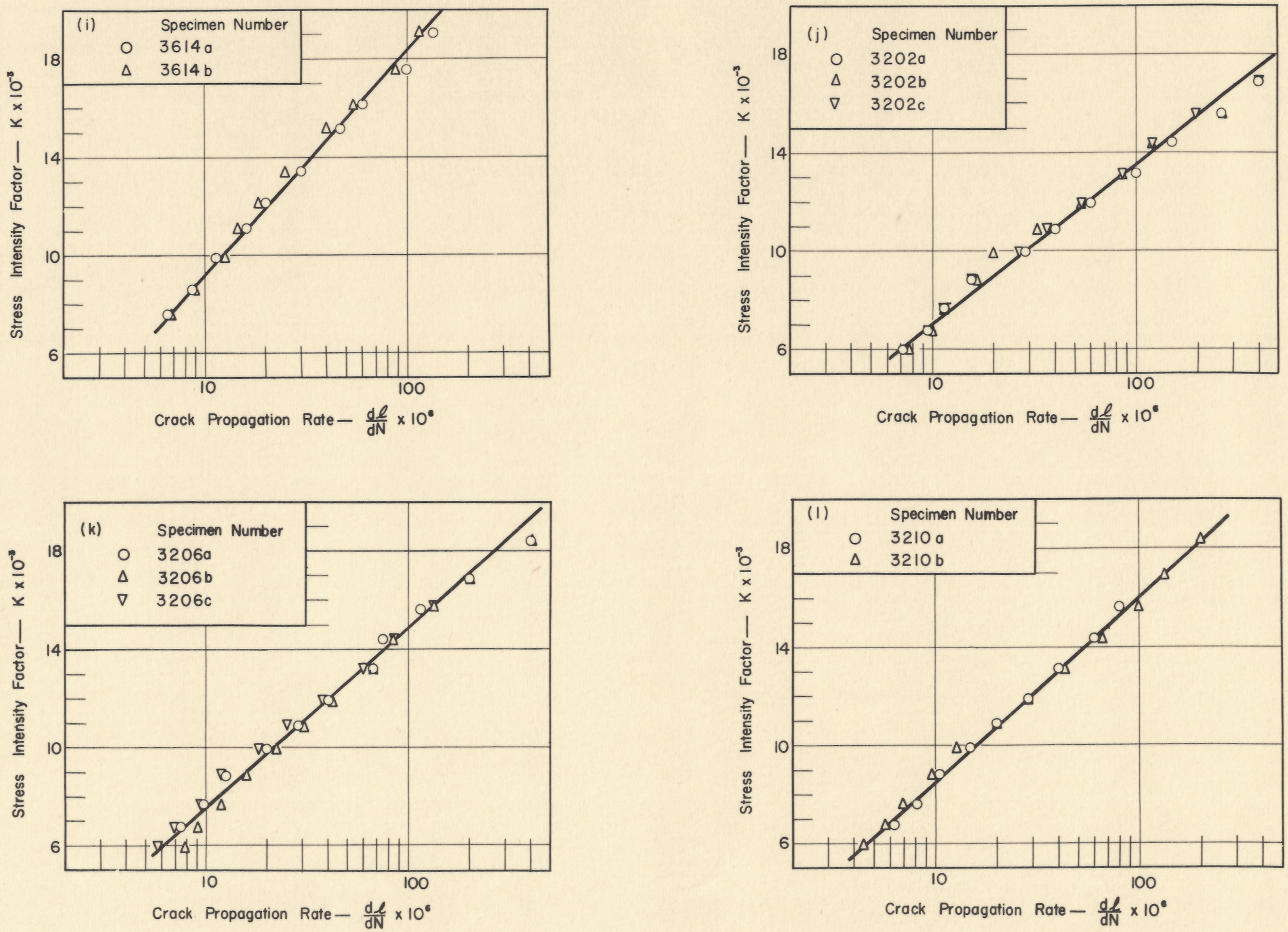

Fig. 49(i,j,k,l) Correlation of Crack Propagation Rate with Stress Intensity Factor

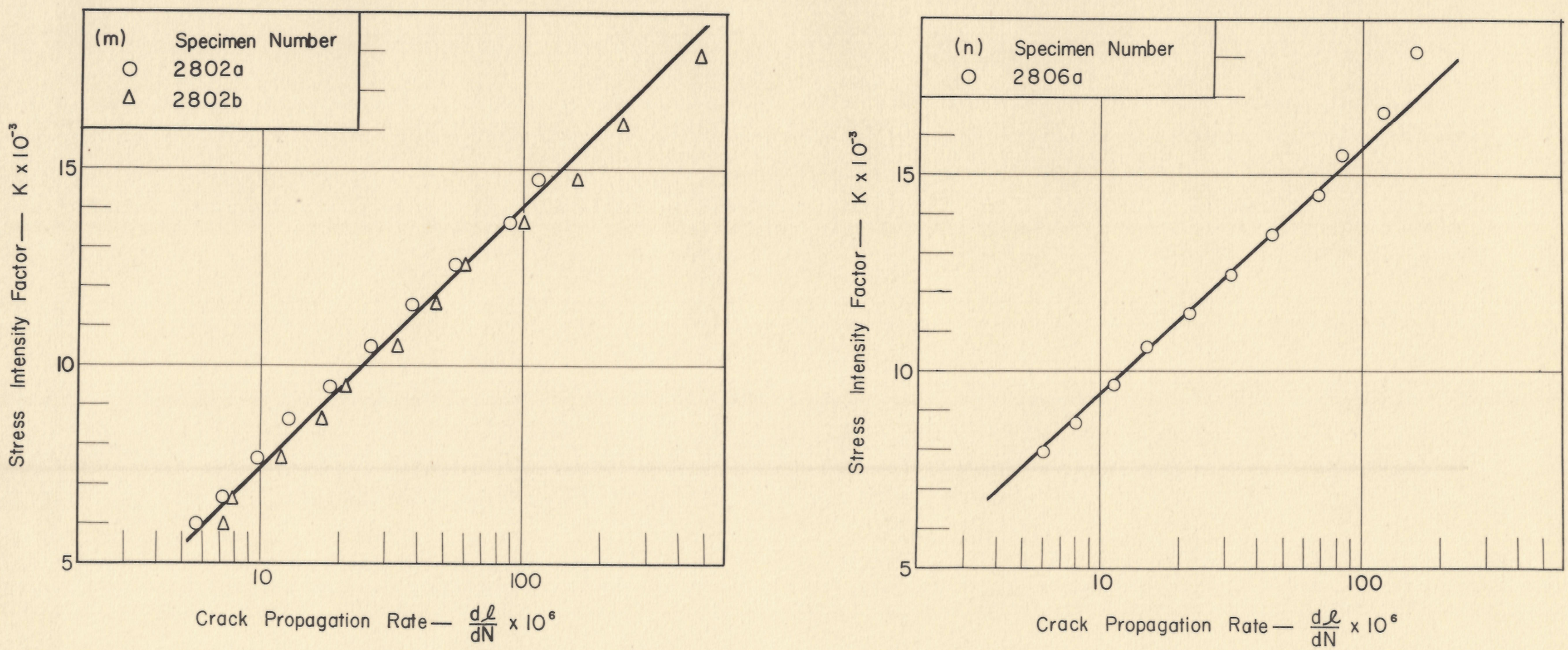

Fig. 49(m,n) Correlation of Crack Propagation Rate with Stress Intensity Factor

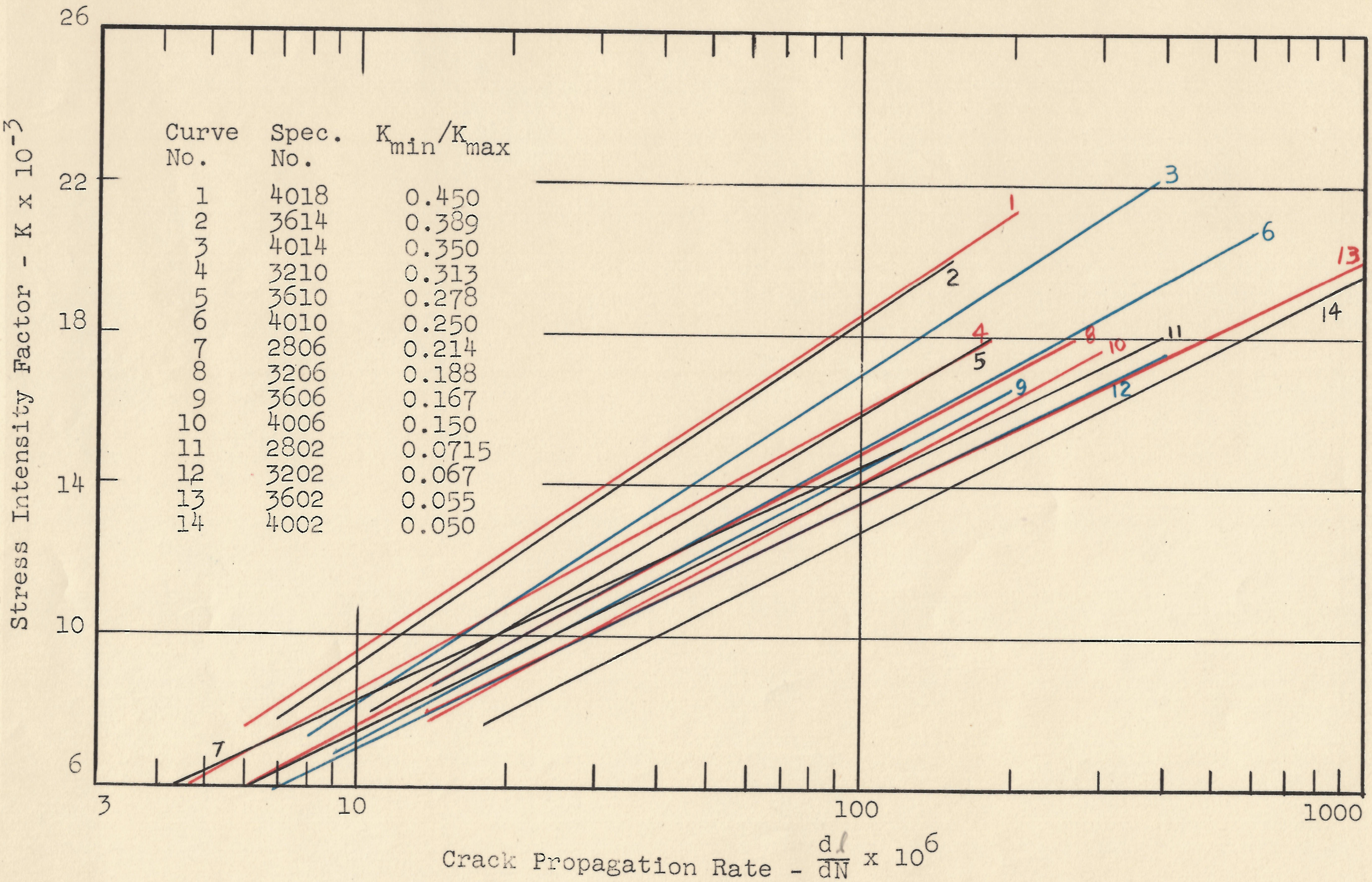

Fig. 50 Diagram Showing Crack Propagation Rate As Influenced By Stress Intensity Factor And The Ratio K_{min}/K_{max}

VITA

Hao Wen Liu was born in Kiangying, Kiangsu, China, August 20, 1926. Prior to his graduation from Miami University in 1951 with a B. S. in Business Administration, he attended the University of Shanghai and Lingnan University in China. He entered graduate school at the University of Illinois in 1951 and received his M. S. in Management in 1952.

In 1952, Mr. Liu changed his major subject to Mechanical Engineering and received his B. S. degree in 1954 and his M. S. degree in 1956. In addition to his graduate studies, Mr. Liu has engaged in research projects in the field of fatigue of metals for the Department of Theoretical and Applied Mechanics.

Mr. Liu is a member of the American Society of Testing Materials and the Society of the Sigma Xi. He has published the following technical articles in the field of fatigue of metals.

H. W. Liu, "Effect of Surface Finish on the Fatigue Strength of Ti 155A Titanium Alloy," T. & A. M. Report No. 526, University of Illinois, January, 1956.

H. W. Liu, "Effect of Surface Finish on the Fatigue Strength of Ti 6Al 4V Titanium Alloy," T. & A. M. Report No. 553, University of Illinois, August, 1956.

H. W. Liu, H. T. Corten, and G. M. Sinclair, "Fretting Fatigue Strength of Titanium Alloy RC 130B," Proceedings ASTM, Vol. 57, 1957, pp. 623-641.

H. W. Liu and H. T. Corten, "Fatigue Damage During Complex Stress Histories," T. & A. M. Report No. 546, University of Illinois, October, 1957.

H. W. Liu and H. T. Corten, "Fatigue Damage During Complex Stress Histories, Final Report," T. & A. M. Report No. 566, University of Illinois, December, 1958.